Carrot & Stick Policies and the Housing Affordability Puzzle[*]

Daniel Lebret[†] Crocker H. Liu[‡] Maxence Valentin[§]

March 26, 2026

Abstract

We study how housing policy affects construction and affordability in cities where supply primarily arises through redevelopment. In these settings, increases in supply change not only the quantity but also the composition of housing. We analyze this mechanism by developing a forward-looking spatial model in which developers choose when to redevelop and how intensively to build in response to affordable housing mandates, density bonuses, and tax incentives. Calibrated to parcel-level data from New York City, the model shows that each instrument operates through parcel-specific redevelopment decisions. Tax incentives accelerate redevelopment, while density bonuses increase project scale but often delay construction. Both instruments increase housing supply but do not reliably lower average rents because redevelopment primarily entails replacing low-rise, depreciated structures with higher-rent construction. The incidence of affordable mandates similarly depends on individual redevelopment decisions, and thus differs across policy instrument bundles. Under fiscal incentives, it falls entirely on the public sector, whereas under density bonuses, it is shared almost equally between landowners and the public sector.

JEL classification: R14, R31, R38, R52
Keywords: Real Estate Development, Land-use regulations, Tax credits, Affordable housing, Capital investment under uncertainty, Public-private partnership

[*]We thank Boaz Abramson (discussant), Franciso Amaral, Nathaniel Baum-Snow, Tom Cui (discussant), Tricia Dietz, Jefferson Duarte (discussant), Antoine Dubus, Gilles Duranton, Pierre-Antoine Erny, Sonia Gilbukh (discussant), Hanchen Jiang, Hans Koster (discussant), Jake Krimmel, Yubei Li, Gabriel Loumeau, John Mangin, Michael Manville, Paavo Monkkonen, Daniel Moran, Shane Phillips, Vincent Rollet, Albert Saiz (discussant), Jaehee Song (discussant), Axel Werwatz (discussant), and Michael Wiebe for insightful discussions and feedback. We are also grateful to the participants of the Seminar of the Institute of Economic Research at the University of Neuchâtel, the 19th North American Meeting of the Urban Economics Association, 4th Workshop on Residential Housing in Zurich, the Economic Research Group Workshop at the University of North Texas, the Barriers to Homeownership, Land-use, and Urban Dynamics workshop at the Chicago FED, the 14th European Meeting of the Urban Economics Association, the 2025 FSU-UF Critical Issues in Real Estate Symposium, Penn State Real Estate Brownbag seminar, the 2024 CRED-MIT Workshop in Real Estate Economics, the 13th European Meeting of the Urban Economics Association, the 2024 AREUEA National Conference, the 15th ReCapNet Conference, and the 2023 AREUEA-International Conference for valuable feedback. This version supersedes a previous version entitled "Carrot & Stick Zoning".

[†]Cornell University. Email: daniel.lebret@cornell.edu.
[‡]Cornell University. Email: chl62@cornell.edu.
[§]ETH Zurich. Email: maxence.valentin@ethz.ch.

Despite extensive policy intervention, housing affordability pressures persist across cities, even in environments with sustained housing production. A central tension is that expanding supply in durable housing markets primarily occurs through redevelopment, which replaces existing structures with new construction that commands higher rents and therefore need not reduce average housing costs. To address this tension, governments often combine incentives with affordable housing mandates. Because real estate investment is however infrequent, irreversible, and forward-looking, these policies shift the conditions under which redevelopment occurs, with long-lasting effects on residents (Rosenthal, 2014), neighborhoods (Brueckner and Rosenthal, 2009), the urban environment (Glaeser and Gyourko, 2018), and the broader economy (Duranton and Puga, 2023; Hsieh and Moretti, 2019). In this study, we formalize this replacement process in a structural model of real estate development to quantify how policy affects housing production, rents, and the cost of affordable housing mandates.

The central implication of the analysis is that new housing does not expand the stock at the margin; it replaces it. As a result, more housing construction fails at lowering average rents, as the replacement effect often dominates the standard supply effect. Because of heterogeneity in the built environment, individual redevelopment decisions also govern how policy instruments affect future supply. Tax exemptions accelerate redevelopment on parcels near their investment threshold, while density bonuses increase project scale but often delay construction. Because policies affect when and how existing assets are replaced heterogeneously, this replacement mechanism also determines the extent to which the cost of mandated affordable units is borne by landlords through lower land values or by the public sector through foregone fiscal revenues. Under fiscal incentives, the cost falls almost entirely on the public sector, whereas under density bonuses, it is shared almost equally between the city's fiscal capacity and landowners, with however substantial heterogeneity among landowners. Together, this replacement mechanism helps reconcile why rents can rise despite substantial building activity, why policies that appear similar in terms of total housing production generate distinct redevelopment patterns, and why different policies are favored by some stakeholders but not others.

To study this mechanism, we develop a forward-looking model of city development in which rational developers decide when to undertake irreversible investments in durable housing and how intensively to build under alternative policy regimes. The city consists of heterogeneous parcels, each potentially containing an income-generating structure defined by its location and building attributes. Developers, who anticipate future rents determined by aggregate and local construction activity, choose the timing and scale of development to maximize asset values subject to zoning constraints and irreversible construction costs. At the parcel level, the model builds on classic frameworks of irreversible investment under uncertainty (Capozza and Li, 1994;

McDonald and Siegel, 1986; Paddock et al., 1988) and extends them to incorporate regulatory and fiscal policy instruments that enter this dynamic optimization problem. Governments may combine incentives (*Carrots*), such as property tax exemptions and density bonuses, with obligations (*Sticks*) requiring in-kind provision of public goods, including infrastructure, environmental improvements, or social housing.[1] We embed these parcel-specific decisions in a citywide spatial environment in which redevelopment on one parcel affects incentives elsewhere. Higher expected construction reduces citywide rent growth through a standard supply effect (Mast, 2023; Rosenthal, 2014), while new market-rate development increases local rent growth through amenity improvements or gentrification, generating positive spillovers across nearby parcels (Almagro and Domínguez-Iino, 2025; Diamond, 2016). Together, these forces determine spatial variation in expected rent growth and, in turn, redevelopment incentives and equilibrium rents across the city.

To illustrate the model's implications, we calibrate it to the New York City (NYC) real estate market, using the affordable housing mandate as the primary policy experiment. The calibration integrates parcel-level data on density, building age, and location with rental data from the American Community Survey and neighborhood-level rental growth and volatility from CoStar. We parameterize rental incomes to decrease with building age and the share of affordable units, and to increase with height (Ahlfeldt and Barr, 2022; Danton and Himbert, 2018; Liu et al., 2018). Construction costs are non-instantaneous and also convex in height (Ahlfeldt et al., 2026; Ahlfeldt and McMillen, 2018; Eriksen and Orlando, 2022). The model matches observed cross-neighborhood property values and predicts out-of-sample construction patterns when calibrated to pre-policy data. The baseline calibration projects 168,395 units over the next decade, closely matching historical construction patterns across neighborhoods.

We then use the model to evaluate policy counterfactuals. We compare affordable mandates, density bonuses, and tax exemptions both in isolation and in combination, focusing on their effects on redevelopment probabilities, citywide housing production, the rent distribution, and the cost and incidence of affordable units. Both density bonuses and tax exemptions expand housing supply relative to the baseline but operate on different margins of the replacement decision. We find that tax exemptions primarily raise redevelopment probabilities by lowering post-construction tax liabilities and bringing forward replacement on parcels near their investment threshold, whereas density bonuses increase optimal density and thus the scope for replacement. As a result, a higher allowable density can delay construction, as developers optimally wait to build taller structures. Because of heterogeneity in the built environment, policy impacts are spa-

[1]The ability of governments to recapture value increases resulting from public actions, often referred to as "land value capture" (OECD and Lincoln Institute of Land Policy, 2022), plays a central role in contemporary urban policy debates. Incentive zoning and related mechanisms are widely used in the United States (Homsy and Kang, 2023), Canada (Moore, 2013), and Europe (Druckenbrod and Beckmann, 2018).

tially heterogeneous. Parcels closer to their redevelopment thresholds respond more strongly to fiscal incentives, while high-quality locations benefit more from density bonuses. Introducing an affordability mandate to either of these policies reduces the number of market-rate units, although substitution toward affordable units partly offsets this effect.

We also evaluate how each policy counterfactual affects expected rents. Rent changes reflect the interaction of three channels: the discount associated with the share of affordable units in new buildings, the replacement premium arising when redevelopment substitutes older, depreciated units with new housing that enters without accumulated depreciation, and the downward (upward) effect of additional citywide (neighborhood market-rate) supply. We observe that policies that expand supply increase the number of units in both the bottom and the top quintiles of the rent distribution, reflecting the competing supply and replacement effects. We find that, in aggregate, the replacement effect, however, dominates, so additional construction does not translate into lower per-unit average rents. Affordability mandates expand access to below-market-rate units in new construction, but these units tend not to be in the bottom quintile of the distribution, because more stringent rent discounts otherwise hinder redevelopment.

Because below-market housing production is not privately profitable, policies with affordability mandates introduce a wedge between private returns and social objectives that must be absorbed through redevelopment. To evaluate the associated implications, we quantify the implied cost of mandated affordable units in terms of changes in land value and foregone fiscal revenues, making explicit how the cost of affordability is distributed between landowners and the public sector. We estimate that each mandated affordable unit entails a cost of approximately $65,000, with the burden depending critically on the policy instrument bundle. Under tax exemptions, the cost falls almost entirely on the public sector through foregone tax revenues, while under density bonuses, it is split roughly evenly between landowners, through lower land values, and the public sector. This result reflects how different policy instruments shift the gains and costs associated with redevelopment, and relates to the broader literature on the incidence of land use regulation (Diamond and McQuade, 2019; Fischel, 2002; Glaeser et al., 2005).

Our paper contributes to two strands of literature. The first concerns the determinants of real estate supply (Baum-Snow and Duranton, 2025; Glaeser and Gyourko, 2018). Prior research emphasizes the role of market structure and productivity in constraining housing growth (D'Amico et al., 2024; Goolsbee and Syverson, 2023), and the role of construction technology in enabling the rise of high-rise buildings (Ahlfeldt and Barr, 2022; Ahlfeldt et al., 2026; Ahlfeldt and McMillen, 2018). A parallel line of research highlights how physical and regulatory constraints generate spatial variation in supply elasticities (Albouy and Ehrlich, 2018; Baum-Snow and Han, 2024;

Brueckner and Singh, 2020; Büchler and v. Ehrlich, 2023; Gyourko et al., 2021; Saiz, 2010). Our study is more specifically related to the literature modeling forward-looking developers in dynamic settings (Cunningham, 2006; Hsiao, 2025; Murphy, 2018; Peng, 2023; Rollet, 2025), which emphasizes the option value embedded in land ownership. More specifically, our models contribute to the long tradition of real options models (McDonald and Siegel, 1986; Myers, 1977) applied to real estate development (Arnott and Lewis, 1979; Capozza and Li, 1994; Grenadier, 1996; Lange and Teulings, 2024; Quigg, 1993; Titman, 1985). Building on the development framework of Lebret and Liu (2023), we extend this class of models by including endogenous feedback between parcels, thereby addressing a central critique of asset-pricing-based development models, which often treat prices as exogenous. The incorporation of parcel-specific development decisions into a spatial equilibrium also enables the evaluation of policy counterfactuals.

Second, our study contributes to the literature on the effects of urban regulatory and fiscal policies (Gyourko and Molloy, 2015; Quigley and Rosenthal, 2005). The existing literature examines the impact of supply-side policies such as tax incentives in opportunity zones (Chen et al., 2023; Corinth and Feldman, 2024), upzoning (Büchler and Lutz, 2024; Freemark, 2020, 2023; Greenaway-McGrevy and Phillips, 2023; Rollet, 2025), affordable housing mandates (Favilukis et al., 2023), and inclusionary housing mandates coupled with density bonuses (Schuetz et al., 2011) or fiscal incentives (Baum-Snow and Marion, 2009; Eriksen and Rosenthal, 2010; Soltas, 2024, 2022). Krimmel and Wang (2026) further show that attaching affordability constraints to upzoning in Seattle shifts development outside targeted areas, underscoring the tension between incentives and constraints. Although these *Carrot and Stick* mechanisms have been examined by urban planners and political scientists (Freemark, 2020; Homsy and Kang, 2023; Kim, 2020; Korngold, 2022), our paper provides a structural analysis that unifies these tools and enables isolating how different policy instruments affect redevelopment, rents, and their incidence.

The paper proceeds as follows. Section 1 presents the model, describing developers' decision rules in a spatial economy. Section 2 illustrates the mechanics of the model on a representative parcel and describes how spatial spillovers operate. Section 3 outlines the empirical setting and calibration. Section 4 reports the outcomes of the status-quo calibration and validation exercises. Section 5 analyzes the effects of policies on housing production and rents. Section 6 describes the costs of each policy and quantifies the cost of mandated affordable units. Section 7 concludes.

1 A Forward-looking Spatial Model of Real Estate Development

We develop a forward-looking model of city redevelopment in which developers decide both when to redevelop a parcel and how intensively to build. We consider a city composed of parcels

$i \in I$, each owned by a price-taking developer. Each parcel may contain an existing building characterized by its built density $F_{B,i}$ and its depreciation level $z_{B,i}$. The location of parcel i determines the market rent per unit of built density, denoted R_{it}, which reflects both local and citywide housing market conditions. Developers form expectations about future rents when making redevelopment decisions. In our environment, the government regulates redevelopment through a policy environment that may change from a baseline regime $\mathcal{P}_0$ to an alternative regime $\mathcal{P}$. Policy affects redevelopment incentives directly through regulatory and fiscal instruments and indirectly by altering future housing supply and, thus, future rent dynamics across the city.

1.1 The Real Estate Developer Decision Rule Under Status Quo Regulation

To characterize the redevelopment decision, we first analyze the problem of a single parcel and suppress the parcel index i for notational simplicity. The market rent per unit of space, R_t, is our fundamental state variable. Under the risk-neutral measure $\mathbb{Q}$, rent evolves according to a geometric Brownian motion:

$$dR_t = \delta R_t \, dt + \sigma R_t \, dW_t \tag{1}$$

where δ is the risk-neutral expected growth rate of rent used for valuation that adjusts with future supply[2] , σ is the volatility, and W_t is a standard Brownian motion on the probability space $(\Omega, \mathcal{F}, \mathbb{Q})$. We describe how δ adjusts endogenously with respect to unexpected future supply in Section 1.3. This process is log-normal, implying that both expected growth and volatility scale proportionally with the current rent level.

Valuation relies on standard assumptions that ensure the existence of a risk-neutral measure. Under these conditions, the stochastic process for rents can serve as the fundamental state variable for arbitrage-free pricing, and development options can be valued as contingent claims on future rents.[3] Denoting R as the market rent per unit of space at $t = 0$, we can rewrite the potential rent at $t \geq 0$ as $R_t = Re^{(\delta - \sigma^2/2)t + \sigma W_t} = Re^{\sigma Z_t}$, where $Z_t = bt + W_t$, and $b = 1/\sigma(\delta - \sigma^2/2)$.

To obtain the rental income of a parcel, we introduce two elements.[4] First, we define $\Gamma(F, z, \alpha)$ as the function that scales the market rent of a unit of density R_t, based on the characteristics of the built property, to yield the stochastic rental income of a developed property. In particular, the

[2]Under standard asset-pricing conditions, the risk-neutral rent growth rate is linked to the observed cap rate c_i through the relationship $\delta_i \approx r - c_i$, where r denotes the risk-free rate.

[3]In practice, rents are not continuously traded and markets are incomplete. The assumption that rents are spanned by traded assets should be interpreted as an analytical convenience supported by the existence of correlated securities (e.g., REIT shares, lease-backed instruments) that allows developers to partially hedge rent risk. We discuss these assumptions in more detail in Appendix A.1.

[4]In this theoretical section, we assume that parcels are of unit size one ($L = 1$). In the model applications, we will make parcel size scale both rents and costs proportionally.

rent increases with the built density F[5], decreases with the accumulated depreciation ($z \in [0,1]$), and decreases with the portion of built space allocated to affordable housing (α). Because market rent R_t is defined on a per unit basis of newly built property, we let $\Gamma(F=1, z=1, \alpha=0)=1$ correspond to a property with a built density of 1 ($F=1$), with no operational efficiency losses due to rental depreciation ($z=1$), and no affordable housing ($\alpha=0$) that would alter the rental incomes. We revert to the full parametrization of $\Gamma(F,z,\alpha)$ in Section 3. Second, we assume the government imposes a tax on developed properties proportional to the rental incomes, reducing the developer's effective payout by ψ. Consequently, the value of the developed parcel without its development option is

$$\mathbf{E}_{\mathbb{Q}}\left\{\int_0^{\infty} e^{-ru}\underbrace{(1-\psi)}_{\text{Net of tax}}\underbrace{\Gamma(F_B,z_B,\alpha_B)R_u}_{\text{Gross rental income}}\,\mathrm{d}u\right\},$$

where the subscript B describes the characteristics of the current building.

Private developers have the option to replace the current building with a new one constructed at density $F \leq \bar{F}_0$, where $\bar{F}_0$ denotes the maximum allowable built density (volume) under the regulatory environment $\mathcal{P}_0$. Exercising this option requires paying an instantaneous demolition cost $\gamma(F_B)$ to remove the existing structure, in addition to incurring an annual construction cost during the construction period of d years, denoted as $\kappa(F,\alpha)$. Construction costs increase with the density of the new construction (F) and vary with the portion of built-up area dedicated to affordable housing (α).

Developers exercise the option to redevelop under $\mathcal{P}_0$ only if favorable market conditions prevail. Because developers already own the parcel and the existing structure, the redevelopment decision corresponds to exercising an embedded option to replace the current building. We denote by R^e the predetermined rent level (the expansion barrier) at which developers initiate construction at density F, and by T_{R^e} the first time this barrier is reached. We assume deterministic time-to-build: completion occurs exactly d years after initiation. Let H_{R^e} denote the time at which the property is fully developed.[6] Consequently, the value of the parcel under $\mathcal{P}_0$ inclusive of the development option is

[5]Throughout the paper, density F should be interpreted as effective built volume per unit of land rather than purely floor-area density. In addition to total floor area, F captures building height that affects the productive space available to tenants.

[6]Formally, $T_{R^e}(R)=\inf\{t\geq 0 : R_t = R^e\}$ and $H_{R^e}(R)=T_{R^e}(R)+d$.

$$\pi_0(R, F_B, z_B, \alpha_B, F; \mathcal{P}_0, \Theta) = \underbrace{\mathbf{E}_{\mathbb{Q}}\left\{ \int_0^{T_{R^e}} e^{-ru}\,(1-\psi)\;\Gamma(F_B, z_B, \alpha_B) R_u \,\mathrm{d}u \right\}}_{\text{Value of existing property}} - \underbrace{\mathbf{E}_{\mathbb{Q}}\left\{ e^{-rT_{R^e}} \gamma(F_B) \right\}}_{\text{Demolition costs}}$$
$$- \underbrace{\mathbf{E}_{\mathbb{Q}}\left\{ \int_{T_{R^e}}^{H_{R^e}} e^{-ru} \kappa(F, \alpha)\,\mathrm{d}u \right\}}_{\text{Construction costs}} + \underbrace{\mathbf{E}_{\mathbb{Q}}\left\{ \int_{H_{R^e}}^{\infty} e^{-ru}(1-\psi)\,\Gamma(F, 1, \alpha) R_u \mathrm{d}u \right\}}_{\text{Value of new property}} \quad (2)$$

where Θ is the vector of parameters. The value of a parcel thus consists of four discounted terms: net-of-taxes rents from the current property until demolition, demolition costs at the stopping time, expenditures during construction, and the net-of-tax rental income from the completed asset.

1.2 Adding Policy Instruments into the Development Decision Rule

We summarize the policy environment by the vector $\mathcal{P} = [\alpha, \phi, \tau]$, where α denotes a mandate requiring that a share of the project be allocated to affordable housing units, ϕ represents additional allowable density, and τ denotes a temporary tax exemption following redevelopment. The status quo corresponds to $\mathcal{P}_0 = [\alpha = 0, \phi = 0, \tau = 0]$.[7]. The three policy instruments affect redevelopment decisions through different channels. The mandate α reduces the market rental income generated by the property and alters construction costs through the functions $\Gamma(.)$ and $\kappa(.)$, respectively. The density bonus ϕ relaxes the density constraint by allowing developers to choose $F \leq \bar{F}$, where $\bar{F} = \bar{F}_0(1+\phi)$. Finally, the tax exemption τ postpones property taxation for τ years after redevelopment is completed.

We can thus rewrite the value of a parcel under the new regulatory environment as:

$$\pi(R, F_B, z_B, \alpha_B, F; \mathcal{P}, \Theta) = \underbrace{\mathbf{E}_{\mathbb{Q}}\left\{ \int_0^{T_{R^e}} e^{-ru}\,(1-\psi)\;\Gamma(F_B, z_B, \alpha_B) R_u \,\mathrm{d}u \right\}}_{\text{Value of existing property}}$$
$$- \underbrace{\mathbf{E}_{\mathbb{Q}}\left\{ e^{-rT_{R^e}} \gamma(F_B) \right\}}_{\text{Demolition costs}} - \underbrace{\mathbf{E}_{\mathbb{Q}}\left\{ \int_{T_{R^e}}^{H_{R^e}} e^{-ru} \kappa(F, \alpha)\,\mathrm{d}u \right\}}_{\text{Construction costs}}$$

[7]Some parcels may already contain units subject to rent stabilization, rent control, or existing affordability requirements. Accordingly, the policy parameter α should be interpreted as an incremental mandate beyond existing regulations. If the current share of regulated or affordable units on a parcel (denoted α_B) already exceeds the policy requirement, the mandate does not bind, and the existing constraint remains in place.

$$+\underbrace{\mathbf{E}_{\mathbb{Q}}\left\{\int_{H_{R^e}}^{\infty} e^{-ru}\,\Gamma(F,1,\alpha)R_u\,\mathrm{d}u\right\}}_{\text{Value of new property gross of tax}}-\underbrace{\mathbf{E}_{\mathbb{Q}}\left\{\int_{H_{R^e}+\tau}^{\infty} e^{-ru}\,\psi\,\Gamma(F,1,\alpha)R_u\,\mathrm{d}u\right\}}_{\text{Property taxes after }\tau\text{ years of exemption}} \quad (3)$$

Similar to Equation (2), the property value consists of the sum of present values with an additional final term that captures the impact of postponing property taxes for τ years after the development has been completed.

We solve the model analytically by first characterizing the five integrals that define parcel value conditional on a given expansion barrier and density. Rational developers maximize their parcel values, which yields a closed-form solution for the optimal expansion barrier and a numerical solution for the optimal density. These expressions allow us to derive the parcel-level outcomes: the probability that a parcel is redeveloped at a future date, and its optimal redevelopment density.

1.2.1 Parcel value

Proposition 1 *In the presence of the expansion threshold R^e and given a construction density $F \leq \bar{F}$, the property value $\pi(.)$ satisfies*

$$\begin{aligned}\pi(R,R^e,F,F_B,z_B,\alpha_B;\mathcal{P},\Theta) = {} & \underbrace{\Gamma(F_B,z_B,\alpha_B)\frac{1-\psi}{r-\delta}\left[R-R^e\left(\frac{R^e}{R}\right)^{\xi}\right]}_{\textit{Value of existing property}}-\underbrace{\gamma(F_B)\left(\frac{R^e}{R}\right)^{\xi}}_{\textit{Demolition costs}}\\ & \underbrace{-\frac{\kappa(F,\alpha)}{r}\left(1-e^{-rd}\right)\left(\frac{R^e}{R}\right)^{\xi}}_{\textit{Construction costs}}+\underbrace{\Gamma(F,1,\alpha)\frac{R^e}{r-\delta}\,e^{-(r-\delta)d}\left(\frac{R^e}{R}\right)^{\xi}}_{\textit{Value of new property gross of tax}}\\ & \underbrace{-\psi\,\Gamma(F,1,\alpha)\frac{R^e}{r-\delta}\,e^{-(r-\delta)(d+\tau)}\left(\frac{R^e}{R}\right)^{\xi}}_{\textit{Property taxes after }\tau\textit{ years of exemption}}, \quad (4)\end{aligned}$$

with $b=(1/\sigma)(\delta-\sigma^2/2)$, $\lambda=\sqrt{2r+b^2}$, and $\xi=(b-\lambda)/\sigma$.

The proof is in Appendix A.2.

1.2.2 Probability of development

Conditional on current market conditions and a given regulatory regime, developers optimally initiate construction when rent reaches a critical expansion threshold R^{e*}. At this threshold,

the expected value of redevelopment exactly outweighs the continuation value of the existing structure, accounting for construction costs, policy distortions, and the stochastic timing of redevelopment.

Proposition 2 *Given a construction density $F \leq \bar{F}$ and a regulatory regime $\mathcal{P}$, the optimal expansion threshold is*

$$R^{e*} = \frac{\xi}{1+\xi} \frac{\gamma(F_B) + \frac{\kappa(F,\alpha)}{r}\left(1 - e^{-rd}\right)}{\vartheta}, \tag{5}$$

where

$$\vartheta = \Gamma(F, 1, \alpha)\frac{1}{r-\delta}\left(e^{-(r-\delta)d} - \psi\, e^{-(r-\delta)(d+\tau)}\right) - \Gamma(F_B, z_B, \alpha_B)\frac{1-\psi}{r-\delta}.$$

The proof is in Appendix A.3.

Proposition 2 characterizes the rent level at which redevelopment becomes optimal. Because market rents evolve stochastically, a higher expansion threshold does not simply delay development deterministically. Instead, it lowers the probability that redevelopment occurs within any finite horizon. Conditional on the current rent level R, the timing of (re)development is governed by the stopping time $T_{R^{e*}}(R) = \inf\{t \geq 0 \mid R_t = R^{e*}\}$, the first time the rent process reaches the optimal expansion threshold.

This formulation allows us to characterize the redevelopment start in probabilistic terms. Policies that raise construction or regulatory costs increase R^{e*} and therefore reduce the likelihood that development is initiated by a given date, even holding fixed the underlying rent dynamics. The next proposition provides a closed-form expression for this probability.

Proposition 3 *Given the expansion threshold R^{e*} and a construction density $F \leq \bar{F}$, the probability that development is completed by horizon h satisfies*

$$\mathbf{P}_{\mathbb{P}}(H_{R^{e*}} \leq h) = \mathbf{P}_{\mathbb{P}}(T_{R^{e*}} \leq h - d)\,, \tag{6}$$

where $H_{R^{e*}} \equiv T_{R^{e*}} + d$. The probability is computed under the physical measure $\mathbb{P}$, under which rent evolves as $dR_t = gR_t\,dt + \sigma R_t\,dW_t^{\mathbb{P}}$. Here g denotes the expected rent growth rate under the physical measure. Section 1.3 allows this growth rate to adjust with policy-induced supply changes.

For $h > d$, letting $a = \ln(R^{e*}/R)/\sigma > 0$ and $m = (g - \sigma^2/2)/\sigma$, the redevelopment probability is

$$\mathbf{P}_{\mathbb{P}}(T_{R^{e*}} \leq h - d) = \mathcal{N}\left(\frac{m(h-d) - a}{\sqrt{h-d}}\right) + e^{2ma}\,\mathcal{N}\left(-\frac{m(h-d) + a}{\sqrt{h-d}}\right), \tag{7}$$

while $\mathbf{P}_{\mathbb{P}}(H_{R^{e*}} \leq h) = 0$ for $h \leq d$.

The proof is in Appendix A.4.

1.2.3 Optimal density

The preceding analytical results characterize optimal redevelopment timing conditional on a chosen construction density $F \leq \bar{F}$. We now turn to the developer's choice of density. For a fixed expansion threshold R^e, the tradeoff between higher post-redevelopment rental income and higher construction costs admits a closed-form solution for the optimal density (see Appendix A.5). Higher density increases post-redevelopment rental income but also raises construction costs, so the optimal choice of F^* balances these competing forces. Once the expansion threshold is chosen optimally as a function of density, the joint problem of selecting both redevelopment timing and density no longer admits a closed-form solution.

As a result, the developer's optimal density must be determined numerically. Formally, we solve

$$\begin{aligned} F^* = \arg\max_{F} \quad & \pi(R, R^{e*}(F), F, F_B, z_B, \alpha_B) \\ \text{s.t.} \quad & 0 \leq F \leq \bar{F}, \end{aligned} \tag{8}$$

where $R^{e*}(F)$ is given by Proposition 2. This numerical optimization yields the optimal density F^*, the associated expansion threshold $R^{e*}(F^*)$, and the associated probability of development $\mathbf{P}^*$. Together, these objects characterize the developer's decision rule, incorporating both the optimal timing and intensity of redevelopment, conditional on replacement construction.[8]

1.3 Accounting for Aggregate and Local Spillovers in Development Decisions

The parcel-level decision rule described above characterizes redevelopment incentives for a given rent process. However, large-scale policy reforms may alter rents by changing construction across the city. To capture this feedback, we embed the parcel-level model in a citywide environment in which redevelopment decisions determine future housing supply, and thus expected rental growth. Changes in supply affect rent growth through both aggregate supply effects and local neighborhood spillovers, consistent with the empirical literature on housing supply and rents.

In equilibrium, the pricing drift δ_i used in the valuation problem and the physical rent growth

[8] In this framework, developers choose *when* to redevelop and *how much* to build, but not the quality of construction conditional on redevelopment. New construction is assumed to enter without accumulated depreciation, reflecting the fact that redevelopment typically replaces aging structures with buildings that must meet current building codes, safety standards, and regulatory requirements. To the extent that developers in high-demand locations could choose to upscale quality, allowing for such choices would tend to amplify replacement-driven rent increases.

rate g_i introduced in the redevelopment probability depend on the policy environment and the evaluation horizon h. We denote these policy-adjusted parameters by $\delta_i(h;\mathcal{P})$ and $g_i(h;\mathcal{P})$. Consistent with the literature on the effects of new supply on rents (Asquith et al., 2023; Li, 2022; Pennington, 2025; Rollet, 2025), we expect rents to respond negatively to *citywide* aggregate rises in housing stock (supply effect) and positively to *neighborhood-level* increases in market-rate units (amenity effect).

Negative supply-induced adjustments. Let $S(h;\mathcal{P})$ denote the expected citywide housing stock at horizon h under policy $\mathcal{P}$, and let $S(h;\mathcal{P}_0)$ denote the corresponding expectation under the status-quo. We measure the policy-induced change in expected total housing stock as the log difference:

$$\Delta S(h;\mathcal{P}) = \ln S(h;\mathcal{P}) - \ln S(h;\mathcal{P}_0).$$

We assume that rental growth responds to this aggregate supply shock with elasticity of rents with respect to housing supply $\zeta_S < 0$, so that larger citywide increases in housing supply reduce expected rent growth.

Positive amenity-induced adjustments. Let $N_i(h;\mathcal{P})$ denote the expected market-rate new housing supply in the neighborhood of parcel i under policy $\mathcal{P}$, and define the associated policy-induced change as the log difference

$$\Delta N_i(h;\mathcal{P}) = \ln N_i(h;\mathcal{P}) - \ln N_i(h;\mathcal{P}_0).$$

The elasticity ζ_A captures how an increase in neighborhood market-rate housing units affects rent growth through local amenity spillovers. We assume that $\zeta_A > 0$ to reflect that new nearby development enhances local amenities and spurs gentrification (Couture et al., 2024), although negative values remain possible when congestion or local opposition dominate.

Combining the aggregate supply and local amenity channels yields a common adjustment summarizing the effect of policy-induced construction on rent growth. For parcel i, define the annualized supply-induced adjustment

$$\Delta\delta_i(h;\mathcal{P}) = \frac{1}{h}\Big(\zeta_S \Delta S(h;\mathcal{P}) + \zeta_A \Delta N_i(h;\mathcal{P})\Big).$$

This term captures the effect of policy-driven supply changes on rent dynamics.[9]

[9]Under the risk neutral measure, the expected potential rent satisfies $\mathbf{E}_{\mathbb{Q}}[R_h] = Re^{\delta h}$. At horizon h under policy $\mathcal{P}$, an exogenous supply shock $\Delta S(h;\mathcal{P})$ scales expected rents by $e^{\zeta_S \Delta S(h;\mathcal{P})}$ and implies $Re^{(\delta+\Delta\delta)h} = Re^{\delta h + \zeta_S \Delta S(h;\mathcal{P})}$, which yields this drift adjustment.

Mapping supply adjustments into rents. We incorporate this supply adjustment into the two drift parameters governing rent dynamics. The *risk-neutral drift* governs valuation under the pricing measure $\mathbb{Q}$. For parcel i, the baseline pricing drift implied by the cap rate c_i is $\delta_i' \equiv r - c_i$. Rent growth, however, evolves under the physical measure $\mathbb{P}$. We denote the baseline physical rent growth rate by g_i', which reflects the expected rent growth consistent with the total return on real estate net of the cap rate absent policy-induced supply shocks.

For a given policy $\mathcal{P}$ and evaluation horizon h, the policy-adjusted parameters are

$$\delta_i(h;\mathcal{P}) = \delta_i' + \Delta\delta_i(h;\mathcal{P}), \qquad g_i(h;\mathcal{P}) = g_i' + \Delta\delta_i(h;\mathcal{P}).$$

Within each policy counterfactual, both parameters remain constant over time in the geometric Brownian motion dynamics. The dependence on h reflects the annualization of the horizon-specific supply adjustment rather than a time-varying drift process.

Fixed point and convergence. In equilibrium, policy-induced supply adjustments must be consistent with developers' redevelopment responses. The policy-induced changes in citywide and neighborhood supply determine the drift adjustment $\Delta\delta_i(h;\mathcal{P})$, which updates both the pricing drift $\delta_i(h;\mathcal{P})$ and the physical rent growth rate $g_i(h;\mathcal{P})$. These updated parameters affect redevelopment probabilities and densities and, therefore, expected supply. The resulting equilibrium corresponds to a fixed point in which supply adjustments and redevelopment responses are mutually consistent. Appendix A.6 describes the numerical procedure used to compute this fixed point.

1.4 Expected Rental Incomes

Using the completion probability from Proposition 3 and the optimal density F^*, we derive the expected parcel-level rental income at horizon h incorporating the redevelopment option and spatial adjustments. These adjustments account for the effects of citywide supply changes and neighborhood spillovers on expected rent levels.

Corollary 1 *For parcel i, the expected rental income at horizon h is*

$$\begin{aligned}\mathbf{E}_{\mathbb{P}}\{RentInc_{ih}\} = &\underbrace{\left[1 - \mathbf{P}_i^*(H_{R^{e*}} \le h;\mathcal{P})\right]}_{\textit{Prob no development}} \times \underbrace{\Gamma(F_{B,i}, z_{B,i}(h), \alpha_{B,i}) \times \mathbf{E}_{\mathbb{P}}\{R_{ih}\}}_{\textit{Rental income of existing property}} \\ &+ \quad \underbrace{\mathbf{P}_i^*(H_{R^{e*}} \le h;\mathcal{P})}_{\textit{Prob development}} \times \underbrace{\Gamma(F_i^*, 1, \alpha) \times \mathbf{E}_{\mathbb{P}}\{R_{ih}\}}_{\textit{Rental income of new property}}.\end{aligned} \tag{9}$$

where $\mathbf{P}_i^*$ and F_i^* are given in Equations (6) and (8), and $z_B(h)$ is the cumulative depreciation of the existing structure after additional h years. The spatially-adjusted physical expectation of rents is

$$\mathbf{E}_{\mathbb{P}}\{R_{ih}\} = R_i \, \exp(g_i(h;\mathcal{P})\, h), \tag{10}$$

Expression (10) reduces to $R_i e^{g_i' h}$ under the status quo.

The proof is in Appendix A.7.

Expression (9) shows that expected rental income is a weighted average of the income generated by the existing structure and the redeveloped property. Spatial effects enter through two channels. First, the drift adjustment $\Delta\delta_i(h;\mathcal{P})$ modifies the pricing drift $\delta_i(h;\mathcal{P})$ and therefore affects the redevelopment probability $\mathbf{P}_i^*(H_{R^{e*}} \leq h)$ and the optimal density F_i^*. The weights in (9) therefore incorporate spatial feedback induced by policy. Second, spatial supply responses also affect the level of expected rents through the physical growth rate $g_i(h;\mathcal{P})$ in (10). These adjustments apply even when redevelopment does not occur, so spatial feedback affects both new and existing structures.

2 Numerical Illustration of the Model

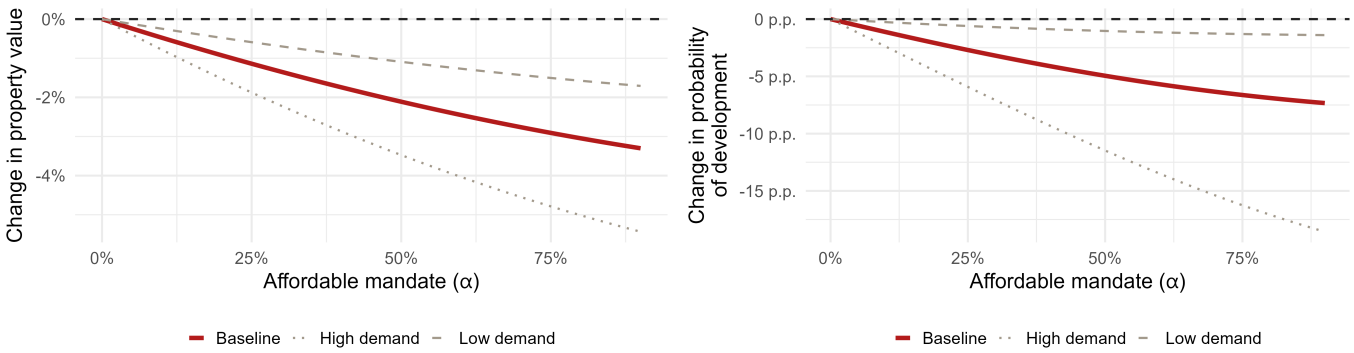
Before calibrating the model to the NYC housing market, we use numerical illustrations to clarify its economic mechanisms. We first examine how policy instruments shape developers' parcel-level redevelopment decisions. We then introduce a stylized simulated city to illustrate how an unexpected supply shock propagates spatially and alters redevelopment incentives through local spillovers and citywide supply responses.

2.1 Impact of Public Policies on Parcel-level Outcomes

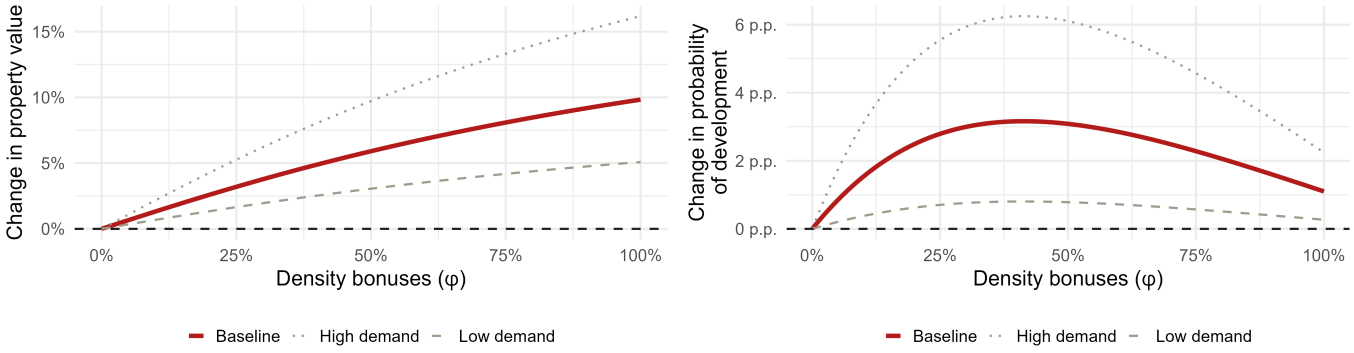
In this section, we show that the model captures the trade-off between *Carrots* (ϕ and τ) and *Sticks* (α) at the parcel level, both in terms of valuation and development probability. We provide additional comparative statics with respect to the remaining parameters as well as more extended discussions related to the effects of key parameters in Appendix B. In particular, we describe the role of parcel heterogeneity and emphasize the importance of modeling non-instantaneous construction durations relative to the existing literature.

For the analysis in this section, we consider a representative parcel near the redevelopment threshold and apply the parametrization and calibration described in Section 3. This calibration incorporates returns and costs to density, as well as an affordability mandate α that simultane-

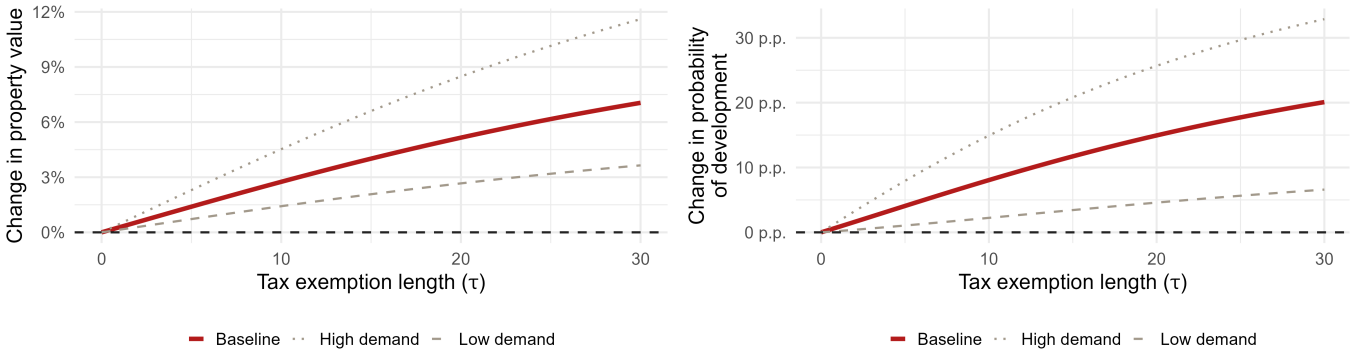
Figure I: Property Value and Development Probability with Respect to Policy Instruments



A. Mandatory share for affordable housing (α)



B. Density bonuses (ϕ)



C. Length of tax exemptions (τ)

Note: These figures show the effects of policy instruments on property value (left panels) and the probability of development within 10 years (right panels). These figures are obtained for a parcel of land built at 66% of its capacity with $F_B = 2$ and $\bar{F} = 3$, aged 150, with a rental return of 4%, a volatility of 15%, and an annual potential rent \$50. All other parameters and elasticities are reported in Table II.

ously reduces rental income and construction costs. We introduce spatial and building heterogeneity in the citywide analysis. Figure I illustrates the effect of each policy instrument on prop-

erty values (left panels) and on the probability of (re)development within 10 years (right panels). The figure also shows how these effects vary with initial demand, by shifting the rent potential R above or below the baseline.

Panel (a) of Figure I shows that raising the affordable share requirement (α) consistently lowers both property values and development probabilities. This decline in property value operates entirely through a reduction in the redevelopment option value, rather than from the value of the existing structure. Affordable housing mandates have a stronger impact in high-demand areas, where, for the same mandate, parcels with higher demand experience a greater decline in property values and a greater reduction in redevelopment probability. Effects are also stronger on parcels closer to the redevelopment threshold, confirming that mandates bind most strongly where redevelopment is most imminent.

Panel (b) of Figure I shows that increasing allowable density (ϕ) unambiguously raises property values. However, the probability of development can increase or decrease with ϕ, depending on the parcel characteristics and underlying housing demand.[10] Because developers retain the option to build at higher density, property value always rises. Yet, when ϕ becomes sufficiently large, developers may delay construction, waiting for market conditions that justify building at the higher density, continuing to collect rental incomes from the existing structure. This reduction in the probability of development with ϕ is more pronounced for parcels near the redevelopment threshold, as additional density offered just before redevelopment postpones redevelopment to justify construction. Panel (c) of Figure I shows that offering tax exemptions unambiguously increases property values and accelerates (re)development. The gain in property value comes entirely from the redevelopment option, since the exemption applies only to newly developed buildings. Unlike the density bonuses, the tax exemption's effect on construction probability is amplified on parcels close to redevelopment.

We then examine parcel-level trade-offs between *Carrots* and *Sticks*, focusing on how affordability mandates interact with zoning and fiscal incentives. Figure B2 shows that, for any level of affordable mandate, there exists a level of density bonuses or tax exemptions that holds property values constant, thus leaving developers indifferent between the status-quo and the combination of instruments (left panels). Other trade-offs hold redevelopment incentives constant (right panels), but the two indifference curves do not coincide. This divergence illustrates the difficulty of aligning public and private objectives when policies simultaneously affect project income and costs. Although zoning in NYC is primarily as-of-right (i.e., development allowed without

[10] In this simple single-parcel analysis, additional supply does not affect market rents, unlike in the citywide model that includes spatial spillovers and citywide supply effects. In other words, the stochastic potential rent R_t is assumed to remain unaffected by the policy ϕ.

discretionary review), these parcel-level results illustrate how the model extends naturally to discretionary zoning environments common in other cities.

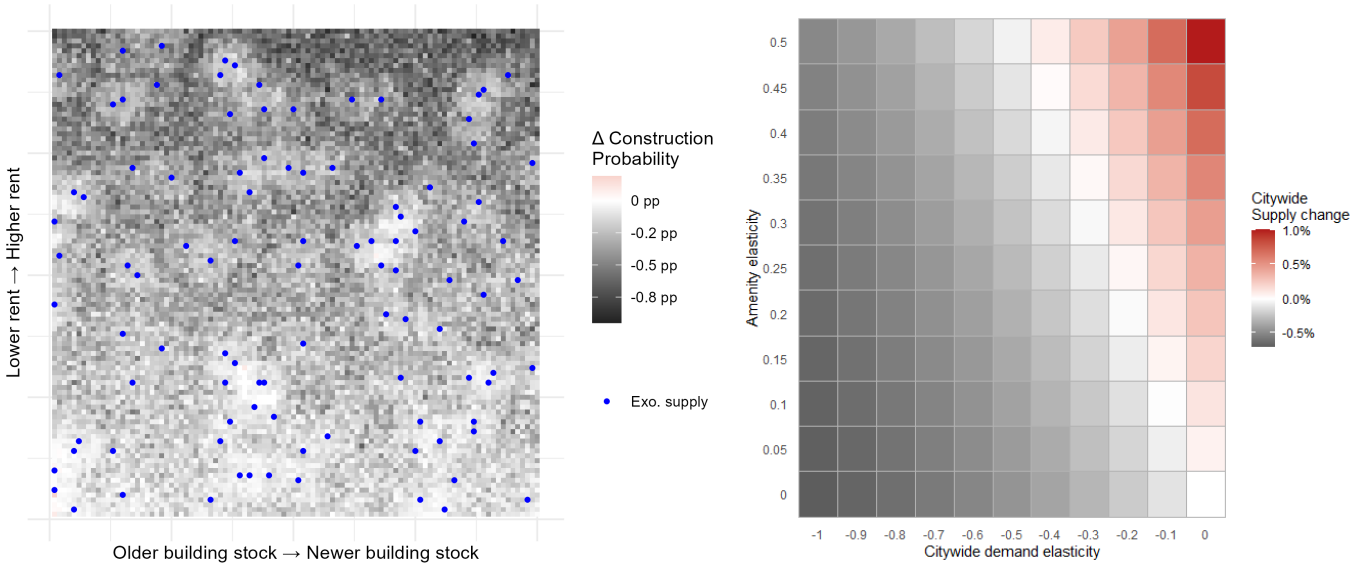
2.2 Spatial Responses to an Exogenous Supply Shock

We illustrate how an exogenous supply increase on a subset of parcels propagates spatially via the local and citywide channels described in Section 1.3. This exercise clarifies how the spatial feedback mechanism reallocates redevelopment incentives across locations in a controlled environment, prior to calibrating the model to NYC. Specifically, we conduct an experiment in which 1% of parcels are forced to redevelop, generating an exogenous increase in housing supply equivalent to 0.92% of the current housing stock. We then examine how this intervention affects construction probabilities on all other parcels as developers endogenously update redevelopment decisions in response to both aggregate and localized supply effects. The experiment is implemented in a stylized city where potential rents R_i increase from South to North, while the building stock becomes progressively older (more obsolete) from West to East.

Panel A of Figure II maps the resulting change in construction probabilities for our preferred elasticity specification ($\zeta_S = -0.50$ and $\zeta_A = 0.10$). Construction probabilities decline overall as the increase in aggregate supply reduces expected rents and weakens redevelopment incentives across parcels. This negative effect is most pronounced for parcels with initially strong demand (high R_i) and for newer buildings, as those are further away from their redevelopment threshold . However, we also observe localized increases in construction probability near exogenously redeveloped parcels, reflecting local amenity spillovers that raise the expected rent growth rate, g_i', and thereby increase the value of redevelopment options. These localized effects are strongest when multiple nearby parcels are forced to redevelop, creating concentrated clusters of elevated redevelopment activity.

The magnitude of these responses remains limited in the aggregate. In an already built-up city, redevelopment is costly due to demolition expenses and lengthy construction timelines. Panel B of Figure II examines how the aggregate supply response varies with the demand elasticity, ζ_S, and the strength of local amenity spillovers, ζ_A. For empirically plausible values of ζ_S, the resulting change in aggregate supply remains modest (less than 1% decrease), even though redevelopment incentives are reallocated spatially. Stronger amenity effects amplify local construction incentives but do not offset the dominant role of aggregate inverse demand elasticity, except under unrealistically large spillover effects that are inconsistent with the empirical literature (Asquith et al., 2023; Li, 2022; Mense, 2025). Although local spillovers meaningfully increase redevelopment incentives near exogenously redeveloped parcels, their aggregate effects on con-

Figure II: Exogenous Supply Change and Other Parcel Responses



A. Parcel-level change in $\mathbf{P}_i^*$

B. Total expected supply change

Note: These figures illustrate the spatial propagation of an exogenous housing supply shock in a stylized city. In the policy experiment, 1% of parcels (shown as blue dots in Panel A) are forced to redevelop ($Prob_i = 1$) at a density 100% higher than the current limit, generating an exogenous increase in housing supply equivalent to 0.92% of the current supply. Potential rents R_i are drawn such that they increase from South to North, and building age becomes older (more obsolete) from West to East. All other parameters are similar across parcels ($F_B = 3$, $\bar{F} = 6$, cap rate = 4%, total return = 8%, $\sigma = 15\%$, and $\alpha_B = 0$). All other elasticities and parameters correspond to the baseline values reported in Table II. Panel B shows the corresponding aggregate change in total housing supply (excluding the exogenously redeveloped parcels) as a function of the citywide inverse demand elasticity ζ_S, and the local amenity elasticity ζ_A.

struction and rents remain moderate for empirically relevant elasticities.

3 Model Quantification

We calibrate the model to NYC's housing market, focusing on affordable-housing mandate policies, which serve as our central case study. The calibration proceeds in three steps. First, we construct the parcel-level dataset, with sources and summary statistics shown in Table I. Second, we specify the functional forms of the key functions, $\Gamma(\cdot)$, $\gamma(\cdot)$, and $\kappa(\cdot)$, that govern the instantaneous return and costs to development. The elasticities and parameters of the model, summarized in Table II, are either estimated from microdata, drawn from the literature, or calibrated to match selected key moments of the model.

Table I: Summary Statistics of Lot-level Data

Statistic	Source	Mean	St. Dev.	Min	Median	Max
Current FAR – $F_{B,i}$	PLUTO	1.05	1.18	0.00	0.73	88.55
Maximum FAR – $\bar{F}_i$	PLUTO	1.44	1.43	0.50	0.90	88.55
Lot size (th. sqft) – L_i	PLUTO	3.75	6.50	1.25	2.50	250.00
Age (years)	PLUTO	72.92	36.63	0	84	302
Depreciation rate (%) – $z_{B,i}$	Estimated	68.98	7.08	58.69	66.08	100.00
Share of aff. units (%) – $\alpha_{B,i}$	DHCR & HPD	0.25	2.98	0	0	50
Annual Rent per sqft ($)	ACS + PLUTO	24.06	7.99	2.48	23.11	99.24
Annual Potential Rent per sqft ($) – R_i	Estimated	35.46	11.08	3.41	34.62	127.05
Expected growth (%) – g_i	Costar	2.25	0.45	1.34	2.32	4.10
Caprate (%) – $r - \delta_i$	Costar	5.34	0.34	4.22	5.21	6.17
Volatility (%) – σ_i	Estimated	8.21	0.39	7.46	8.26	11.08

Notes: *This table presents summary statistics for the 765,830 parcels included in the baseline analysis. The majority of parcel-level data is sourced from the Primary Land Use Tax Lot Output (PLUTO). Age measures the number of years since the last recorded renovation or construction. Obsolescence captures the rental discount associated with property aging, with 1 representing newly constructed building. Annual rent per square foot is derived from the 2023 ACS 5-Year data at the census block-group or tract level. Potential rent reflects market-rate rents for one non-depreciated square foot at FAR=1, obtained by adjusting observed rent for the typical building within each geography. Cap rates, rental returns, and volatility are sourced from CoStar, following their definitions for New York City residential markets, as detailed in Appendix C.*

3.1 Parcel-level Data

Each parcel i is characterized by its current density $F_{B,i}$, maximum allowable density $\bar{F}_i$, rental income depreciation $z_{B,i}$, share of current affordable units $\alpha_{B,i}$, and location. Location, in turn, determines the potential rent per square foot R_i, as well as the expected return and volatility of rental income. We restrict the sample to parcels zoned or partially zoned for residential use, excluding parcels designated exclusively for public or other non-residential purposes. Appendix C details the data cleaning process, which yields a final sample of 765,830 parcels, and shows additional summary statistics, including maps of key parcel-level data.

Built and maximum allowed density ($F_{B,i}$ and $\bar{F}_i$). We calibrate $F_{B,i}$ and $\bar{F}_i$ using the built Floor-Area-Ratio (FAR) and the maximum allowable FAR from the Primary Land Use Tax Lot Output (PLUTO) dataset. We also record lot size L_i in square feet, which implies that a building contains $s_i = F_{B,i}L_i$ square feet of residential space. Parcel size scales rents and construction costs through the functions $\gamma()$, $\kappa()$, and $\Gamma()$, but does not affect developers' optimal decision rules at the parcel level because the expansion threshold is homogeneous of degree zero with respect to lot size. In the baseline calibration, the average built density $F_{B,i}$ is 1.05, the average building size is approximately 5,000 square feet, and the average maximum allowable density $\bar{F}_i$ is 1.44. 36.8% of parcels are built to the maximum allowable density. As shown in Figure D1, the unused capacity

is, however, spatially heterogeneous, with greater potential for increased density particularly in the Southern Bronx.

Rental depreciation ($z_{B,i}$). To account for rental depreciation, we assume that the current asset yields lower rental income as the structure ages. Specifically, we use the functional form $z_i = \text{Age}_i^{\epsilon_z}$, where Age_i measures the number of years since the last recorded renovation or construction, and $\epsilon_z < 0$ denotes the age elasticity of rental income. This form implies steeper depreciation at early ages, consistent with (Lopez and Yoshida, 2022). To estimate ϵ_z, we follow Rosenthal (2014) and regress transaction prices on building age in a hedonic pricing framework, as detailed in Appendix C.2. Estimated elasticities range from -0.096 to -0.089, implying an average annual decline of approximately 2% over the first 10 years, with slower depreciation thereafter. We calibrate ϵ_z to -0.093 in the baseline calibration, which yields a mean $z_{B,i}$ of 0.69 and a standard deviation of 0.07.

Current share of affordable units ($\alpha_{B,i}$). Because there is no comprehensive building-level dataset that reports the share of affordable units, we combine multiple administrative data sources to approximate $\alpha_{B,i}$. First, we use publications from the New York State Division of Housing and Community Renewal (DHCR) to identify buildings that received a 421-a or J-51 tax exemptions, two popular programs that offer property tax exemptions to buildings in exchange for affordable units. We identify 4,611 parcels with a 421-a exemption and 1,486 parcels with a J-51 exemption, and assign a value of $\alpha_{B,i} = 30\%$ for 421-a properties and $\alpha_{B,i} = 50\%$ for J-51 properties, consistent with the stronger affordability mandate of the latter. Second, we add buildings recorded by the Department of Housing Preservation & Development as participating in MIH or VIH programs, which require the provision of affordable units.[11] In total, we observe 104 MIH/VIH buildings and assign a value of $\alpha_{B,i} = 30\%$ to those parcels.

Potential rent per square foot (R_i). We estimate R_i primarily using block-group–level median rents from the 2023 American Community Survey (ACS) 5-year data (see Appendix C.3 for details). We first convert reported rents to a per–square-foot measure by normalizing ACS rents by the median residential unit size ($UnitSize_i$), computed using PLUTO. In our sample, the average annual rent per square foot is \$24.06. Because R_i represents the potential rent of *market-rate*, non-depreciated square footage at FAR $= 1$, we adjust observed rent per square foot in geography j to net-out the effects of depreciation, built density, and existing affordability requirements.[12]

[11] VIH allows FAR bonuses to be transferred to parcels other than those hosting affordable units. We assign a positive $\alpha_{B,i}$ only to the "generating" sites.

[12] For instance, low observed rent per square foot in a block-group may reflect low potential rent R_i or a high prevalence of obsolete structures.

Specifically, we define

$$R_{i(j)} = \frac{\text{Rent}_{i(j)}}{\Gamma\Big(\tilde{F}_{B,i(j)},\, \tilde{z}_{B,i(j)},\, \tilde{\alpha}_{B,i(j)}\Big)},$$

where $R_{i(j)}$ denotes the potential rent assigned to the geography j where parcel i is located, $\tilde{F}_{B,i(j)}$, $\tilde{z}_{B,i(j)}$, and $\tilde{\alpha}_{B,i(j)}$ are the weighted median built density, rental depreciation, and affordable unit share across parcels in geography j, respectively. Weighting by built square footage $F_{B,i} \times L_i$ ensures that the representative building characteristics reflect the stock of space actually inhabited by renters, consistent with the ACS rent measure. After this adjustment, the average annual potential rent in the sample is \$35.46 per square foot.

Rental return and volatility (δ_i, g_i and σ_i). We calibrate the baseline pricing drift δ_i' using observed capitalization rates $caprate_i$ (rent-to-price ratio), setting $\delta_i' = r - caprate_i$. This interpretation treats δ_i' as a reduced-form, risk-neutral measure of expected rental growth that incorporates both fundamentals and the required risk premium. We obtain capitalization rates from CoStar market data and assign them to each parcel after having manually geocoded the 37 CoStar-defined New York submarkets. We describe the procedure and show summary statistics in Appendix C.4. We also calibrate the physical rent growth rate g_i' using Costar data, defining g_i' as the difference between the expected total return on real estate and the cap rate, $g_i' = \text{Total Return}_i - caprate_i$. This decomposition follows from the standard identity that total return equals income yield plus capital appreciation. The resulting average implied rent growth rate across submarkets is 2.25%, and incorporates developers' expectations about future rental growth under the status-quo policy. To compute σ_i, we use asset and rental returns for multifamily properties over the past 20 years in each CoStar submarket, and take the standard deviations of these return series, which we denote by σ_i. Across the 37 submarkets, the average annual unlevered volatility is 8.21%.

3.2 Parametrization

3.2.1 The rental income scaling function

In our model, the underlying rent per square foot R is scaled by the function $\Gamma(\cdot)$, which maps parcel characteristics into annual rental income. We parametrize this scaling function as

$$\Gamma(F, z, \alpha, L) = LF^{(1+\epsilon_F)}z(1 - \alpha\epsilon_\alpha), \tag{11}$$

where L is the size of the parcel, F is the FAR, $z \in (0, 1)$ is the discount associated with depreciation, and α is the share of affordable units in the building.[13] The parameter $\epsilon_F > 0$ denotes the height elasticity of rents, while $\epsilon_\alpha > 0$ captures the rental discount associated with non-market-unit. We calibrate ϵ_F at 0.07 using estimates from the skyscraper literature (Ahlfeldt and Barr, 2022; Ahlfeldt et al., 2026; Danton and Himbert, 2018). The positive ϵ_F reflects the capitalization of height advantages, including better views and reduced street-level noise, into market rents.

The rental discount associated with affordable housing ϵ_α could, in principle, be a policy parameter in $\mathcal{P}$. To limit the scope of the counterfactual space, we focus on mandates that vary only the share of affordable units α, while fixing the rental discount ϵ_α, guided by estimates from Favilukis et al. (2023). Specifically, they find that rent-stabilized units in NYC rent at an average 26.6% discount relative to market-rate units, while rent-controlled units rent at an average discount of 77.7%. To span this empirical range, we consider values of $\epsilon_\alpha \in \{0.25, 0.50, 0.75\}$. Our main counterfactuals use a 25% discount, while Section 5 examines how results vary as the implied rental discount increases, with particular attention to developer's voluntary adoption of policy $\mathcal{P}$.

3.2.2 The demolition cost function

We parametrize demolition costs as

$$\gamma(F, L) = k_d L F^{\eta_D}, \tag{12}$$

where η_D governs how demolition costs scale with existing built density and k_d is a cost shifter. To calibrate these parameters, we use information obtained from interviews with developers. They reported that the fixed cost components –invariant to structure size– typically represent 50–60% of total demolition expenses. We therefore calibrate η_D such that the average ratio of the cost of demolishing a building with a FAR of 0.1 to the cost of demolishing the entire structure equals 55%. The resulting estimate, $\eta_D = 0.296$, implies substantial returns to scale in demolition. Developers we interviewed also reported that demolition costs typically account for 13–20% of total redevelopment costs when an existing structure is removed. This statistic pins down the relationship between k_d and the construction cost parameter k_c, which is jointly determined as discussed in Section 3.2.4.

[13] The theoretical model abstracts from the size of the parcel because the optimal decision rule is unaffected by it. Because it influences aggregate outcomes, such as total housing production, we explicitly consider parcel size in the calibration.

Table II: Baseline Model Elasticities and Parameters

Parameters	Description	Value	Methods & main sources
	The Rental Scaling function		
ε_F	Density elasticity of rent	0.07	Calibration – Literature
ε_z	Age elasticity of rent	-0.093	Estimation – Table C2
ε_α	Affordable units rental discount	$\{\mathbf{0.25}; 0.50; 0.75\}$	Calibration – Literature
	The demolition cost function		
η_D	Demolition cost elasticity of density	0.296	Target: Fixed cost demolition (55%)
k_d	Baseline demolition cost per density unit	73.91	Target: Share of development cost (15%)
	The construction cost function		
η_F	Density elasticity of construction cost	0.60	Calibration – Literature
η_α	Affordable housing construction cost discount	0.20	Estimation - RCLO report
k_c	Baseline construction cost per density unit	436.37	Target: Land-value ratio (23.68%)
	Spatial supply spillovers		
ζ_S	Global Supply elasticity of rent	-0.50	Calibration – Literature
ζ_A	Local Supply elasticity of rent	0.10	Calibration – Literature
	Distance for local supply spillovers	500 feet	Calibration – Literature
	Others		
ψ	Real estate tax rate (% of rental income)	20.15	Estimation - DoF & Costar
d	Construction periods (years)	3.08	Estimation – DCP
r	Risk free rate (%)	1.90	Estimation – FED

3.2.3 The construction cost function

We parametrize annual construction costs as

$$\kappa(F, \alpha, d, L) = \frac{1}{d} k_c L F^{(1+\eta_F)} (1 - \alpha\eta_\alpha), \tag{13}$$

where k_c is the baseline cost of constructing per square foot, $\eta_F > 0$ is the height elasticity of construction cost, and η_α captures the cost adjustment associated with space allocated to the public good α. We set $\eta_F = 0.60$ to reflect the convex relation between height and construction costs. This value is consistent with existing estimates: Ahlfeldt and McMillen (2018) report an elasticity of 0.61 for residential buildings above five floors, Ahlfeldt et al. (2026) calibrate an elasticity at 0.55, and Ahlfeldt and Barr (2022) estimate 0.56 for tall residential buildings.

The second elasticity, η_α, reflects systematic differences in per–square-foot construction expenditures between market-rate and non-market units. To calibrate η_α, we use data from the National Apartment Association's Income and Expenses Report, cited in the RCLO report on The Affordable Housing Asset Class. This report documents capital expenditures per square foot for market-rate and subsidized units from 2012 to 2021. On average, subsidized units receive 19.9%

lower capital expenditure per square foot than market-rate units. Although capital expenditures are not identical to construction costs, we treat this differential as a reasonable proxy for calibration purposes and set $\eta_\alpha = 0.20$.

3.2.4 Baseline construction and demolition costs

The model's monetary level is governed by three parameters: the market rent of a non-depreciated square foot, R_i, the demolition cost, k_d, and the construction cost, k_c, all expressed per square foot in our calibration. Because the probability of development and property value are homogeneous of degree zero and one, respectively, in R, k_d, and k_c, only their relative magnitudes matter for computing development probabilities, and thus counterfactual analyses. Given R_i, we therefore calibrate k_d and k_c by targeting empirical moments of the model. We treat these parameters as constant across neighborhoods, since labor, material, and regulatory costs are broadly similar within the city (Glaeser and Gyourko, 2018).

To identify k_c, we use PLUTO data on the ratio of land to property values. For each parcel, we compute the model-implied land-value ratio as $LandRatio_i = \pi_i(F_{B,i} = 0; \Theta)/\pi_i(F_{B,i} = F_{B,i}; \Theta)$, that is, the ratio of the parcel's value absent any structure to its value at the observed density. This approach interprets land value as the option value of redevelopment when the existing structure is removed. Intuitively, a lower construction cost k_c increases redevelopment incentives, raising land values relative to current property values, thereby increasing the land-value ratio. We can therefore identify k_c by matching the average model-implied $LandRatio_i$ to the observed value of 23.7%.

To identify k_d, we use evidence that demolition costs account for 13–20% of total development costs when an existing structure is removed. We target this statistic by imposing

$$\frac{1}{n_B} \sum_{i:F_{B,i}>0} \frac{\gamma(F_{B,i}, L_i)}{d \cdot \kappa_i(F_i^*, \alpha_i, d, L_i) + \gamma(F_{B,i}, L_i)} = 0.15$$

in the model, where $n_B \equiv \#\{i : F_{B,i} > 0\}$. This matching pins down k_d, the baseline demolition cost parameter, because higher demolition costs k_d increase the share of total redevelopment costs attributable to demolition. Matching this target jointly with the land-value ratio target yields calibrated values of $k_c = 436.37$ and $k_d = 73.91$. For reference, the mean value of R_i in the model is \$35.46, implying that the cost of constructing one unit of density is about twelve times the annual rental income.

3.3 Calibration of Other Parameters

Amenity and demand elasticities (ζ_S and ζ_A). As described in Section 1.3, policy-induced construction affects rents and development probabilities of other parcels through two channels: a negative citywide supply effect, captured by the inverse demand elasticity $\zeta_S < 0$, and a local amenity effect, captured by $\zeta_A > 0$. Existing reduced-form estimates do not separately identify these two components. However, recent evidence provides guidance on their combined net effect at relevant spatial scales. In NYC, Li (2022) estimates that an unanticipated increase in nearby housing supply reduces local rents with an elasticity of approximately -0.10 within a 500-foot radius, while Rollet (2025) finds a larger elasticity of -0.42 at a similar spatial scale. Together with evidence from Mense (2025), Asquith et al. (2023), and Pennington (2025), these findings suggest that, although local amenity gains may partially offset supply effects, the net impact of new construction on local rents is negative on average. In other words, the total effect of adding new housing units reduces rents in the surrounding area, after accounting for all offsetting forces.

Guided by this empirical evidence, we impose that the combined elasticity satisfies $\zeta_S + \zeta_A = -0.40$ and define the neighbors of parcel i as all parcels that fall within 500 feet of the centroid of parcel i. To account for endogenous amenities (Almagro and Domínguez-Iino, 2025; Diamond, 2016) that may increase redevelopment incentives for nearby parcels as described by Pennington (2025), we assume a baseline value of $\zeta_A = 0.10$. Given the lack of separate empirical identification of ζ_S and ζ_A, we assess robustness by considering alternative decompositions of the combined elasticity in the counterfactual analysis.

Construction length (d) We calibrate the construction period using data from the DCP Housing Database Project-Level Files, defining duration as the interval between permit issuance and building completion. This interval corresponds to the period during which developers incur construction costs but receive no rental incomes. The sample is restricted to multi-family buildings developed by private for-profit firms, excluding outliers completed in less than three months or more than ten years. Our baseline calibration sets $d = 3.08$ years, the average time between permit issuance and completion.

Risk-free rate (r) We calibrate r using the average one-year yield on U.S. Treasury securities reported by the Board of Governors of the Federal Reserve System (FRED), used as the discount rate in the risk-neutral valuation. Over the period from January 2000 to December 2023, the average yield is 1.90%, which we use as the model's risk-free rate.

Property tax rate (ψ) We compute the effective property tax rate on residential properties by combining multiple datasets. First, we link assessment data for multi-family properties from PLUTO with statutory tax rates (NYC Department of Finance) to construct parcel-level tax liabilities since 2000. These tax liabilities are then merged with 36,000 transactions of multi-family properties from CoStar, and effective asset-based tax rates are obtained by dividing tax bills by corresponding sale prices. Since 2000, the median effective tax rate has been 1.1%, with an interquartile range of 0.57–1.83%. Because the model requires a tax rate on rental flows, we map this asset-based rate into an income-based rate by dividing by the sample's average cap rate of 5.34%, translating observed property tax liabilities into the flow-based tax wedge relevant for development incentives in the model.

4 Baseline Model Outcomes and Validation

Using the calibrated parameterization from the previous section, we compute key outcomes under the baseline scenario $\mathcal{P}_0 = [\alpha = 0, \phi = 0, \tau = 0]$, which provides the reference point against which all counterfactuals are evaluated. The baseline outcomes at the parcel-level are:

1. $\mathbf{P}_i(\mathcal{P}_0; \Theta|t)$, the probability that parcel i is redeveloped within a t-year horizon;
2. $\pi_i(\mathcal{P}_0; \Theta)$, the parcel value including both current use and redevelopment option value;
3. $F_i^*(\mathcal{P}_0; \Theta)$, the optimal redevelopment density;
4. $\mathbf{E}[R_{it}|\mathcal{P}_0; \Theta]$, the expected potential rent per square foot.

From these parcel-level outcomes, we compute the expected number of housing units and expected rental income on each parcel. We present aggregate outcomes by summing parcel-level results across all parcels. Although our model describes outcomes in square footage, we ease discussion and interpretation by presenting all quantitative results in number of housing units, obtained by dividing square footage outcomes by the typical unit size within each census tract. We correspondingly present all rent results in dollars per month and per housing unit. In Appendix D, we detail how we aggregate the outcomes and provide additional baseline results.

4.1 Baseline Results

Baseline citywide outcomes: The first row of Table III reports the citywide aggregates under the baseline scenario. The model implies construction of 168,395 housing units over ten years, consistent with NYC's historical production of 10,000–28,000 units annually since 2010 (NYC housing production). After accounting for demolitions, net new construction is 125,685 units. Panel A of Figure D1 illustrates the spatial distribution of new housing, concentrated in Brooklyn and

Table III: Baseline Calibration Outcomes and Robustness to Parameter Changes

	$E[Units]$ # of Apt.	$E[unitsNet]$ # of Apt	$E[Rent]$ $ per month	$E[Density]$ Sqft per acre	PV(taxes) ($billion)	PV ($billion)	Option Value (%)
	(1)	(2)	(3)	(4)	(5)	(6)	(7)
Baseline	168,395	125,685	2,682	56,877	407.78	1,574.13	0.81
			Varying key underlying model's elasticities				
Shorter duration time ($d = d/2$)	275,227	181,601	2,727	57,647	414.81	1,578.91	1.11
Higher cost to height ($\eta_F = 2\eta_F$)	192,387	135,036	2,673	57,210	410.34	1,581.01	1.24
Higher return to height ($\epsilon_F = 2\epsilon_F$)	196,595	143,401	2,903	57,070	443.12	1,703.79	0.79
Higher depreciation ($\epsilon_z = 2\epsilon_z$)	321,393	177,542	2,010	57,586	304.73	1,127.91	1.55
			Other model benchmarks				
No development ($k_c = \infty$)	0	0	2,612	55,126	393.97	1,561.34	0
No endogenous density choice ($F_i^* = \bar{F}_i$)	171,581	130,594	2,689	56,948	406.43	1,569.88	0.54
No maximum allowable density ($\bar{F}_i = \infty$)	417,328	321,509	2,797	59,610	417.78	1,529.06	1.67

Notes: *This table reports the aggregate outcomes of our baseline calibration and additional sensitivity analyses performed by varying underlying model parameter. Column (1) shows the expected number of housing units constructed (or under construction) over a 10-year horizon, Column (2) shows expected net unit addition, Column (3) shows expected monthly rent, Column (4) shows expected residential density at the 10-year horizon, Columns (5) and (6) show the present value of the property tax revenues and parcel values, and Column (7) shows the average value of the redevelopment option. The first row reports results under the baseline calibration described in Table II, and subsequent rows report the same outcomes under alternative parameter assumptions, varied one at a time as described in the text.. The "No development" scenario imposes an infinite cost of redevelopment. Except for the last specification (No maximum allowable density), the rent drift is is held fixed at its baseline value in these exercises and does not adjust with excess supply.*

Queens along the East River and in Staten Island. Citywide rent rises from $2,107 to $2,682 per unit per month at the 10-year horizon. This increase reflects three components: (1) additional discount from another decade of depreciation on non-redeveloped properties, (2) replacement effects $\Gamma(\cdot)$, whereby older depreciated units are substituted with newer construction that commands higher rents, and (3) the positive rental growth captured by the g_i'.[14]

Density, asset valuation, and option value. At the 10-year horizon, average residential density rises from 55,125 to 56,877 built square footage per acre. As expected, density declines with distance from central Manhattan, consistent with the classical urban model. The model implies a total residential asset value of NYC's residential assets at $1.57 trillion, comparable to the $1.83 trillion Department of Finance's reported valuation (Tax Lot Assessment Portal) despite our focus on residential parcels. The redevelopment option accounts for 0.81% of total residential asset value, indicating that most parcel value derives from the existing structure.

Parcel-level heterogeneity. Figure D2 reports the average development probability by (i) current built space (Panel A) and (ii) potential rent (Panel B).[15] In Panel A, the probability of redevelopment rises with building age (as depreciation reduces the value of existing cash flows) and with unused capacity (the gap between maximum and built FAR). By contrast, higher existing density raises the opportunity cost of redevelopment, which delays investment. Panel B shows that parcels with higher potential rents (R_i) have higher redevelopment probabilities.

4.2 Robustness to underlying parameters

In the remaining panels of Table III, we assess the sensitivity of aggregate outcomes to alternative elasticity assumptions, highlighting how the model captures the trade-off between development costs and returns. In these scenarios, we do not endogenize developers' expectations about future supply and thus do not update rental growth due to excess supply. The objective of this exercise is to illustrate how baseline outcomes vary with underlying parameters, not to evaluate a counterfactual in which a given parameter shifts exogenously.

Sensitivity to elasticity assumptions. Shorter construction durations increase expected apartment production, density, and property values by raising the value of the redevelopment option. Higher height elasticity of construction costs also increases new development, despite the higher

[14] In the baseline scenario, δ_i' and g_i' do not vary with future expected supply, $\Delta S(\mathcal{P}_0|t)$, because the calibrated cap rate already incorporates developers' expectations under the status quo.

[15] Table D1 reports conditional partial correlations between parcel characteristics and model outputs, showing that built space is a key determinant of both the probability and intensity of redevelopment.

costs of building taller structures. This reflects an adjustment in margins: developers build earlier but at lower density, with the timing effect dominating the reduction in scale in determining total expected supply. These results underscore the central role of construction technology in shaping urban outcomes (Ahlfeldt et al., 2026). Higher returns to height and faster rental depreciation both stimulate redevelopment, but through distinct mechanisms. Greater returns to height increase the payoff from new projects, while faster depreciation erodes the value of existing assets, raising the relative attractiveness of redevelopment. Together, these comparative statics illustrate how technological parameters and asset aging jointly shape baseline supply and valuation outcomes.

Alternative models. The final panel of Table III reports baseline outcomes under alternative model assumptions. The first row shows that without construction, rent per month is 2.61% lower than in the baseline scenario, highlighting how new construction tends to increase rents by replacing older, low-rise buildings with newer, taller ones. The second row indicates that when developers are required to build at the maximum allowable density, aggregate outcomes remain largely unchanged, although the sum of present values declines, reflecting the role of optimizing F^*. This result reflects the fact that in NYC zoning regulations are often binding (Brueckner et al., 2024), so developers tend to build up to the regulatory limit. In contrast, when density is unconstrained, construction activity increased by a factor of 2.5. Under this benchmark, which includes a supply effect ($\zeta_S + \zeta_A < 0$) to avoid unrealistic infinite construction, average rents rise to \$2,797, indicating that the supply response is still insufficient to offset the replacement effect observed in the baseline.

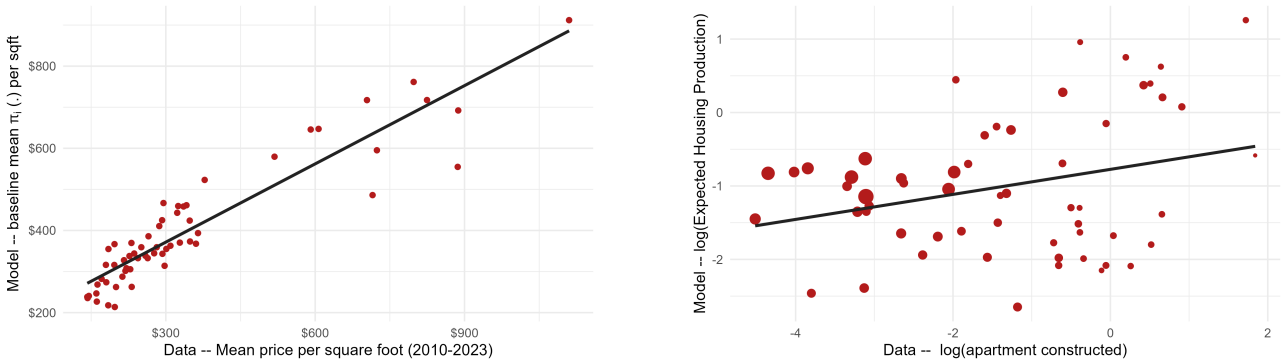
4.3 Model Validation

Does the model predict real estate values? We validate the model by comparing its present value predictions to observed property transaction prices. For each community district j, we compute the average model-implied value per housing unit as

$$\frac{1}{n_j} \sum_{i \in j} \frac{\pi_i(\mathcal{P}_0; \Theta)}{F_{B,i} L_i / \text{UnitSize}_i},$$

where UnitSize_i denotes the median apartment size in the block group of property i. This adjustment accounts explicitly for heterogeneity in unit sizes when constructing district-level averages. Panel A of Figure III compares model-implied values to average price per unit observed in multifamily transactions from CoStar over the 2010–2023 period. The correlation between the two series is 0.93, indicating that the calibration reflects cross-neighborhood variation in real estate market valuations. This fit is particularly important because developers' decision rules depend directly

Figure III: Model Validation



A. Real estate value

B. Construction activity

Note: Panel A shows the relation between the log mean price per housing unit of Multi-Family buildings, using transaction from CoStar since 2010, and the log of the model-implied mean price per unit in each community district. Panel B plots the log number of housing units constructed in each community district between 2013 and 2022, scaled by the number of parcels, against the corresponding model-implied construction outcomes based on the 2013 calibration.

on relative differences in present values across policy environments.

Does the model predict real estate construction activity? To confirm that our model predicts outcomes beyond prices, we compare its predictions to observed construction patterns. We collect data on the number of housing units constructed in each community district between 2013 and 2022 from NYC Planning and recalibrate parcel-level characteristics to their 2013 values, following the same methodology described in Section 3. As in the baseline analysis, we compute the model-implied number of housing units constructed in each community district j as

$$\sum_{i \in j} \mathbf{E}\left[\mathbf{P}_i(\mathcal{P}_0, \Theta \mid t = 10)\, \frac{F_i^*(\mathcal{P}_0, \Theta)\, L_i}{\text{UnitSize}_i}\right],$$

expressed in housing units. Panel B of Figure III compares model-implied construction to observed construction, with both measures scaled by community-district acreage to account for differences in district size. The figure shows that the model tracks the cross-sectional distribution of observed construction across neighborhoods well.

5 Policy Counterfactuals

We examine how policy interventions affect redevelopment decisions and, through them, housing production, rents, and affordability outcomes. Policy interventions modify the regulatory framework at $t = 0$, shifting from the baseline environment $\mathcal{P}_0$ to $\mathcal{P} = [\alpha \geq 0, \phi \geq 0, \tau \geq$

0], thereby changing developers' redevelopment incentives and expectations about future rental growth. Deviations from baseline outcomes are denoted by Δ. For example, the aggregate change in expected net housing units under $\mathcal{P}$ is

$$\Delta \mathbf{E}[AptNet|\mathcal{P}, t = 10] \quad = \quad \mathbf{E}[AptNet|\mathcal{P}, t = 10] - \mathbf{E}[AptNet|\mathcal{P}_0, t = 10]$$

We report monetary outcomes as percentage deviations from the baseline to facilitate comparisons across policy instruments and policy bundles.

Although the model admits arbitrary combinations of policy instruments, we focus on six environments that span commonly used regulatory approaches: (1) upzoning, which raises allowable density by 50%; (2) a 20-year property tax exemption; (3) an affordability mandate requiring 30% of units to be affordable; (4) incentive zoning, which combines affordability mandates with density bonuses; (5) fiscal incentive zoning, which pair mandates with tax exemptions; and (6) a fully combined policy that stacks all three instruments.

We present the counterfactual results in three blocks, corresponding to how policy affects redevelopment outcomes and their implications for production, rents, and affordability. First, we examine how different policies affect housing production, distinguishing between market-rate and affordable units. Second, we analyze the effects of each policy on expected rents, decomposing the relative contributions of the model's main channels. Finally, in the subsequent section, we document the policy tradeoffs governments face when attempting to expand affordability, with particular emphasis on fiscal and negative land capitalization.

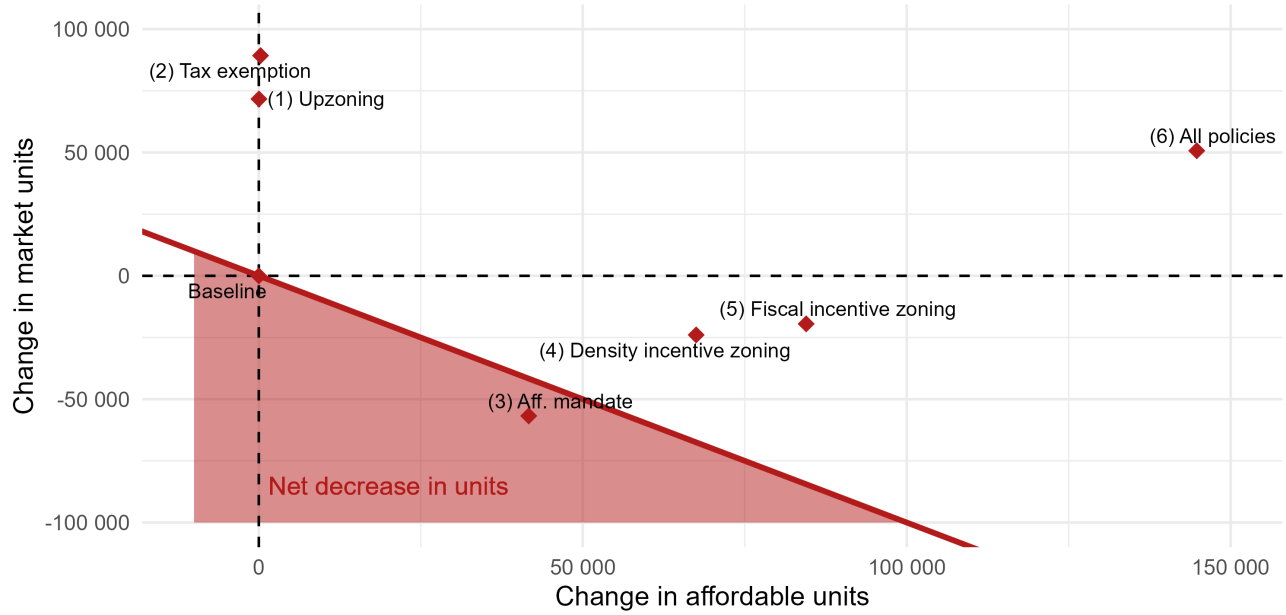
5.1 Housing Production

5.1.1 Market-rate vs affordable units: aggregate effects

Figure IV summarizes the aggregate housing production effects of the six policy interventions by plotting changes in affordable units against changes in market-rate units. The downward-sloping line provides a benchmark for interpreting how gains in affordability units map into changes in market-rate housing units. Movements along the line correspond to one-for-one reallocation between affordable and market-rate units, leaving aggregate supply approximately unchanged. Points above the line indicate net expansions of the housing stock, while points below the line indicate net contractions relative to the baseline. Detailed numerical outcomes are reported in Table E2 in the Appendix.

The figure reveals stark differences in aggregate production responses across policy instruments. Unilateral upzoning and tax exemptions lie in the vertical line, reflecting increases in

Figure IV: Policy Counterfactuals – Housing Production



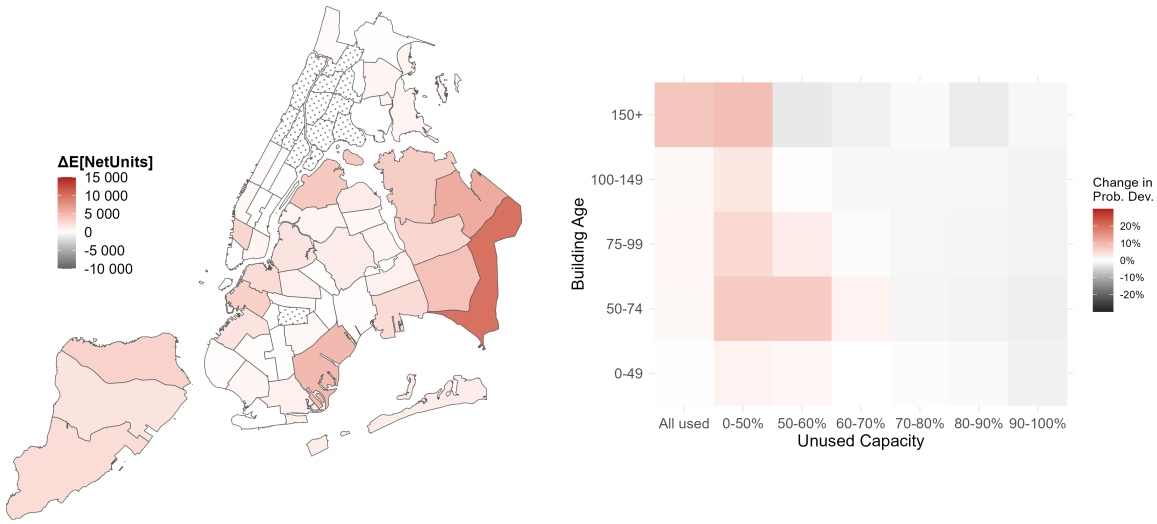
Note: This scatter plot shows the expected change in affordable housing units (x-axis) and market-rate housing units (y-axis) relative to the baseline over a 10-year horizon. Policy (1) Upzoning corresponds to a 50% increase in allowable density; Policy (2) Tax exemption corresponds to a 20-year property tax exemption; and Policy (3) corresponds to a 30% affordability mandate. Policies (4), (5), and (6) combine these instruments.

market-rate housing with negligible effects on affordable supply. A standalone affordability mandate, by contrast, shifts production sharply toward affordable units but lies below the 45-degree line, indicating that increases in affordable housing are accompanied by a contraction in total housing production. Policies that combine affordability mandates with incentives occupy intermediate positions. Density Incentive Zoning and Fiscal Incentive Zoning both lie above the 45-degree line, indicating net expansions of the housing stock, but affordability gains in these cases arise primarily through reallocation, with increases in affordable units offset by reductions in market-rate production. Only the fully combined policy lies in the upper-right quadrant, expanding both affordable and market-rate housing simultaneously.

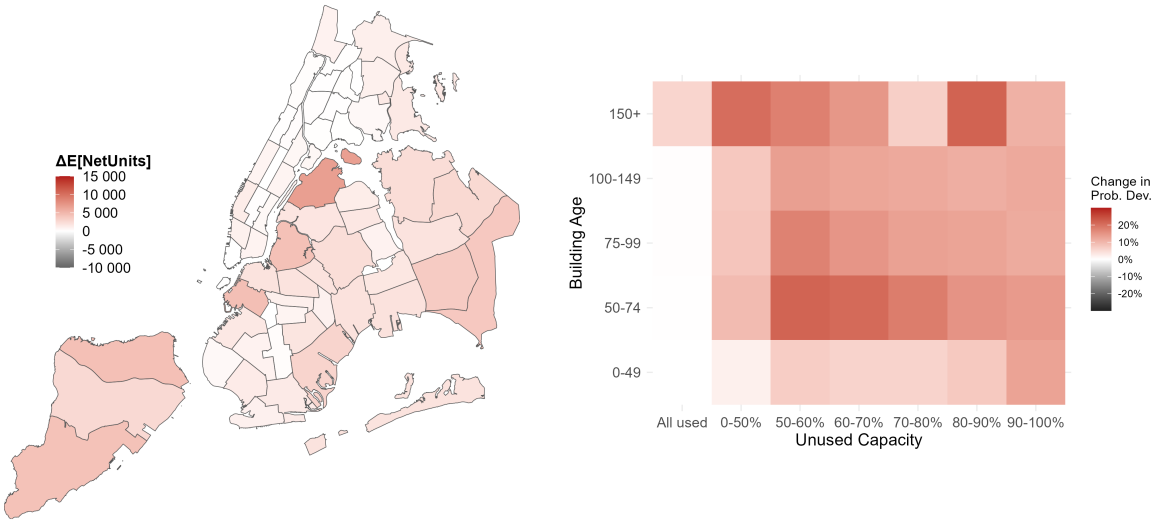
5.1.2 Spatial heterogeneity is driven by parcel heterogeneity

Figure V highlights spatial heterogeneity in housing production, focusing on unilateral upzoning and tax exemption policies for illustration. Although both policies increase aggregate housing production at the citywide level, their spatial incidence differs markedly across neighborhoods. Areas with parcels near their redevelopment threshold and strong underlying demand—such as Western Brooklyn and Queens—exhibit larger responses to fiscal incentives, while

Figure V: Policy Counterfactuals – Housing Production Heterogeneity



A. Upzoning ($\phi = .50$)



B. Tax exemptions ($\tau = 20$)

Note: The maps report the expected net change in the number of housing units under each counterfactual policy, aggregated at the community-district level. The right-hand panels report changes in redevelopment probabilities, grouping parcels by deciles of unused density ($\bar{F}_i - F_{B,i}$) and building age. Panel A reports results for an upzoning policy allowing a 50% increase in maximum density, and Panel B reports results for a 20-year exemption from property taxes on newly developed buildings.

the effects of upzoning are more uniformly distributed spatially.

The right-hand panels of Figure V illustrate the mechanisms underlying these spatial patterns

by reporting changes in redevelopment probabilities across parcels grouped by deciles of unused density and building age. Tax exemptions raise redevelopment probabilities for parcels with older structures and substantial unused density. By contrast, upzoning lowers redevelopment probabilities for many of these same parcels. In the model, this occurs because higher allowable density raises the optimal expansion threshold, inducing developers to delay redevelopment until rents justify larger projects. As a result, although both policies expand aggregate housing supply, they operate through distinct channels, generating different spatial responses even when applied uniformly across the city.

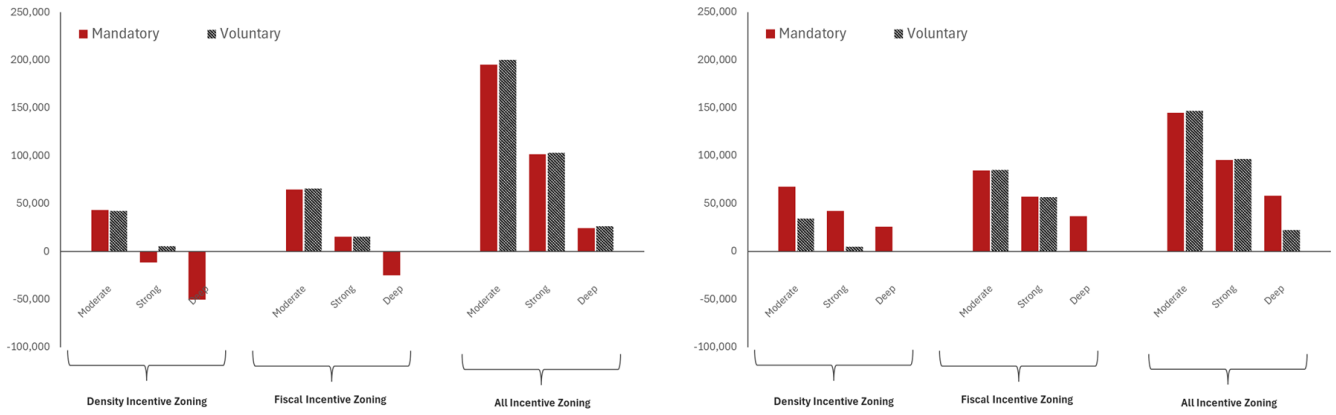
5.1.3 Voluntary *Carrot* & *Stick* policies and affordability levels

We next examine how voluntary adoption and the depth of affordability requirements affect housing production under the *Carrot & Stick* policies. We model voluntary regimes such that developers adopt a policy bundle $\mathcal{P}$ only if it raises property value relative to the baseline, i.e., if $\pi_i(\mathcal{P}) > \pi_i(\mathcal{P}_0)$. Parcels for which regulatory requirements dominate incentives remain under the baseline regulatory environment.[16] We provide additional results on the types of parcels that adopt different policy bundles in Appendix E.2. We also vary the depth of affordability requirements through the rent discount ϵ_α, holding the affordable-share requirement fixed. Figure VI summarizes the results. Panel A reports changes in total net housing production, and Panel B reports changes in net affordable housing production. Within each policy environment, outcomes are shown for moderate, strong, and deep affordability requirements.

Under mandatory regimes, deepening affordability requirements progressively weakens redevelopment incentives and reduces both total and affordable housing production. Although the affordable-share requirement is unchanged ($\alpha = 0.30$), higher rent discounts lower project profitability and cause fewer parcels to redevelop. In several cases, total housing production becomes negative relative to the baseline even as affordable production remains positive, indicating that the contraction operates primarily through market-rate units rather than through a collapse of affordable construction itself. As rent discounts rise, parcels for which regulatory costs outweigh available incentives optimally remain under the baseline environment, reducing aggregate redevelopment activity. At moderate affordability levels, voluntary adoption yields housing production outcomes similar to those under mandatory regimes. As affordability requirements deepen further, participation declines sharply, and both total and affordable housing production converge back toward the baseline.

[16]The voluntary-adoption counterfactual introduces a binary participation decision that can create discontinuities in the fixed-point iteration described in Appendix A.6. To ensure numerical stability, we smooth adoption beliefs during the iteration using a logit approximation and recover the binary adoption rule once the algorithm has converged. Appendix A.8 provides details.

Figure VI: Affordability Levels and *Voluntary* Policy Interventions



A. Total net housing production

B. Total affordable production

Notes: The figures report changes in expected housing production relative to the baseline calibration $\mathcal{P}_0$ over a 10-year horizon. Panel A reports the change in total housing units net of demolitions, while Panel B reports the change in affordable housing units. Bars are grouped by policy regime, Density Incentive Zoning, Fiscal Incentive Zoning, and the Combined Incentive Policy, and by the depth of the affordability requirement. Affordability depth is parameterized by the rent discount ϵ_α, which scales the rental income of affordable units relative to market-rate units: $\epsilon_\alpha = 0.25$ (moderate), $\epsilon_\alpha = 0.50$ (strong), and $\epsilon_\alpha = 0.75$ (deep). Red bars correspond to mandatory policy regimes, in which all new construction must comply with the specified requirements. Stripped black bars correspond to voluntary policy regimes, in which developers choose whether to adopt the policy bundle or remain under the baseline regulatory environment. In voluntary counterfactuals, adoption decisions are made assuming all other parcels adopt the policy.

The Combined Incentive Policy constitutes a notable exception to this pattern. By bundling density bonuses and tax exemptions, it sustains redevelopment under voluntary adoption even at high affordability discounts. Under deep affordability ($\epsilon_\alpha = 0.75$), the combined policy continues to generate positive affordable housing production. Relative to the other regimes, stacking incentives preserves redevelopment across a broader set of parcels, allowing affordable production to remain positive despite stringent requirements.

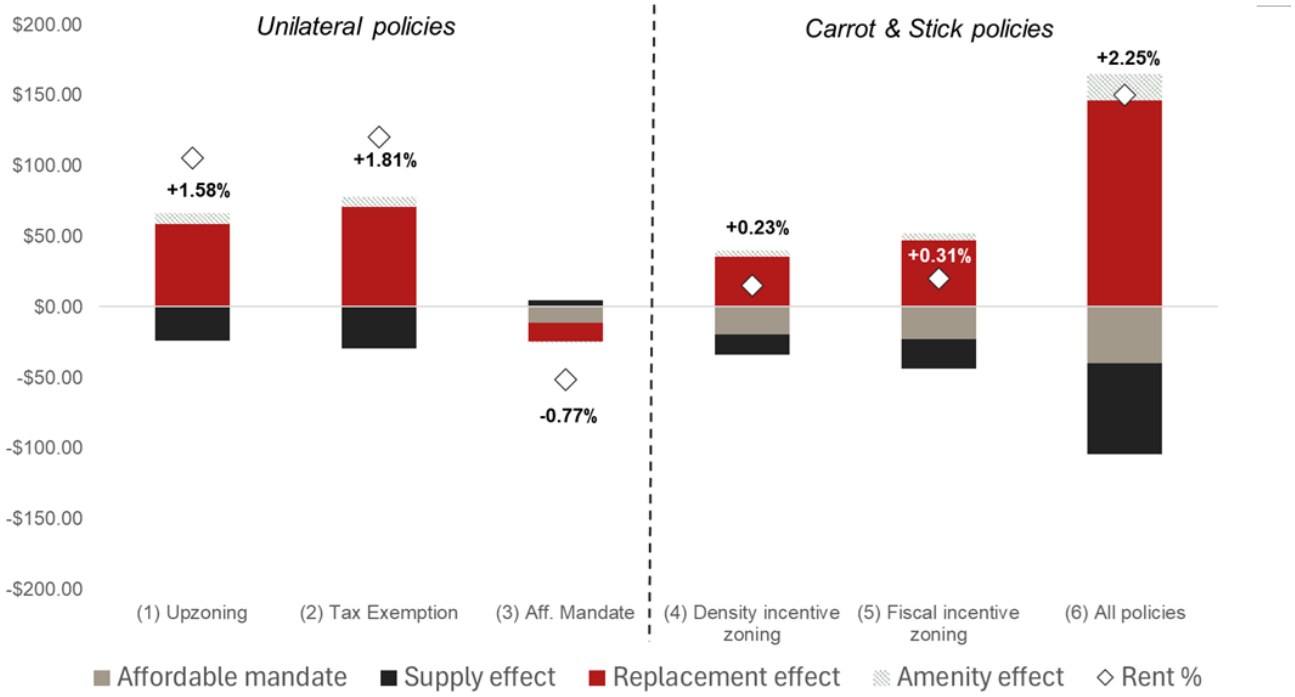
5.2 Expected Rent

5.2.1 Average expected housing rent and its decomposition

Figure VII reports the change in average citywide expected rent relative to the baseline. Across counterfactuals, policies generate heterogeneous rent responses, reflecting the combined effects of additional supply, affordability requirements, and the replacement of older, depreciated housing stock through redevelopment.

Under Density and Fiscal Incentive Zoning, average expected rents decline modestly, by 0.11% and 0.15%, respectively, relative to the baseline. By contrast, the largest rent increases oc-

Figure VII: Counterfactual Results – Expected Rents



Note: The points report the average expected rent change under each counterfactual policy relative to the baseline at a 10-year horizon. The stacked bars decompose this change into four components. The Affordable Mandate component isolates the direct effect of the affordable share α on rental income, holding expected construction activity fixed. The Supply effect captures the change in expected rents attributable to additional citywide housing supply. The Amenity effect is computed analogously and reflects the impact of local supply increases on neighborhood rents. The Replacement effect is defined as the residual component and captures rent changes associated with replacing older, depreciated structures with new construction, including changes in redevelopment probabilities and endogenous updates to expected rental growth. Policies (1)–(3) correspond to unilateral interventions—upzoning, tax exemption, and affordability mandate—while policies (4)–(6) combine these instruments.

cur under policies associated with the strongest redevelopment activity, notably upzoning (Policy [1]), tax exemption (Policy [2]), and the combined bundle (Policy [6]), which increase expected rents by 1.58%, 1.81%, and 2.25%, respectively. In these cases, expanded supply coincides with substantial replacement of older, depreciated housing stock by new construction.[17]

To interpret these patterns, we decompose rent changes into four components: (i) the affordable share effect, reflecting shifts in average rent due to the inclusion of below-market units in new buildings; (ii) the supply effect, capturing downward pressure from additional citywide supply; (iii) the amenity effect, capturing the impact of nearby construction on local rents; and (iv) the replacement effect, which reflects higher rents associated with replacing older, lower-rent structures with new construction. Across policies, replacement effects account for a substantial

[17]Figure E2 provides spatial context by mapping changes in average expected rent across community districts. Neighborhoods experiencing larger increases in redevelopment activity—such as parts of Brooklyn, Queens, and Staten Island—exhibit larger rent responses, while districts with limited redevelopment display more muted changes.

Table IV: Counterfactual Results – Change in Rent Distribution across Quintiles

		Q1	Q2	Q3	Q4	Q5
	Range	\$0–1,840	\$1,840–2,260	\$2,260–2,700	\$2,700–3,550	\$3,550+
	Baseline	20%	20%	20%	20%	20%
			Unilateral Policy			
(1)	*Upzoning*	20.28%	19.89%	19.14%	19.15%	21.53%
(2)	*Tax abatement*	20.23%	19.61%	18.77%	19.36%	22.02%
(3)	*Affordable mandate*	20.01%	20.08%	20.35%	20.33%	19.23%
			Mandatory Carrot & Stick Zoning			
(4)	*Density Incentive Zoning*	20.24%	20.01%	19.73%	19.7%	20.32%
(5)	*Fiscal Incentive Zoning*	20.23%	19.87%	19.47%	19.92%	20.52%
(6)	*All Policies*	20.69%	19.5%	18.21%	18.98%	22.62%

Notes: *This table reports the share of expected housing supply falling within each rent quintile under each counterfactual policy relative to the baseline calibration $\mathcal{P}_0$. Quintile thresholds are defined from the baseline rent distribution.*

share of rent responses and often offset downward pressure from added supply and affordability requirements. For example, under upzoning, expected rent rises by approximately \$60 per unit per month due to replacement, while the supply effect lowers rent by approximately \$24. Introducing an affordability mandate (Policy [4]) dampens this increase by allocating a share of new construction to below-market units, which—together with the supply effect—largely neutralize replacement effects.

5.2.2 Rent distribution

To describe how policy interventions affect rents beyond changes in averages, we examine shifts in the distribution of expected rents at the housing-unit level. Table IV reports the share of expected housing supply falling within each rent quintile under each counterfactual, relative to quintiles computed under the baseline. Policies without affordability mandates redistribute the housing stock toward both ends of the rent distribution. Under upzoning and tax abatements, the share of units in the highest rent quintile (more than \$3,550 per month) increases, reflecting the expansion of new market-rate construction. At the same time, the share of units in the lowest quintile (less than \$1,840) increases modestly, reflecting a citywide decline in rents associated with the supply response.

Similar policies, with however an affordability mandate (Policies 4 to 6), exhibit similar patterns, with reductions in the middle three quintiles offset by modest increases in both the bottom and top quintiles. To further examine this pattern, Figure E1 plots changes in the expected num-

ber of apartments across $500 rent bins. Positive (negative) bars indicate rent ranges in which the expected mass of units increases (decreases) relative to baseline. The stacked bars distinguish changes in market-rate units from those attributable to units subject to affordability mandates. Under both density and fiscal incentive zoning, most additional mandated affordable units fall above the mean rather than at the bottom of the distribution. This reflects how mandates interact with developers' optimization decisions: mandates are adopted primarily on high-value parcels where the ϵ_α% rent discount remains bearable. As a result, the lower end of the distribution continues to be supplied primarily by the existing stock rather than by newly built affordable units.

5.2.3 Robustness to demand elasticity assumptions

In the model, expected rents are determined by the built housing stock and the stochastic process governing potential rents R_i. Developers' expectations about future rents enter redevelopment decisions through the elasticity parameters ζ_S and ζ_A, which capture, respectively, citywide supply effects and local amenities spillovers. This subsection examines how alternative values of these elasticities affect rent and housing production outcomes.

When does the supply effect dominate rent outcomes? Figure E3 reports how average rent changes and housing production vary with the citywide inverse demand elasticity ζ_S, focusing on upzoning (left panel) and tax exemptions (right panel). Under the baseline calibration, both policies generate positive average rent changes, reflecting redevelopment activity that replaces older housing stock with new construction, while the net effect of additional supply on expected rents remains limited.

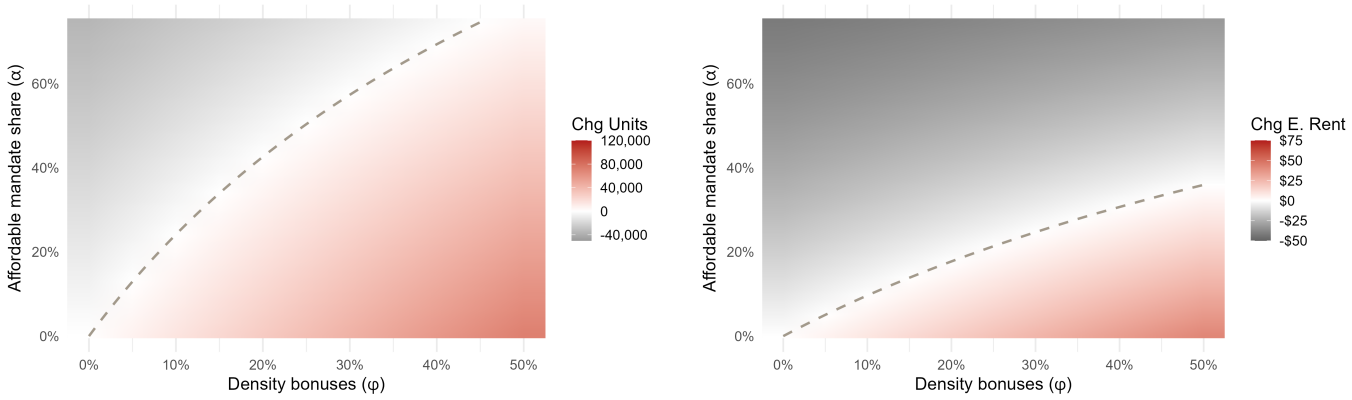
As the elasticity becomes more negative, the downward pressure from aggregate supply increases and progressively offsets this effect. However, reversing the sign of the average rent response requires an inverse demand elasticity with absolute values close greater than unity. However, at such a level, the model predicts a decline in housing production, as developers delay or forgo redevelopment in anticipation of larger future rent reductions from aggregate supply expansion. Consequently, rent reductions through the traditional supply mechanism occur in parameter ranges in which redevelopment incentives are substantially weakened.

Amenity spillovers and spatial clustering. To shed light on the role of local amenity effects, we measure how rents spatially cluster across housing units using Moran's I's spatial correlation. We compute Moran's I correlation using inverse-distance weights with a maximum radius of 250 meters. Under the baseline policy, it equals 0.53, indicating a strong spatial correlation in NYC rents.

Figure E4 reports changes in this spatial correlation under upzoning ($\phi = 0.50$) and tax exemptions ($\tau = 20$) for alternative values of the amenity elasticity ζ_A. Notably, the two policies move spatial correlation in opposite directions. Density bonuses raise it, tax exemptions reduce it. This divergence reflects where each instrument concentrates new development. Density bonuses attract construction on high-value parcels surrounded by expensive units, while tax exemptions target depreciated low-rise buildings, which tend to concentrate in lower-rent areas. Both effects amplify as local spillovers strengthen. When ζ_A approaches the magnitude of the aggregate inverse demand elasticity ζ_S, spatial correlation in rents rises by approximately six percentage points under upzoning, or 10% increase relative to the baseline.

5.3 Policy Trade-offs

Figure VIII: Continuous Policies Outcomes - Density Incentive Zoning



A. Change in housing unit

B. Change in expected average rent

Note: These heatmaps report changes in model outcomes under a Density Incentive Zoning program across continuous values of the density bonus ϕ (horizontal axis) and the affordable housing requirement α (vertical axis). All changes are measured relative to the status-quo policy $\mathcal{P}_0$ at the 10-year horizon. Panel A shows the net change in the expected number of housing units $E[AptNet|\mathcal{P}]$. Panel B reports the change in average expected rents per housing unit. Dotted contour lines indicate combinations of (ϕ, α) that leave the corresponding outcome equal to its baseline level under the status-quo policy $\mathcal{P}_0$.

The results presented so far focus on a discrete set of policy values for density bonuses, tax exemptions, and affordability mandates. However, our model allows us to evaluate any combination of these instruments. Figure VIII shows the change in housing production and expected average rents for Density Incentive Zoning across continuous values of ϕ (horizontal axis) and α (vertical axis). An analogous figure for policies combining tax exemptions and an affordable mandate is reported in Figure E7.

Two patterns emerge. First, proportional increases in density bonuses and affordability requirements do not translate proportionally into changes in aggregate outcomes, implying that

policy effects are not locally linear. This nonlinearity reflects the complexity of developers' optimal decisions within the real option framework as well as the spatial feedback effects that impact parcels heterogeneously. Second, the dashed contours show that policy combinations that hold housing production constant relative to the baseline generally differ from those that stabilize expected rents, indicating that no single combination of ϕ and α simultaneously offsets policy-induced changes across these margins.

6 Policy Incidence and the Cost of Mandated Affordable Units

Having shown how policy affects redevelopment and rents through the replacement margin, we now examine how these same mechanisms determine the cost and incidence of affordable mandates. We do not measure welfare, but instead, focus on how policy-induced changes in redevelopment translate into changes in private land values and the fiscal position of the city. Because policies affect when and how existing assets are replaced, they determine who bears the cost of affordable mandates.

6.1 Public and Private Costs of Policy Interventions

We evaluate how each policy affects the distribution of costs between the public sector and private landowners. We measure changes in the present value of property tax revenues and in parcel values, which together capture how policy-induced changes in redevelopment are reflected in fiscal revenues and land value capitalization. Because policies affect when and how existing assets are replaced, they determine whether these costs are absorbed through fiscal channels or capitalized into land values.

Table V reports both dimensions for each counterfactual policy. Although Upzoning (Policy [1]) modestly raises tax revenues by 0.44%, it reduces aggregate residential asset values by -1.20%. This decrease reflects the downward pressure of additional supply on existing properties, a pattern consistent with concerns over land value dilution following land-use deregulation Ahlfeldt et al. (2026); Duranton and Puga (2023).Tax exemptions (Policy 2), by contrast, impose the highest fiscal cost among unilateral interventions (-2.61%), mechanically reducing tax revenues during the exemption window. The affordable mandate (Policy 3) has comparatively modest fiscal consequences (-0.42%) but is distinctive in that it generates the smallest share of losers (14%) as the reduction in construction benefits landlords through higher future rental incomes. The Combined Incentive Zoning (Policy 6) produces the largest aggregate decline in both parcel values (-2.74%) and the greatest reduction in tax revenues (-3.89%). At the same time, winners under this policy

Table V: Counterfactual Results – Costs of Interventions

		Private Gain/Loss				Public
		ΔPV (%)	Shr. PV-losers (%)	Avg. Gain (000's $ per parcel)	Avg. Loss	ΔPV^{Tax} (%)
		Unilateral Policy				
(1)	*Upzoning* - $\phi = 50\%$	-1.20	0.87	47.04	-35.73	0.44
(2)	*Tax abatement* - $\tau = 20$	-0.93	0.86	110.31	-40.27	-2.61
(3)	*Affordable mandate* - $\alpha = 30\%$	0.17	0.14	7.13	-18.57	-0.42
		Mandatory Carrot & Stick Zoning				
(4)	*Density Incentive Zoning*	-0.85	0.87	30.45	-24.31	-0.25
(5)	*Fiscal Incentive Zoning*	-0.75	0.87	78.23	-29.15	-2.73
(6)	*Combined Incentive Zoning*	-2.74	0.84	117.64	-90.58	-3.89

Notes: *This table reports the private and public cost outcomes under each counterfactual policy relative to the baseline calibration $\mathcal{P}_0$. Each row corresponds to a counterfactual regulatory environment $\mathcal{P}$. ΔPV reports the percentage change in the aggregate present value of residential parcels. The share of PV-losers is the fraction of parcels whose present value declines under the policy ($\pi_i(\mathcal{P}) < \pi_i(\mathcal{P}_0)$). Average gain and average loss report the average change in present value (in thousands of dollars per parcel) among PV-winners and PV-losers, respectively. ΔPV^{Tax} reports the percentage change in the present value of property tax revenues collected by the city.*

experience the largest average gains ($117.64k per acre), while losers face the steepest average losses ($90.58k per acre), highlighting the redistribution generated by the policy.

Heterogeneous Impact on Landlords. The aggregate statistics in Table V mask substantial heterogeneity in how policies affect individual landowners. Across all policies, a large majority of parcels — between 84% and 88% — experience a decline in present value, while a small minority capture gains. This pattern reflects two opposing forces. The supply effect of new construction reduces expected rental income for all parcels through downward pressure on rents, generating diffuse losses across the parcel distribution. Meanwhile, the redevelopment option creates large gains for the subset of parcels at the margin of redevelopment, where the combined effect of density bonuses, tax relief, and higher post-redevelopment income outweighs the costs of construction and the affordability mandate.

Figure E8 illustrates this asymmetry for the Combined Incentive Policy. The distribution of present value changes is highly skewed, with the mass of PV-losers concentrated just below zero, while the distribution of winners has a long right tail extending beyond 50%, reflecting large option value gains for parcels that redevelop under the new policy environment. The average loss among losers is $750.58k per acre, while the average gain among winners is $1,292.96k per acre — a ratio of approximately 1.7, indicating that each winner gains nearly twice as much as each loser

loses on a per-acre basis. These results exemplify why these policies are often exposed to NIMBY opposition (Diamond and McQuade, 2019) and voters' opposition (Fischel, 2002).

6.2 Cost of Mandated Affordable Units

Although the results above describe the fiscal and private costs of each policy, they are not directly comparable across interventions, as policies differ in their effects on total housing supply. To isolate the cost of mandated affordable units, we focus on policy comparisons that hold total expected net housing supply fixed, $\Delta E[\text{NetUnit} \mid \mathcal{P}] = 0$. Under this restriction, policies operate by reallocating units from market-rate to affordable rather than by expanding supply. This restriction keeps equilibrium population and density constant and allows us to evaluate the incidence of one additional affordable unit without conflating it with welfare changes arising from aggregate densification.[18]

We construct the cost measure as follows. For each affordable mandate $\alpha \in \{0.01, \ldots, 0.50\}$, we search over the incentive ϕ (holding $\tau = 0$) or τ (holding $\phi = 0$) that restores total housing supply to its baseline level. The existence of such a compensating incentive follows from the monotonicity of redevelopment incentives established in Appendix A.9. For a fixed mandate α, increasing either ϕ or τ weakly raises parcel values and expands the set of parcels that would redevelop. As a result, aggregate housing supply is weakly increasing in incentives and continuous in aggregate.

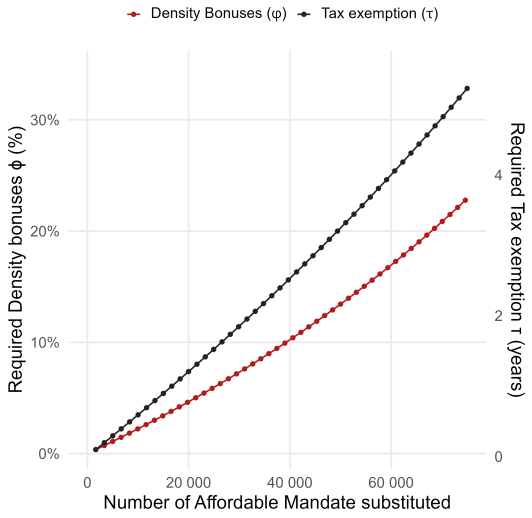
With each policy bundle, we compute $\Delta E[\text{Aff}Net \mid \mathcal{P}]$, the change in expected affordable units, as well as the private cost $\Delta\Pi(\mathcal{P})$ and the fiscal cost $\Delta PV^{\text{tax}}(\mathcal{P})$. The total cost per mandated affordable unit is then summarized as

$$\omega_A(\mathcal{P}) = \frac{\Delta\Pi(\mathcal{P}) + \Delta PV^{\text{tax}}(\mathcal{P})}{\Delta E[\text{Aff}Net \mid \mathcal{P}]}, \qquad \Delta E[\text{Aff}Net \mid \mathcal{P}] > 0. \tag{14}$$

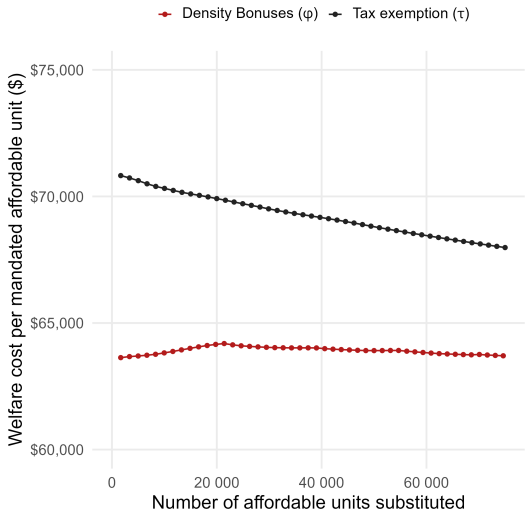
The wedge ω_A measures the total cost of generating one additional affordable unit while holding aggregate supply constant. It therefore isolates the cost of the mandate from broader rent or density effects, and provides a metric for comparing policies that differ in their design (ϕ vs. τ) but are equated on their supply implications. We further decompose ω_A into private and public components, where the private component captures the reduction in parcel values borne by landowners,

[18] Abstracting from supply growth allows us to set aside changes in consumer surplus and agglomeration externalities (Duranton and Puga, 2020). Under this controlled comparison, welfare effects reduce to incidence on landlords and on the fiscal position of the public sector.

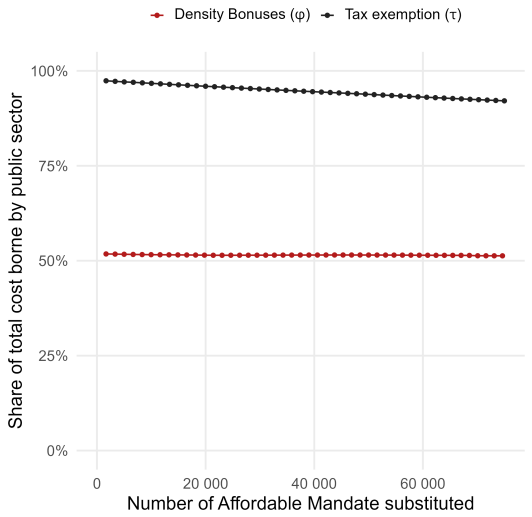
Figure IX: Cost of Mandated Affordable Housing



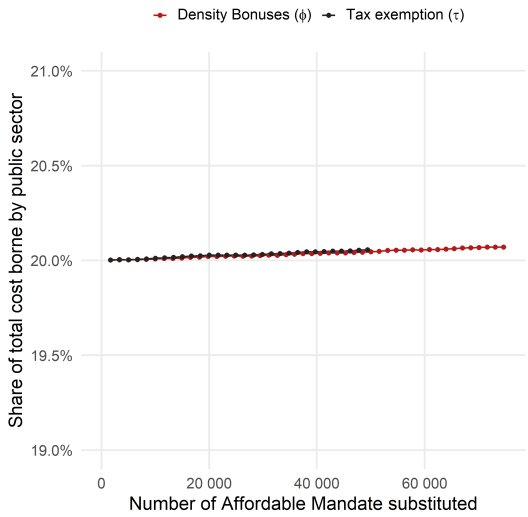
A. Required Incentives



B. Cost per unit



C. Share borne by public sector



D. Share of units in bottom quintile

Note: These figures show outcomes against the number of affordable units substituted for market-rate units, holding total net housing supply fixed ($\Delta E[NetUnit \mid \mathcal{P}] = 0$). Panel A shows the level of the incentives required to achieve supply neutrality under various affordable mandate α. Panel B reports the welfare cost per mandated affordable unit, $\omega_A(\mathcal{P})$. Panel C shows the share of this cost borne by the public sector. Panel D reports the share of units in the bottom quintile of the baseline rent distribution.

and the public component captures the fiscal cost of the incentive:

$$\omega_A^{\text{private}}(\mathcal{P}) = \frac{\Delta\Pi(\mathcal{P})}{\Delta E[\text{Aff}Net \mid \mathcal{P}]}, \qquad \omega_A^{\text{public}}(\mathcal{P}) = \frac{\Delta PV^{\text{tax}}(\mathcal{P})}{\Delta E[\text{Aff}Net \mid \mathcal{P}]}.$$

Panel A of Figure IX shows the level of incentives required to maintain supply neutrality as the affordable mandate increases. For instance, replacing roughly 40,000 market-rate units with affordable ones requires a density bonus of 10% or a tax exemption of 2.60 years. Both density bonuses and tax exemptions must increase with the mandate. The convexity of both schedules indicates that affordability is not scalable without progressively larger compensation. Panel B reports the cost per mandated affordable unit, $\omega_A(\mathcal{P})$. The per-unit cost remains relatively stable across mandate levels and policy instruments, averaging approximately \$63,820 under density-based policies and \$69,054 under fiscal policies. Panel C shows how this cost is distributed between the public and private sectors. Under density-based policies, the burden is roughly evenly split: landowners lose about \$30,000 per unit through negative capitalization, while the city experiences a comparable reduction in the present value of tax revenues. In contrast, under fiscal policies, most of the cost is borne by the public sector, particularly at low mandate levels where up to 95% of the cost arises from reduced tax revenues. As the mandate increases, a larger share of the burden is absorbed by private landowners through declining parcel values, but this share rarely exceeds 10% (approximately \$7,000 per unit). This asymmetry illustrates the political tensions surrounding densification reform (Fischel, 2002): fiscal instruments benefit landowners but are fiscally costly, while regulatory instruments preserve public revenues at the expense of private asset values. Finally, Panel D shows the share of housing units in the bottom quintile of the baseline rent distribution. It shows that, despite the mandate and the increase in the number of affordable units created by the policy, the share of housing units in the bottom quintile does not increase substantially. At most, we see that 20.08% fall within that quintile, highlighting the limits of achieving truly affordable housing through such a mandate.

6.3 Synthesis and Policy Implications

Throughout the paper, the results reflect a common mechanism: policies operate by shifting the conditions under which existing assets are redeveloped. Across policies, redevelopment is endogenous, forward-looking, and selective. Policies that aim to stimulate development do not add housing units mechanically but instead shift the thresholds at which parcels are redeveloped or left unchanged. As a result, policy interventions affect where construction occurs, when it occurs, and what replaces the existing stock, rather than aggregate quantities alone. Because developers optimally target parcels with greater unused density and more depreciated structures, new construction predominantly takes the form of replacement rather than pure expansion.

Consequently, supply expansions do not mechanically lower observed rents. Across policies, expected rent changes reflect the interaction of aggregate and local supply effects, affordability allocations, and changes in the built environment associated with redevelopment. Although

additional construction exerts downward pressure on rents, this effect is often offset by the replacement effect: new buildings enter without accumulated depreciation and typically command higher rents than the average stock in the city. As redevelopment concentrates on older, lower-rent structures, replacement effects often offset supply effects even when total housing production rises.

This result highlights that affordability is fundamentally a question of housing stock composition rather than quantity alone. Most low-rent housing is supplied by aging structures, while affordability mandates reallocate access to new construction at discounted rents rather than creating deeply low-rent units. Consistent with the rent distribution results, mandate-based policies do not generate units in the lowest rent quintile, which remains largely tied to the existing housing stock. In addition, generating affordable units through policy entails non-negligible costs, either through reductions in land values, through public resources, or through a combination of both.

Taken together, these results imply that housing policy design is inherently multidimensional. Density bonuses expand supply but alter the composition of the housing stock. Fiscal incentives accelerate redevelopment but impose public costs. Mandates generate targeted affordability but weaken development incentives and create an implicit cost shared across private and public stakeholders. Because development decisions are individual and parcel-specific, different policy mixes shift not only housing production dynamics and the distribution of rents, but also the distribution of costs across private and public actors. Effective policy, therefore, requires evaluating outcomes jointly across production, rents, land value capitalization, and public costs, rather than along any single dimension.

7 Conclusion

We develop a forward-looking spatial framework in which housing policy operates through endogenous redevelopment decisions. By embedding parcel-level investment choices within a spatial environment with aggregate and local spillovers, the model enables the evaluation of how regulatory and fiscal instruments affect the timing, scale, and location of housing development, and thereby shape the evolution of the housing stock.

A central implication of the analysis is that, in durable housing markets, supply largely operates through replacement rather than expansion of the housing stock. Policy interventions affect housing outcomes by shifting when and how existing assets are replaced, which in turn determines the composition of the housing stock, the evolution of rents, and the incidence of public policies. As a result, policies that expand construction do not mechanically lower average rents,

and observed relations between construction and rents often reflect changes in composition as much as changes in supply.

These findings have direct implications for policy design. Instruments that appear similar when evaluated through their effects on aggregate supply can generate different redevelopment dynamics, rent paths, and incidence patterns because they operate on different margins of the replacement decision. Effective policy therefore requires evaluating how instruments jointly shape redevelopment incentives, housing composition, and cost allocation, rather than focusing on any single outcome in isolation. Although calibrated to New York City, the framework provides a tractable approach to analyzing housing policy in environments where investment is irreversible, forward-looking, and spatially interconnected.

References

Ahlfeldt, G. M. and Barr, J. (2022). The economics of skyscrapers: A synthesis. *Journal of Urban Economics*, 129:103419.

Ahlfeldt, G. M., Baum-Snow, N., and Jedwab, R. (2026). The skyscraper revolution: Global economic development and land savings. *CESifo Working Paper*.

Ahlfeldt, G. M. and McMillen, D. P. (2018). Tall buildings and land values: Height and construction cost elasticities in Chicago, 1870–2010. *Review of Economics and Statistics*, 100(5):861–875.

Albouy, D. and Ehrlich, G. (2018). Housing productivity and the social cost of land-use restrictions. *Journal of Urban Economics*, 107:101–120.

Almagro, M. and Domínguez-Iino, T. (2025). Location sorting and endogenous amenities: Evidence from amsterdam. *Econometrica*, 93(3):1031–1071.

Amaral, F., Dohmen, M., Kohl, S., and Schularick, M. (2025). Superstar returns? spatial heterogeneity in returns to housing. *The Journal of Finance*, 80(5):3057–3094.

Arnott, R. J. and Lewis, F. D. (1979). The transition of land to urban use. *Journal of Political Economy*, 87(1):161–169.

Asquith, B. J., Mast, E., and Reed, D. (2023). Local effects of large new apartment buildings in low-income areas. *Review of Economics and Statistics*, 105(2):359–375.

Bar-Ilan, A. and Strange, W. C. (1999). The timing and intensity of investment. *Journal of Macroeconomics*, 21(1):57–77.

Baum-Snow, N. and Duranton, G. (2025). Housing supply and housing affordability. *NBER Working Paper Series*.

Baum-Snow, N. and Han, L. (2024). The microgeography of housing supply. *Journal of Political Economy*, 132(6):000–000.

Baum-Snow, N. and Marion, J. (2009). The effects of low income housing tax credit developments on neighborhoods. *Journal of Public Economics*, 93(5-6):654–666.

Brueckner, J. K., Leather, D., and Zerecero, M. (2024). Bunching in real-estate markets: Regulated building heights in new york city. *Journal of Urban Economics*, 143:103683.

Brueckner, J. K. and Rosenthal, S. S. (2009). Gentrification and neighborhood housing cycles: will america's future downtowns be rich? *The Review of Economics and Statistics*, 91(4):725–743.

Brueckner, J. K. and Singh, R. (2020). Stringency of land-use regulation: Building heights in us cities. *Journal of Urban Economics*, 116:103239.

Büchler, S., Ehrlich, M. v., and Schöni, O. (2021). The amplifying effect of capitalization rates on housing supply. *Journal of Urban Economics*, 126:103370.

Büchler, S. and Lutz, E. (2024). Making housing affordable? The local effects of relaxing land-use regulation. *Journal of Urban Economics*, 143:103689.

Büchler, S. and v. Ehrlich, M. (2023). Quantifying land-use regulation and its determinants. *Journal of Economic Geography*, 23(5):1059–1096.

Capozza, D. and Li, Y. (1994). The intensity and timing of investment: The case of land. *The American Economic Review*, pages 889–904.

Chen, J., Glaeser, E., and Wessel, D. (2023). Jue insight: The (non-) effect of opportunity zones on housing prices. *Journal of Urban Economics*, 133:103451.

Cochrane, J. H. and Saa-Requejo, J. (2000). Beyond arbitrage: Good-deal asset price bounds in incomplete markets. *Journal of Political Economy*, 108(1):79–119.

Corinth, K. and Feldman, N. (2024). Are opportunity zones an effective place-based policy? *Journal of Economic Perspectives*, 38(3):113–136.

Couture, V., Gaubert, C., Handbury, J., and Hurst, E. (2024). Income growth and the distributional effects of urban spatial sorting. *Review of Economic Studies*, 91(2):858–898.

Cunningham, C. R. (2006). House price uncertainty, timing of development, and vacant land prices: Evidence for real options in Seattle. *Journal of Urban Economics*, 59(1):1–31.

D'Amico, L., Glaeser, E. L., Gyourko, J., Kerr, W. R., and Ponzetto, G. A. (2024). Why has construction productivity stagnated? The role of land-use regulation. *NBER Working Paper Series*.

Danton, J. and Himbert, A. (2018). Residential vertical rent curves. *Journal of Urban Economics*, 107:89–100.

Diamond, R. (2016). The determinants and welfare implications of us workers' diverging location choices by skill: 1980–2000. *American Economic Review*, 106(3):479–524.

Diamond, R. and McQuade, T. (2019). Who wants affordable housing in their backyard? an equilibrium analysis of low-income property development. *Journal of Political Economy*, 127(3):1063–1117.

DiPasquale, D. and Wheaton, W. C. (1992). The markets for real estate assets and space: A conceptual framework. *Real Estate Economics*, 20(2):181–198.

Druckenbrod, C. and Beckmann, V. (2018). Production-integrated compensation in environmental offsets—a review of a German offset practice. *Sustainability*, 10(11):4161.

Duranton, G. and Puga, D. (2020). The economics of urban density. *Journal of economic perspectives*, 34(3):3–26.

Duranton, G. and Puga, D. (2023). Urban growth and its aggregate implications. *Econometrica*, 91(6):2219–2259.

Eriksen, M. D. and Orlando, A. W. (2022). Returns to scale in residential construction: The marginal impact of building height. *Real Estate Economics*, 50(2):534–564.

Eriksen, M. D. and Rosenthal, S. S. (2010). Crowd out effects of place-based subsidized rental housing: New evidence from the LIHTC program. *Journal of Public Economics*, 94(11-12):953–966.

Favilukis, J., Mabille, P., and Van Nieuwerburgh, S. (2023). Affordable housing and city welfare. *The Review of Economic Studies*, 90(1):293–330.

Fischel, W. A. (2002). *The homevoter hypothesis: How home values influence local government taxation, school finance, and land-use policies?* Harvard University Press Cambridge, MA.

Freemark, Y. (2020). Upzoning Chicago: Impacts of a zoning reform on property values and housing construction. *Urban Affairs Review*, 56(3):758–789.

Freemark, Y. (2023). Zoning change: Upzonings, downzonings, and their impacts on residential construction, housing costs, and neighborhood demographics. *Journal of Planning Literature*, 38(4):548–570.

Glaeser, E. and Gyourko, J. (2018). The economic implications of housing supply. *Journal of Economic Perspectives*, 32(1):3–30.

Glaeser, E. L., Gyourko, J., and Saks, R. E. (2005). Why have housing prices gone up? *American Economic Review*, 95(2):329–333.

Goolsbee, A. and Syverson, C. (2023). The strange and awful path of productivity in the US construction sector. *NBER Working Paper Series*.

Greenaway-McGrevy, R. and Phillips, P. C. (2023). The impact of upzoning on housing construction in auckland. *Journal of Urban Economics*, 136:103555.

Grenadier, S. R. (1996). The strategic exercise of options: Development cascades and overbuilding in real estate markets. *The Journal of Finance*, 51(5):1653–1679.

Gyourko, J., Hartley, J. S., and Krimmel, J. (2021). The local residential land use regulatory environment across US housing markets: Evidence from a new Wharton index. *Journal of Urban Economics*, 124:103337.

Gyourko, J. and Molloy, R. (2015). Regulation and housing supply. In *Handbook of Regional and Urban Economics*, volume 5, pages 1289–1337. Elsevier.

Homsy, G. C. and Kang, K. E. (2023). Zoning incentives: Exploring a market-based land use planning tool. *Journal of the American Planning Association*, 89(1):61–71.

Hsiao, A. (2025). Sea level rise and urban adaptation in Jakarta. *Working Paper*.

Hsieh, C.-T. and Moretti, E. (2019). Housing constraints and spatial misallocation. *American Economic Journal: Macroeconomics*, 11(2):1–39.

Kim, M. (2020). Upzoning and value capture: How US local governments use land use regulation power to create and capture value from real estate developments. *Land Use Policy*, 95:104624.

Korngold, G. (2022). *Land Value Capture in the United States: Funding Infrastructure and Local Government Services*. Lincoln Institute of Land Policy.

Krimmel, J. and Wang, B. X. (2026). Upzoning with strings attached: Evidence from Seattle's affordable housing mandate. *Regional Science and Urban Economics*, page 104219.

Lange, R.-J. and Teulings, C. N. (2024). Irreversible investment under predictable growth: Why land stays vacant when housing demand is booming. *Journal of Economic Theory*, 215:105776.

Lebret, D. and Liu, C. H. (2023). Creating value out of thin air. *Working Paper*.

Li, X. (2022). Do new housing units in your backyard raise your rents? *Journal of Economic Geography*, 22(6):1309–1352.

Liu, C. H., Rosenthal, S. S., and Strange, W. C. (2018). The vertical city: Rent gradients, spatial structure, and agglomeration economies. *Journal of Urban Economics*, 106:101–122.

Lopez, L. A. and Yoshida, J. (2022). Estimating housing rent depreciation for inflation adjustments. *Regional Science and Urban Economics*, 95:103733.

Lyons, R. C., Shertzer, A., Gray, R., and Agorastos, D. (2026). The price of housing in the United States, 1890–2006. *The Quarterly Journal of Economics*, 141(1):559–603.

Mast, E. (2023). JUE insight: The effect of new market-rate housing construction on the low-income housing market. *Journal of Urban Economics*, 133:103383.

McDonald, R. and Siegel, D. (1986). The value of waiting to invest. *The Quarterly Journal of Economics*, 101(4):707–727.

Mense, A. (2025). The impact of new housing supply on the distribution of rents. *Journal of Political Economy Macroeconomics*, 3(1):1–42.

Moore, A. A. (2013). *Trading density for benefits: Toronto and Vancouver compared*. Institute on Municipal Finance and Governance.

Murphy, A. (2018). A dynamic model of housing supply. *American Economic Journal: Economic Policy*, 10(4):243–267.

Myers, S. C. (1977). Determinants of corporate borrowing. *Journal of Financial Economics*, 5(2):147–175.

OECD and Lincoln Institute of Land Policy (2022). *Global Compendium of Land Value Capture Policies, OECD Regional Development*. OECD Publishing, Paris.

Paddock, J. L., Siegel, D. R., and Smith, J. L. (1988). Option valuation of claims on real assets: The case of offshore petroleum leases. *The Quarterly Journal of Economics*, 103(3):479–508.

Peng, X. E. (2023). The dynamics of urban development: Evidence from zoning reform in New York. *Working Paper*.

Pennington, K. (2025). Rents, movers, and stayers: The spillover effects of construction in San Francisco. *Working Paper*.

Quigg, L. (1993). Empirical testing of real option-pricing models. *The Journal of Finance*, 48(2):621–640.

Quigley, J. M. and Rosenthal, L. A. (2005). The effects of land use regulation on the price of housing: What do we know? What can we learn? *Cityscape*, pages 69–137.

Rollet, V. (2025). Zoning and the dynamics of urban redevelopment. *Working Paper*.

Rosenthal, S. S. (2014). Are private markets and filtering a viable source of low-income housing? Estimates from a "repeat income" model. *American Economic Review*, 104(2):687–706.

Saiz, A. (2010). The geographic determinants of housing supply. *The Quarterly Journal of Economics*, 125(3):1253–1296.

Schuetz, J., Meltzer, R., and Been, V. (2011). Silver bullet or trojan horse? the effects of inclusionary zoning on local housing markets in the united states. *Urban Studies*, 48(2):297–329.

Soltas, E. (2024). Tax incentives and the supply of low-income housing. *Working Paper*.

Soltas, E. J. (2022). The price of inclusion: Evidence from housing developer behavior. *Review of Economics and Statistics*, pages 1–46.

Titman, S. (1985). Urban land prices under uncertainty. *The American Economic Review*, 75(3):505–514.

Online Appendix

A Proofs

A.1 Foundations for Risk-Neutral Pricing of Rents.

To obtain analytical valuations of development options, we represent rent R_t as a geometric Brownian motion under the risk-neutral measure $\mathbb{Q}$. Rents are not traded claims, but their risk can be priced consistently through a common kernel linked to traded real-estate instruments. Residential property values are therefore the present value of net rents:

$$V_t = \mathbf{E}_{\mathbb{Q}}\left[\int_0^{\infty} e^{-ru} R_{t+u}\, du\right] = \frac{R_t}{r-\delta}, \qquad \delta < r.$$

This parallels rent-capitalization approaches used to relate the rental and asset markets through a capitalization rate – or rent-to-price ratio (Büchler et al., 2021; DiPasquale and Wheaton, 1992). Thus, with V_t inheriting rent dynamics and applying Itô's Lemma gives

$$dV_t = \delta V_t\, dt + \sigma V_t\, dW_t.$$

Four assumptions underlie this representation: (1) asset value derives solely from net rental income; (2) rents equal net operating income, so there is no wedge with value; (3) rents are discounted at a constant r; and (4) rent risk is spanned by traded real-estate instruments such as REITs or CMBS. The measure $\mathbb{Q}$ is thus viewed as a pricing device calibrated to observed valuations. Although real estate markets are incomplete, *good-deal bounds* narrow admissible measures, permitting valuation under $\mathbb{Q}$ without perfect replication (Cochrane and Saa-Requejo, 2000). It will follow from the empirical work that we calibrate δ from observed capitalization rates c_{obs} via $\delta = r - c_{\text{obs}}$, treating δ as a reduced-form risk premium.

A.2 Proof of Proposition 1: Parcel Value

Let $T_{R^e} \equiv \inf\{t \geq 0 : R_t = R^e\}$ with $R^e > R$, and $H_{R^e} \equiv T_{R^e} + d$, with $d > 0$.

Under $\mathbb{Q}$, $dR_t = \delta R_t dt + \sigma R_t dW_t^{\mathbb{Q}}$ with $r > \delta$, so

$$R_t = R\exp\Big((\delta - \frac{1}{2}\sigma^2)t + \sigma W_t^{\mathbb{Q}}\Big) = Re^{\sigma Z_t}, \qquad Z_t \equiv bt + W_t^{\mathbb{Q}}, \qquad b \equiv \frac{\delta - \frac{1}{2}\sigma^2}{\sigma}.$$

Define

$$a \equiv \frac{1}{\sigma}\ln\Big(\frac{R^e}{R}\Big) > 0, \qquad T_{R^e} = \inf\{t \geq 0 : Z_t = a\} \equiv T_a.$$

Parcel value is

$$\pi(R, F_B, z_B, \alpha_B, F; \mathcal{P}, \Theta) = \underbrace{\mathbf{E}_{\mathbb{Q}}\Big\{\int_0^{T_{R^e}} e^{-ru}(1-\psi)\Gamma(F_B, z_B, \alpha_B) R_u\, \mathrm{d}u\Big\}}_{\text{Value of existing property}}$$

$$- \underbrace{\mathbf{E}_{\mathbb{Q}}\Big\{e^{-rT_{R^e}}\gamma(F_B)\Big\}}_{\text{Demolition costs}} - \underbrace{\mathbf{E}_{\mathbb{Q}}\Big\{\int_{T_{R^e}}^{H_{R^e}} e^{-ru}\kappa(F,\alpha)\,\mathrm{d}u\Big\}}_{\text{Construction costs}}$$
$$+ \underbrace{\mathbf{E}_{\mathbb{Q}}\Big\{\int_{H_{R^e}}^{\infty} e^{-ru}\Gamma(F,1,\alpha)R_u\,\mathrm{d}u\Big\}}_{\text{Value of new property gross of tax}} - \underbrace{\mathbf{E}_{\mathbb{Q}}\Big\{\int_{H_{R^e}+\tau}^{\infty} e^{-ru}\psi\Gamma(F,1,\alpha)R_u\,\mathrm{d}u\Big\}}_{\text{Property taxes after }\tau\text{ years of exemption}}. \quad \text{(A.1)}$$

Drift removal. Define an auxiliary measure $\widetilde{\mathbb{P}}$ by

$$\left.\frac{\mathrm{d}\mathbb{Q}}{\mathrm{d}\widetilde{\mathbb{P}}}\right|_{\mathcal{F}_t} = \exp\left(bZ_t - \frac{1}{2}b^2t\right), \qquad t \geq 0, \quad \text{(A.2)}$$

so Z_t is standard Brownian motion under $\widetilde{\mathbb{P}}$. Let

$$\lambda \equiv \sqrt{2r+b^2}, \qquad \xi \equiv \frac{b-\lambda}{\sigma}.$$

1. Existing cash flows.

$$\mathbf{E}_{\mathbb{Q}}\left[\int_0^{T_{R^e}} e^{-ru}(1-\psi)\Gamma(F_B,z_B,\alpha_B)R_u\,du\right] = (1-\psi)\Gamma(F_B,z_B,\alpha_B)R\,\mathbf{E}_{\mathbb{Q}}\left[\int_0^{T_a} e^{-ru}e^{\sigma Z_u}\,du\right].$$

Using (A.2),

$$\mathbf{E}_{\mathbb{Q}}\left[\int_0^{T_a} e^{-ru}e^{\sigma Z_u}\,du\right] = \mathbf{E}_{\widetilde{\mathbb{P}}}\left[\int_0^{T_a} e^{-\frac{\lambda^2}{2}u}e^{(\sigma+b)Z_u}\,du\right] = \mathbf{E}_{\widetilde{\mathbb{P}}}\left[\int_0^{\infty}\cdots du\right] - \mathbf{E}_{\widetilde{\mathbb{P}}}\left[\int_{T_a}^{\infty}\cdots du\right].$$

The resolvent identity yields

$$\mathbf{E}_{\widetilde{\mathbb{P}}}\left[\int_0^{\infty} e^{-\frac{\lambda^2}{2}u}e^{(\sigma+b)Z_u}\,du\right] = \frac{1}{\lambda}\int_{-\infty}^{\infty} e^{-|y|\lambda}e^{(\sigma+b)y}\,dy = \frac{1}{r-\delta}. \quad \text{(A.3)}$$

By the strong Markov property at T_a and $Z_{T_a} = a$,

$$\mathbf{E}_{\widetilde{\mathbb{P}}}\left[\int_{T_a}^{\infty} e^{-\frac{\lambda^2}{2}u}e^{(\sigma+b)Z_u}\,du\right] = e^{(\sigma+b)a}\mathbf{E}_{\widetilde{\mathbb{P}}}\left[e^{-\frac{\lambda^2}{2}T_a}\right]\cdot\frac{1}{r-\delta},$$

and the Laplace transform of T_a gives $\mathbf{E}_{\widetilde{\mathbb{P}}}[e^{-(\lambda^2/2)T_a}] = e^{-\lambda a}$. Hence

$$\mathbf{E}_{\mathbb{Q}}\left[\int_0^{T_a} e^{-ru}e^{\sigma Z_u}\,du\right] = \frac{1}{r-\delta}\left[1-e^{(\sigma+b-\lambda)a}\right] = \frac{1}{r-\delta}\left[1-\left(\frac{R^e}{R}\right)^{1+\xi}\right].$$

Therefore,

$$\mathbf{E}_{\mathbb{Q}}\left[\int_0^{T_{R^e}} e^{-ru}(1-\psi)\Gamma(F_B,z_B,\alpha_B)R_u\,du\right] = \Gamma(F_B,z_B,\alpha_B)\frac{1-\psi}{r-\delta}\left[R - R^e\left(\frac{R^e}{R}\right)^{\xi}\right]. \quad \text{(A.4)}$$

2. Demolition.

$$\mathbf{E}_{\mathbb{Q}}\left[e^{-rT_{R^e}}\right] = \mathbf{E}_{\tilde{\mathbb{P}}}\left[e^{-\frac{\lambda^2}{2}T_a}\right] = e^{-\lambda a} = \left(\frac{R^e}{R}\right)^{\xi},$$

so

$$\mathbf{E}_{\mathbb{Q}}\left[e^{-rT_{R^e}}\gamma(F_B)\right] = \gamma(F_B)\left(\frac{R^e}{R}\right)^{\xi}. \tag{A.5}$$

3. Construction costs on $[T_{R^e}, T_{R^e}+d]$.

$$\mathbf{E}_{\mathbb{Q}}\left[\int_{T_{R^e}}^{T_{R^e}+d} e^{-ru}\kappa(F,\alpha)\,du\right] = \kappa(F,\alpha)\mathbf{E}_{\mathbb{Q}}\left[e^{-rT_{R^e}}\right]\int_0^d e^{-rs}\,ds = \frac{\kappa(F,\alpha)}{r}(1-e^{-rd})\left(\frac{R^e}{R}\right)^{\xi}.$$

4. New value after completion. Conditioning on $\mathcal{F}_{T_{R^e}}$ and using $R_{T_{R^e}} = R^e$,

$$\mathbf{E}_{\mathbb{Q}}\left[\int_{T_{R^e}+d}^{\infty} e^{-ru}R_u\,du\right] = \mathbf{E}_{\mathbb{Q}}\left[e^{-rT_{R^e}}\right]\int_d^{\infty} e^{-rs}\mathbf{E}_{\mathbb{Q}}[R_{T_{R^e}+s} \mid R_{T_{R^e}} = R^e]\,ds = \left(\frac{R^e}{R}\right)^{\xi}\frac{R^e}{r-\delta}e^{-(r-\delta)d},$$

hence

$$\mathbf{E}_{\mathbb{Q}}\left[\int_{H_{R^e}}^{\infty} e^{-ru}\Gamma(F,1,\alpha)R_u\,du\right] = \Gamma(F,1,\alpha)\frac{R^e}{r-\delta}e^{-(r-\delta)d}\left(\frac{R^e}{R}\right)^{\xi}. \tag{A.6}$$

5. Taxes after τ. By the same argument with lower limit $d+\tau$,

$$\mathbf{E}_{\mathbb{Q}}\left[\int_{H_{R^e}+\tau}^{\infty} e^{-ru}\psi\,\Gamma(F,1,\alpha)R_u\,du\right] = \psi\,\Gamma(F,1,\alpha)\frac{R^e}{r-\delta}e^{-(r-\delta)(d+\tau)}\left(\frac{R^e}{R}\right)^{\xi}. \tag{A.7}$$

Closed form. Combining (A.4), (A.5), Step 3, (A.6), and (A.7) gives

$$\begin{aligned}\pi(R,R^e,F,F_B,z_B,\alpha_B;\mathcal{P},\Theta) = \Gamma(F_B,z_B,\alpha_B)\frac{1-\psi}{r-\delta}\left[R - R^e\left(\frac{R^e}{R}\right)^{\xi}\right] - \gamma(F_B)\left(\frac{R^e}{R}\right)^{\xi}\\ - \frac{\kappa(F,\alpha)}{r}\left(1-e^{-rd}\right)\left(\frac{R^e}{R}\right)^{\xi} + \Gamma(F,1,\alpha)\frac{R^e}{r-\delta}e^{-(r-\delta)d}\left(\frac{R^e}{R}\right)^{\xi}\\ - \psi\,\Gamma(F,1,\alpha)\frac{R^e}{r-\delta}e^{-(r-\delta)(d+\tau)}\left(\frac{R^e}{R}\right)^{\xi}.\end{aligned} \tag{A.8}$$

A.3 Proof of Proposition 2: Optimal Expansion Barrier

Fix $F \le \bar{F}$ and regime $\mathcal{P}$. Under deterministic time-to-build d, parcel value is

$$\begin{aligned}\pi = \Gamma(F_B,z_B,\alpha_B)\frac{1-\psi}{r-\delta}\left[R - R^e\left(\frac{R^e}{R}\right)^{\xi}\right] - \gamma(F_B)\left(\frac{R^e}{R}\right)^{\xi}\\ - \frac{\kappa(F,\alpha)}{r}(1-e^{-rd})\left(\frac{R^e}{R}\right)^{\xi} + \Gamma(F,1,\alpha)\frac{R^e}{r-\delta}e^{-(r-\delta)d}\left(\frac{R^e}{R}\right)^{\xi}\end{aligned}$$

$$- \psi\, \Gamma(F,1,\alpha)\frac{R^e}{r-\delta}e^{-(r-\delta)(d+\tau)}\Big(\frac{R^e}{R}\Big)^{\xi}, \tag{A.9}$$

with $\xi = \frac{b-\lambda}{\sigma}$, $b = \frac{\delta-\frac{1}{2}\sigma^2}{\sigma}$, $\lambda = \sqrt{2r+b^2}$.

Define

$$K(F) = \gamma(F_B) + \frac{\kappa(F,\alpha)}{r}(1-e^{-rd}),$$

$$\vartheta = \Gamma(F,1,\alpha)\frac{e^{-(r-\delta)d} - \psi e^{-(r-\delta)(d+\tau)}}{r-\delta} - \Gamma(F_B,z_B,\alpha_B)\frac{1-\psi}{r-\delta}.$$

Then

$$\pi = \Gamma(F_B,z_B,\alpha_B)\frac{1-\psi}{r-\delta}R + \Big[\vartheta R^e - K(F)\Big]\Big(\frac{R^e}{R}\Big)^{\xi}.$$

Maximizing in R^e is equivalent to maximizing

$$g(R^e) = \Big[\vartheta R^e - K(F)\Big]\Big(\frac{R^e}{R}\Big)^{\xi}.$$

FOC.

$$g'(R^e) = \vartheta\Big(\frac{R^e}{R}\Big)^{\xi} + \Big[\vartheta R^e - K(F)\Big]\frac{\xi}{R}\Big(\frac{R^e}{R}\Big)^{\xi-1}.$$

Setting $g'(R^e)=0$ yields

$$\vartheta(1+\xi)R^e = \xi K(F),$$

so, for $\vartheta > 0$,

$$R^{e*}(F) = \frac{\xi}{1+\xi}\frac{K(F)}{\vartheta}.$$

SOC. Since

$$g(R^e) = R^{-\xi}\big(\vartheta(R^e)^{1+\xi} - K(F)(R^e)^{\xi}\big),$$

$$g''(R^e) = R^{-\xi}\big[\vartheta(1+\xi)\xi(R^e)^{\xi-1} - K(F)\xi(\xi-1)(R^e)^{\xi-2}\big].$$

Using the FOC,

$$g''(R^{e*}) = R^{-\xi}\vartheta(1+\xi)(R^{e*})^{\xi-1}.$$

Under $r>\delta$, $\xi<-1$, hence $(1+\xi)<0$ and $g''(R^{e*})<0$. Thus R^{e*} is a strict local maximizer.

A.4 Proof of Proposition 3: Probability of Development

Under the physical measure $\mathbb{P}$, rent follows

$$dR_t = g(h;\mathcal{P})R_t dt + \sigma R_t dW_t^{\mathbb{P}}, \qquad R_t = R\exp\Big((g(h;\mathcal{P}) - \frac{1}{2}\sigma^2)t + \sigma W_t^{\mathbb{P}}\Big).$$

Define

$$X_t = \frac{1}{\sigma}\ln\Big(\frac{R_t}{R}\Big) = m(h;\mathcal{P})t + W_t^{\mathbb{P}}, \qquad m(h;\mathcal{P}) = \frac{g(h;\mathcal{P}) - \frac{1}{2}\sigma^2}{\sigma}.$$

Let $R^{e*} > R$ and

$$a = \frac{1}{\sigma} \ln\Big(\frac{R^{e*}}{R}\Big) > 0.$$

The initiation time is

$$T_{R^{e*}} = \inf\{t \geq 0 : R_t = R^{e*}\} = \inf\{t \geq 0 : X_t = a\} \equiv T_a.$$

For Brownian motion with drift, the first-passage distribution satisfies

$$\mathbf{P}_{\mathbb{P}}(T_a \leq t) = \mathcal{N}\Big(\frac{m(h;\mathcal{P})t - a}{\sqrt{t}}\Big) + \exp(2m(h;\mathcal{P})a)\mathcal{N}\Big(-\frac{m(h;\mathcal{P})t + a}{\sqrt{t}}\Big), \qquad t > 0.$$

Applying this result to the stopping time $T_{R^{e*}}$ gives the redevelopment probability $\mathbf{P}_{\mathbb{P}}(T_{R^{e*}} \leq t)$.

With deterministic construction length d, completion occurs at $H = T + d$. Therefore, for horizon h,

$$\mathbf{P}_{\mathbb{P}}(H \leq h) = \begin{cases} \mathbf{P}_{\mathbb{P}}(T \leq h - d), & h > d, \\ 0, & h \leq d. \end{cases}$$

Substituting $t = h - d$ yields

$$\mathbf{P}_{\mathbb{P}}(H \leq h) = \mathcal{N}\Big(\frac{m(h;\mathcal{P})(h-d) - a}{\sqrt{h-d}}\Big) + \exp(2m(h;\mathcal{P})a)\mathcal{N}\Big(-\frac{m(h;\mathcal{P})(h-d) + a}{\sqrt{h-d}}\Big),$$

which establishes the result.

A.5 Optimal Density Conditional on a Fixed-expansion Threshold

Fix R^e and deterministic time-to-build d (so $H_{R^e} = T_{R^e} + d$). From (A.8), the terms that depend on F can be written as

$$\pi(F; R^e) = \text{const} - D(d)\,\kappa(F, \alpha) + M(d, \tau)\,\Gamma(F, 1, \alpha),$$

where const is independent of F and

$$D(d) \equiv \frac{1 - e^{-rd}}{r}\left(\frac{R^e}{R}\right)^{\xi}, \qquad M(d, \tau) \equiv \frac{e^{-(r-\delta)d}(1 - \psi e^{-(r-\delta)\tau})}{r - \delta} R^e \left(\frac{R^e}{R}\right)^{\xi},$$

with $\xi = (b - \lambda)/\sigma$ as in the main text. Using the calibration functional forms from subsection 3.2

$$\kappa(F, \alpha) = \frac{k_c L}{d}\,(1 - \alpha\eta_\alpha)\,F^{1+\eta_F}, \qquad \Gamma(F, 1, \alpha) = L\,(1 - \alpha\epsilon_\alpha)\,F^{1+\epsilon_F},$$

the objective becomes $\pi(F; R^e) = \text{const} - K_1 F^{1+\eta_F} + K_2 F^{1+\epsilon_F}$ with

$$K_1 = D(d)\frac{k_c L}{d}(1 - \alpha\eta_\alpha), \qquad K_2 = M(d, \tau)L(1 - \alpha\epsilon_\alpha).$$

Assuming an interior optimum with $\eta_F \neq \epsilon_F$, the first-order condition is

$$-(1 + \eta_F)K_1 F^{\eta_F} + (1 + \epsilon_F)K_2 F^{\epsilon_F} = 0,$$

which yields

$$\begin{aligned} F^*(R^e) &= \left[\frac{(1+\epsilon_F)K_2}{(1+\eta_F)K_1}\right]^{\frac{1}{\eta_F-\epsilon_F}} \\ &= \left[\frac{rd}{k_c(1-e^{-rd})}\cdot\frac{e^{-(r-\delta)d}(1-\psi e^{-(r-\delta)\tau})}{r-\delta}\cdot R^e\cdot\frac{(1+\epsilon_F)(1-\alpha\epsilon_\alpha)}{(1+\eta_F)(1-\alpha\eta_\alpha)}\right]^{\frac{1}{\eta_F-\epsilon_F}} \end{aligned}$$

As in the main text, once R^{e*} is substituted back as a function of F, the joint choice of (R^e, F) generally does not admit a closed-form solution. The optimal density must therefore be obtained numerically from the reduced-form objective $\pi(R, R^{e*}(F), F, \cdot)$.

A.6 Iterative Algorithm for the Spatial Fixed Point

The equilibrium drift vector is defined as the fixed point of a mapping from expected housing supply to parcel-level redevelopment decisions and back to aggregate supply. Policy-induced construction alters expected supply, which modifies the rent dynamics entering both the valuation problem and the redevelopment probability. These changes affect optimal redevelopment timing and density and therefore expected supply. Equilibrium requires consistency between supply adjustments and developers' responses. This appendix describes the fixed-point algorithm under policy $\mathcal{P}$ at horizon h.

Measures. Under the pricing measure $\mathbb{Q}$, rent evolves as $dR_t = \delta_i R_t\,dt + \sigma_i R_t\,dW_t^{\mathbb{Q}}$, where the risk-neutral drift δ_i governs valuation and determines optimal redevelopment thresholds and densities.

Under the physical measure $\mathbb{P}$, rent evolves as $dR_t = g_i R_t\,dt + \sigma_i R_t\,dW_t^{\mathbb{P}}$, where the physical growth rate g_i governs expected rent growth and redevelopment probabilities.

Initialization. Let δ_i' denote the baseline pricing drift implied by the cap rate and let g_i' denote the baseline physical rent growth rate. Initialize

$$\delta_i^{(0)} = \delta_i', \qquad g_i^{(0)} = g_i', \qquad \Delta S^{(0)} = 0, \qquad \Delta N_i^{(0)} = 0.$$

Iteration $k \geq 1$. Given the previous supply adjustments, compute the common supply-induced drift adjustment

$$\Delta\delta_i^{(k)} = \frac{1}{h}\zeta_S \Delta S^{(k-1)} + \frac{1}{h}\zeta_A \Delta N_i^{(k-1)}.$$

Update both the pricing drift and the physical growth rate:

$$\delta_i^{(k)} = \delta_i' + \Delta\delta_i^{(k)}, \qquad g_i^{(k)} = g_i' + \Delta\delta_i^{(k)}.$$

Using $\delta_i^{(k)}$, solve the parcel valuation problem under $\mathbb{Q}$ to obtain the optimal redevelopment trigger and density, $R_i^{e*,(k)}$ and $F_i^{*,(k)}$. Using the physical growth rate $g_i^{(k)}$, compute the probability of

redevelopment

$$\mathbf{P}_i^{(k)}(H \le h) = \mathbf{P}_{\mathbb{P}}\Big(T_i^{(k)} \le h - d\Big).$$

Expected supply on parcel i is therefore

$$s_i^{(k)} = \mathbf{P}_i^{(k)} F_i^{*,(k)} L_i + (1 - \mathbf{P}_i^{(k)}) F_{B,i} L_i.$$

Aggregate and neighborhood supply changes are updated as

$$\Delta S^{(k)} = \ln\Big(\sum_i s_i^{(k)}\Big) - \ln\Big(\sum_i s_i^{(0)}\Big), \qquad \Delta N_i^{(k)} = \ln\Big(\sum_{j\in\mathcal{L}_i} s_j^{(k)}\Big) - \ln\Big(\sum_{j\in\mathcal{L}_i} s_j^{(0)}\Big).$$

Convergence. The algorithm iterates until $|\Delta S^{(k)} - \Delta S^{(k-1)}| <$ tol. At convergence the equilibrium parameters satisfy

$$\delta_i(h;\mathcal{P}) = \delta_i' + \Delta\delta_i(h;\mathcal{P}), \qquad g_i(h;\mathcal{P}) = g_i' + \Delta\delta_i(h;\mathcal{P}),$$

which aligns supply adjustments with developers' optimal redevelopment responses.

A.7 Proof of Corollary 1: Expected Rental Incomes

Under the physical measure $\mathbb{P}$, rent evolves as

$$dR_t = g_i(h;\mathcal{P}) R_t\, dt + \sigma R_t\, dW_t^{\mathbb{P}}, \qquad R_t = R_i \exp\Big((g_i(h;\mathcal{P}) - \frac{1}{2}\sigma^2)t + \sigma W_t^{\mathbb{P}}\Big).$$

Since $W_t^{\mathbb{P}} \sim \mathcal{N}(0,t)$ and $\mathbf{E}_{\mathbb{P}}\{e^{\sigma W_t^{\mathbb{P}}}\} = e^{\frac{1}{2}\sigma^2 t}$, the expected rent level at horizon h is $\mathbf{E}_{\mathbb{P}}\{R_{ih}\} = R_i \exp(g_i(h;\mathcal{P})h)$.

Let $\mathbf{P}_i^*(H_{R^{e*}} \le h;\mathcal{P})$ denote the completion probability defined in Proposition 3. With deterministic construction time d, completion occurs at $H_{R^{e*}} = T_{R^{e*}} + d$, so that $\mathbf{P}_i^*(H_{R^{e*}} \le h) = \mathbf{P}_i^*(T_{R^{e*}} \le h - d)$ for $h > d$ and 0 otherwise.

Conditional on the redevelopment outcome, if redevelopment has not occurred, rental income at horizon h equals $\Gamma(F_{B,i}, z_{B,i}(h), \alpha_{B,i})\, R_{ih}$, and $\Gamma(F_i^*, 1, \alpha)\, R_{ih}$ if redevelopment is completed. Taking expectations under $\mathbb{P}$ yields

$$\begin{aligned}\mathbf{E}_{\mathbb{P}}\{RentInc_{ih}\} = \Big[1 - \mathbf{P}_i^*(H_{R^{e*}} \le h;\mathcal{P})\Big] &\times \Gamma(F_{B,i}, z_{B,i}(h), \alpha_{B,i}) \times \mathbf{E}_{\mathbb{P}}\{R_{ih}\} \\ + \quad \mathbf{P}_i^*(H_{R^{e*}} \le h;\mathcal{P}) &\times \Gamma(F_i^*, 1, \alpha) \times \mathbf{E}_{\mathbb{P}}\{R_{ih}\}\end{aligned}$$

which corresponds to Equation (9).

A.8 Fixed-Point Computation under Voluntary Policy Adoption

In the voluntary-adoption counterfactual, developers choose whether to adopt the policy bundle $\mathcal{P}$ or remain under the baseline regime $\mathcal{P}_0$. Parcel i adopts the policy if and only if it increases project value:

$$\pi_i(\mathcal{P}) > \pi_i(\mathcal{P}_0).$$

Because equilibrium is computed as a fixed point, adoption decisions depend on expectations about other parcels' participation. The resulting binary rule introduces a discontinuity in the mapping from supply adjustments to aggregate supply, which can generate oscillations in the iteration.

To stabilize the algorithm, we smooth adoption beliefs during the fixed-point iteration using a logit approximation. The perceived probability that parcel i adopts the policy is

$$P_i(\mathcal{P}) = \frac{1}{1 + \exp\left(-\dfrac{\pi_i(\mathcal{P}) - \pi_i(\mathcal{P}_0)}{\lambda}\right)}. \tag{A.10}$$

The probabilities $P_i^{(k)}(\mathcal{P})$ enter the supply update step of the fixed-point iteration described in Appendix A.6. Expected supply on parcel i during iteration k is

$$s_i^{(k)} = P_i^{(k)}(\mathcal{P})\, s_i^{(k)}(\mathcal{P}) + (1 - P_i^{(k)}(\mathcal{P}))\, s_i^{(k)}(\mathcal{P}_0).$$

This smoothing replaces the discontinuous adoption rule during the iteration and yields a continuous mapping from drift adjustments to aggregate supply. Once the fixed point has converged, the smoothing device is removed and the final adoption decision reverts to the deterministic rule

$$\text{parcel } i \text{ adopts } \mathcal{P} \quad \Longleftrightarrow \quad \pi_i(\mathcal{P}) > \pi_i(\mathcal{P}_0).$$

The parameter λ governs the degree of smoothing. As $\lambda_i \to 0$, equation (A.10) converges to the deterministic adoption rule.

A.9 Feasibility and Compensating Incentives

This appendix characterizes the properties of parcel value that underlie the feasibility and participation results discussed in Section 6.

Proposition 1 (Continuity, Monotonicity, and Feasibility Thresholds) *Fix a mandate intensity $\alpha > 0$. Let parcel value be defined as in Proposition 1, where for each (α, ϕ, τ) the developer chooses optimal redevelopment timing and density:*

$$\pi_i(\alpha, \phi, \tau) = max_{0 \le F \le \bar{F}(\phi)} \pi(R, R^{e*}(F; \alpha, \phi, \tau), F, F_B, z_B, \alpha_B)\,.$$

Then: (i) $\pi_i(\alpha, \phi, \tau)$ is continuous in (ϕ, τ) on the admissible policy domain; (ii) $\pi_i(\alpha, \phi, \tau)$ is weakly increasing in the fiscal incentive τ; (iii) $\pi_i(\alpha, \phi, \tau)$ is weakly increasing in the density bonus ϕ through expansion of the feasible set $F \le \bar{F}(\phi)$; (iv) Define $\lambda_i(\phi, \tau) = \pi_i(\alpha, \phi, \tau) - \pi_i(\mathcal{P}_0)$. Then the compensating set $\mathcal{C}_i(\alpha) = \{(\phi, \tau) : \lambda_i(\phi, \tau) \ge 0\}$ is monotone in incentives: if $(\phi, \tau) \in \mathcal{C}_i(\alpha)$ and $(\phi', \tau') \ge (\phi, \tau)$ componentwise, then $(\phi', \tau') \in \mathcal{C}_i(\alpha)$; (v) Feasibility is characterized by parcel-specific thresholds: the boundary $\{(\phi, \tau) : \lambda_i(\phi, \tau) = 0\}$ separates infeasible and feasible policy combinations.

The proofs proceed in steps:

Step 1: Continuity. For any fixed construction density F, parcel value $\pi(\cdot)$ is given in Proposition 1. This expression is continuous in (ϕ, τ) on the admissible domain. The optimized value $\pi_i(\alpha, \phi, \tau)$ is obtained by maximizing this continuous function over the compact set $F \in [0, \bar{F}(\phi)]$.

Standard arguments imply that the resulting value function is continuous in (ϕ, τ).

Step 2: Monotonicity in τ. From (4), a longer tax exemption reduces the present value of property taxes paid after redevelopment. Holding F fixed, this increases project value. Since the developer optimizes over F, the optimized value $\pi_i(\alpha, \phi, \tau)$ is weakly increasing in τ.

Step 3: Monotonicity in ϕ. A higher density bonus increases the upper bound $\bar{F}(\phi)$ on feasible construction density. This expands the feasible set of the developer's optimization problem. Since the objective is maximized over this set, enlarging the feasible set cannot reduce the optimized value. Hence $\pi_i(\alpha, \phi, \tau)$ is weakly increasing in ϕ. Note that although a higher density bonus raises optimized parcel value, it may also increase the optimal expansion threshold $R^{e*}(F)$ and delay redevelopment. This affects development probabilities but does not overturn the monotonicity of the value function.

Step 4: Compensating set. Define $\lambda_i(\phi, \tau) = \pi_i(\alpha, \phi, \tau) - \pi_i(\mathcal{P}_0)$. By Steps 1–3, λ_i is continuous and weakly increasing in each argument. The compensating set $(\phi, \tau) : \lambda_i(\phi, \tau) \geq 0\}$ is therefore a superlevel set of a continuous, monotone function. It follows that if $(\phi, \tau) \in \mathcal{C}_i(\alpha)$, any $(\phi', \tau') \geq (\phi, \tau)$ also belongs to $\mathcal{C}_i(\alpha)$.

Step 5: Threshold structure. Continuity of λ_i implies that the boundary $\{(\phi, \tau) : \lambda_i(\phi, \tau) = 0\}$ separates the feasible and infeasible regions. This boundary defines parcel-specific thresholds for incentives required to restore feasibility.

B Additional Comparative Statics of the Model

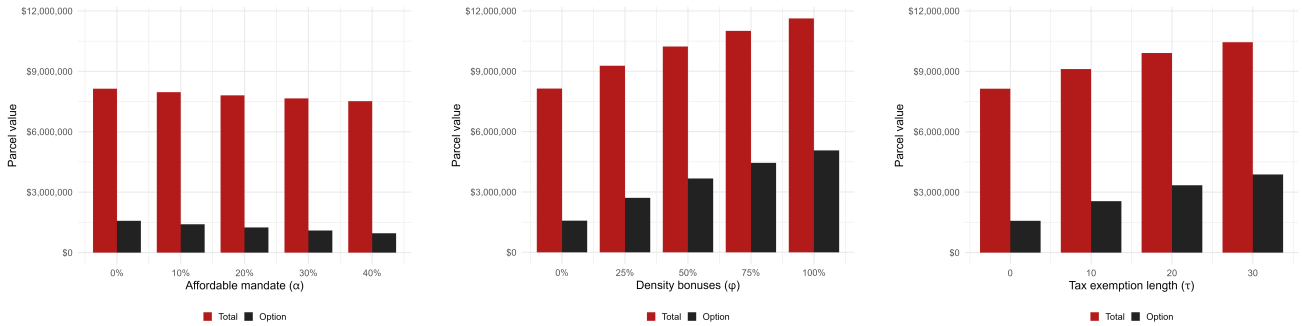
In this appendix, we present additional results and figures illustrating how our model, applied to a single parcel, responds to changes in parameters. We first provide more detail on how policy instruments affect model outcomes. Next, we report the complete set of comparative statics, accompanied by a brief discussion related to the importance of parcel heterogeneity. We finally provide an extended discussion of the role of non-instantaneous construction duration in an investment model under uncertainty. The results are derived for a single parcel, implying that the effect of supply on rents does not operate here. Unless specified otherwise, the comparative statics are obtained for a parcel close to its redevelopment threshold built at 66% of its capacity, with $F_B = 2$ and $\bar{F} = 3$, an age of 150 years, an expected rental growth rate of 4% (total return of 8% and a caprate of 4%), an annual potential rent per sqft of 50, and a lot size of 2,500 sqft. All other elasticities correspond to the values shown in Table II.

B.1 Policy Instruments Effects

In Table B1, we report changes in parcel value and in the probability of redevelopment associated with the enactment of a single policy. More importantly, the table shows how these results vary with key elasticity assumptions. Figure B1 highlights the effects of each policy instrument on the value of the redevelopment option, and Figure B2 shows the outcomes when policies are combined.

Affordable mandate (α). As highlighted in the main text, mandating affordable units on a given parcel unambiguously reduces both parcel value and the probability of (re)development, because

Figure B1: Policy Instruments Influence the (Re)development Option Value



A. Affordable mandate (α) B. Density bonuses (ϕ) C. Length of tax exemptions (τ)

Note: These figures show the effects the policy instruments on the present value of the current building and the present values of the redevelopment option. This option value is calculated as the difference between the total parcel value and its counterpart, where no development is allowed. These figures are obtained for a parcel of land built at 66% of its capacity with $F_B = 2$ and $\bar{F} = 3$, of age 150, with a rental growth of 4%, a volatility of 15%, a potential rent of 100, and a lot size of 2,500 sqft. All other parameters and elasticities are shown in Table II.

of the decline in the redevelopment option value (Panel A of Figure B1). For instance, Table B1 shows that a 20% mandate lowers parcel value by 0.49% and development probability by 1.15 percentage points. The impact is stronger in high-demand areas where the same 20% mandate leads to a 0.91% drop in value and a 2.69 percentage-point reduction in development probability. Effects are also stronger for parcels closer to the redevelopment threshold (i.e., with more unused density and older buildings). If the rental discount on affordable units doubles (ϵ_α), a 20% mandate reduces property values by 1.08% and development probability by 2.76 percentage points, consistent with the idea that deeper rent discounts further reduce the incentive to develop. In contrast, if developers can reduce construction costs for affordable units (higher η_α), the 20% mandate only modestly lowers property values, suggesting that cost savings can partially offset the mandate's negative effects.

Density bonuses (ϕ). Although density bonuses unambiguously increase parcel value through a higher redevelopment option value (Figure B1), they may also delay redevelopment as developers may require stronger market potential to justify the higher cost of construction. As an example, the second panel of Table B1 shows that a 50% increase in allowable density ($\phi = 0.5$) raises parcel value by 2.68% and development probability by 0.93 percentage points. In high-demand areas, property values and development probability increase more strongly with ϕ. For parcels closer to the redevelopment threshold, the parcel value still increases, but the probability of redevelopment declines sharply as developers would rationally wait to construct a taller building rather than build a lower one earlier. If the marginal benefit of height is higher (ϵ_F), a ϕ of 50% raises property values by 4.07% and development probability by 1.52 percentage points. In contrast, if we set a higher height elasticity of construction cost, the parcel value increases modestly, and redevelopment probabilities remain essentially unchanged. These results highlight that the impact of density policy depends critically on construction technology. (Ahlfeldt et al., 2026).

Tax exemptions (τ). Offering tax exemptions consistently increases parcel values and accelerates (re)development. The increase in value arises entirely from the redevelopment option, since the

Table B1: Policy's Effects on Single Parcel Outcomes and Sensitivity Analyses

	Change in Property Value (%)	Change in Prob. Dev. (p.p.)
Mandating 20% of Affordable Housing ($\alpha = 0.20$)		
Baseline	-0.93	-2.19
Higher potential rent ($R = 1.25R$)	-1.52	-4.75
Parcel closer to redevelopment ($F_0 = F_0/2$ and $age = 2age$)	-3.08	-3.07
Higher affordable rental discount ($\epsilon_\alpha = 2\epsilon_\alpha$)	-1.99	-5.02
Higher affordable construction discount ($\eta_\alpha = 2\eta_\alpha$)	-0.57	-0.69
Increase Maximum Allowed Density by 50% ($\phi = 0.50$)		
Baseline	5.91	3.08
Higher potential rent ($R = 1.25R$)	9.72	6.10
Parcel closer to redevelopment ($F_0 = F_0/2$ and $age = 2age$)	7.95	-12.82
Higher return to height ($\epsilon_F = 1.5\epsilon_F$)	7.36	4.64
Higher cost from height ($\eta_F = 1.5\eta_F$)	1.57	-0.43
20-years Property Tax Exemption ($\tau = 20$)		
Baseline	5.15	14.95
Higher potential rent ($R = 1.25R$)	8.48	25.68
Parcel closer to redevelopment ($F_0 = F_0/2$ and $age = 2age$)	20.10	21.43
Higher property tax rate ($\psi = 1.5\psi$)	7.92	19.48

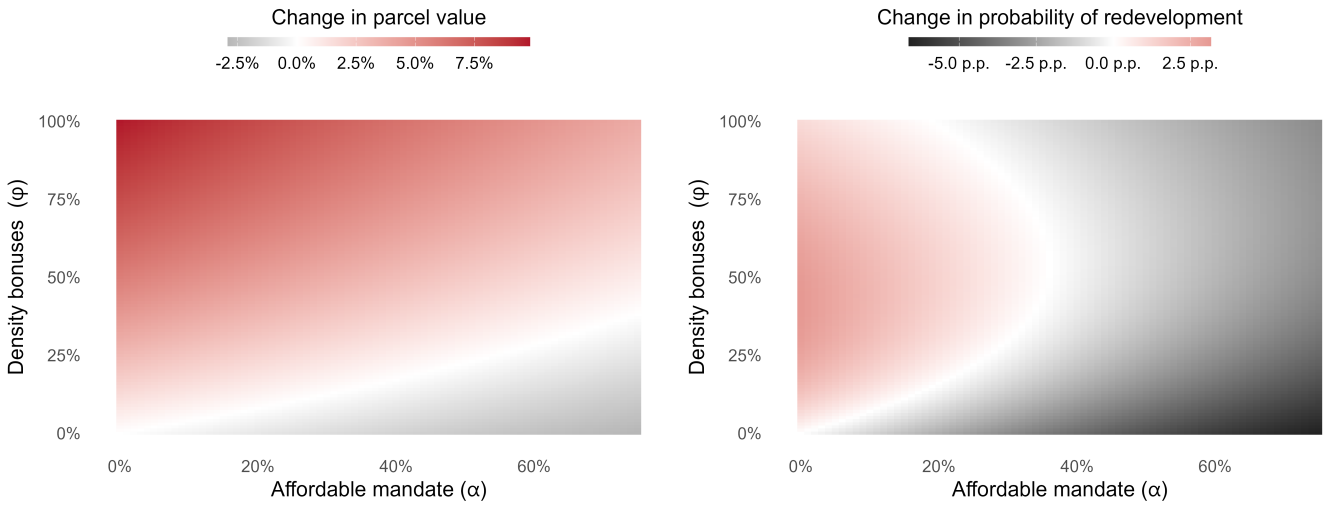
Notes: *This table reports the change in property value and the change in the probability of development within 10 years with respect to the policy instruments. These figures are obtained for a parcel of land built at 66% of its capacity with $F_B = 2$ and $\bar{F} = 3$, of age 150, with a rental growth of 4%, a volatility of 15%, and a potential rent of 50. All other parameters and elasticities are shown in Table II.*

exemption applies only to new construction (Figure B1). As exemplified by the third panel of Table B1, a 20-year exemption increases parcel value by 2.98% and development probability by 8.25 percentage points. These effects are amplified for parcels closer to redevelopment, where probabilities rise by 16.24 percentage points, and in high-demand areas, where values increase by 5.5% and redevelopment probabilities by 16.5 percentage points. As expected, the impact of exemptions grows with higher property tax rates.

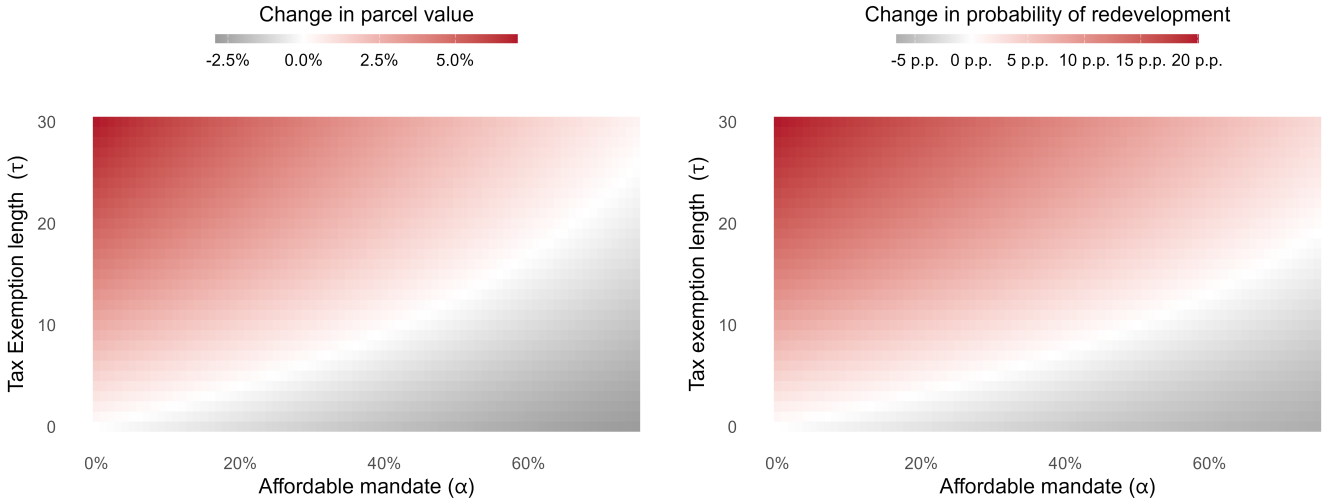
B.2 Parcel Heterogeneity and the Probability of Development

In this subsection, we show how the model predicts parcel value and redevelopment probability as functions of the parcel's characteristics: built form (age and current FAR) and location, which in our framework operates primarily through potential rent (R) and expected rent growth (g). These results highlight that heterogeneity in age, density, and local demand fundamentals is central to explaining spatial variation in redevelopment activity and, therefore, essential for understanding both the distributional and aggregate effects of policy interventions. Figure B4 further illustrates marginal effects with respect to the remaining parameters of the parcel-level model.

Figure B2: Trade-offs Between Carrots and Sticks in Simple Parcel Analysis



A. Density incentive zoning

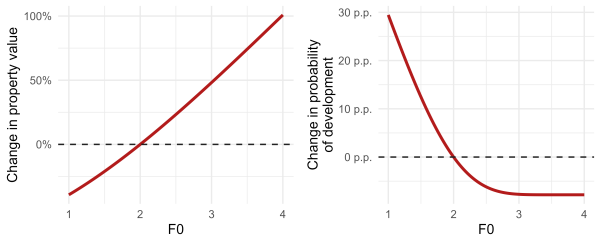


B. Fiscal incentive zoning

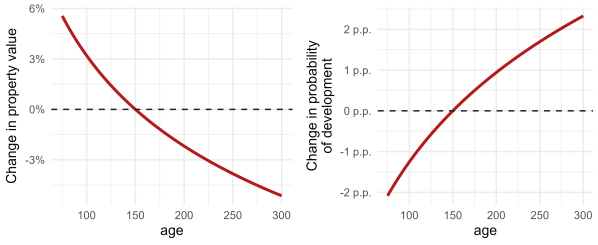
Note: These figures show the effects of combining an affordable mandate with either density bonuses (Panel A) or with a property tax exemption (Panel B) on the change in the property value (left panels) and the change in the probability of development completion within 10 years (right panels). These figures are obtained for a parcel of land built at 66% of its capacity with $F_B = 2$ and $\bar{F} = 3$, of age 150, with a rental growth of 4%, a volatility of 15%, and an annual potential rent of 50. All other parameters and elasticities are shown in Table II.

Panel A of Figure B3 shows that parcels with low initial built density (F_B) have lower property values than more intensively developed sites but exhibit the highest redevelopment probabilities, reflecting the larger embedded option value of underbuilt parcels. As current density approaches its maximum, the potential for value creation through rebuilding declines sharply, even though the standing property retains a high value. Panel B shows that redevelopment incentives rise with building age. Older structures face greater physical and economic obsolescence, which increases the value of the redevelopment option, while property values decline with age as rental income from existing buildings deteriorates. Together, these panels show that redevel-

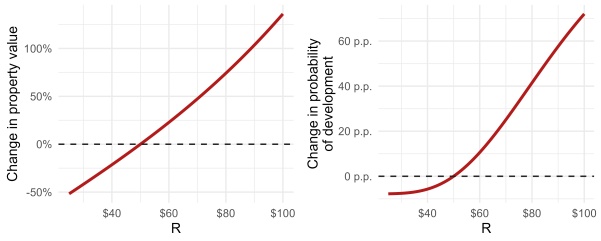
Figure B3: Effects of key Parcel Heterogeneity on Value and Probability of Development



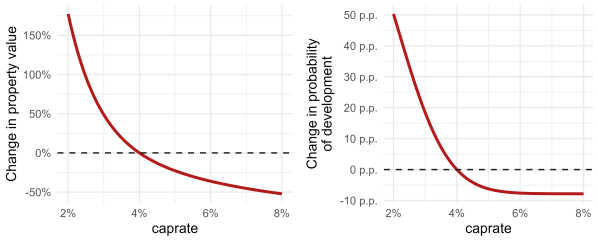
A. Current built density – F_B



B. Property age – $z^{-1}(age)$



C. Potential rent per unit – R



D. Caprate – $(r - \delta)$

Note: These figures show the effects of changing the one input parameter on the change in the property value (left panels) and the change in the probability of development starting within 10 years (right panels). These figures are obtained for a parcel of land built at 66% of its capacity with $F_B = 2$ and $\bar{F} = 3$, of age 150, with a rental growth of 4%, a volatility of 15%, and a potential rent of 50. All other parameters and elasticities are shown in Table II.

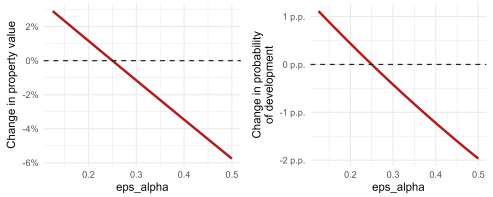
opment becomes more likely when the expected gains from rebuilding outweigh the opportunity cost of preserving the existing structure—an essential mechanism for understanding redevelopment activity across the city.

Spatial heterogeneity further amplifies these dynamics. In our framework, spatial variation operates through potential rent (R) and caprate (c), which together summarize local demand fundamentals. Panels C and D show that higher rent levels (R) or lower caprate (i.e., higher expected rental growth) both increase parcel value and sharply raise redevelopment probabilities, with effects that intensify at higher R and δ. Small differences in neighborhood demand can therefore translate into disproportionately large differences in redevelopment activity, illustrating how micro-level heterogeneity aggregates into uneven spatial patterns of urban growth.

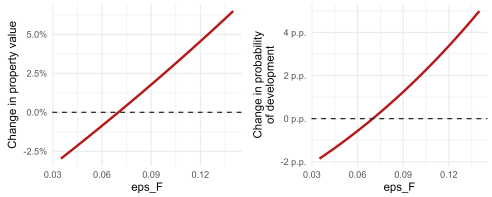
B.3 Relevance of Non-instantaneous Construction Duration

The impact of uncertainty on investment behavior changes fundamentally when construction is not instantaneous. Panels A and B of Figure B5 show the probability of development for various construction duration d and cost shifter k_c, respectively. The development probability increases with uncertainty for large d but decreases with uncertainty with instantaneous construction. For long construction periods d, developers hesitate at low uncertainty, waiting for clearer signals. Once uncertainty is high enough, the probability of investment rises sharply. This pattern differs from the *incremental* investment framework in Bar-Ilan and Strange (1999), where uncertainty lowers investment intensity at every stage by discouraging additional capital, paralleling the results of shorter d in Panel A. Unlike with *lumpy* investment, with *incremental* investment, firms make many small decisions over time, each negatively affected by uncertainty. In

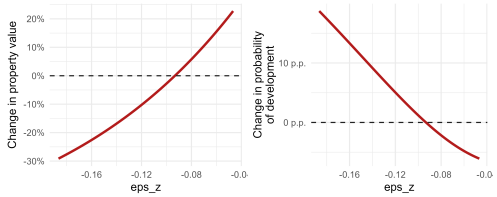
Figure B4: Effects of Parameter Changes on Parcel Value and Probability of Development



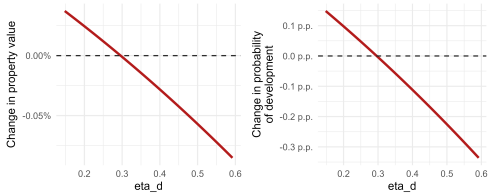
A. Affordable rental discount – ϵ_α



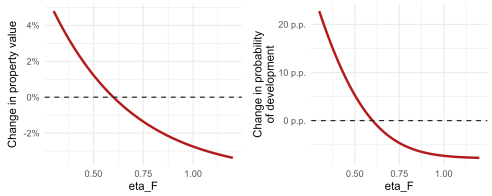
B. Height elasticity of rent – ϵ_F



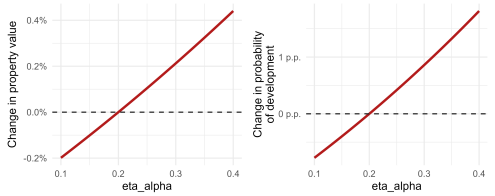
C. Age elasticity of rent – ϵ_z



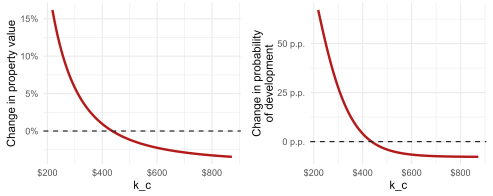
D. Height elasticity of demolition – η_D



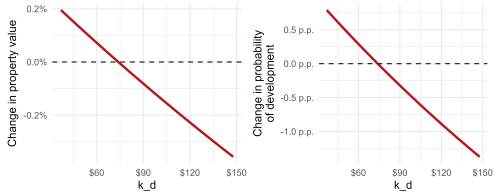
E. Height elasticity of construction – η_F



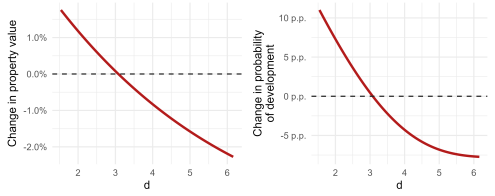
F. α elasticity of construction – η_α



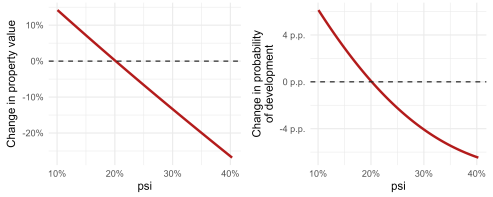
G. Construction cost shifter – k_c



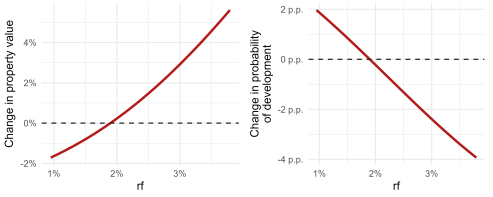
H. Demolition cost shifter – k_d



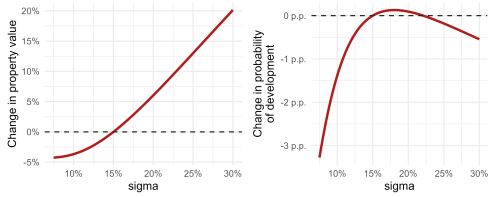
I. Construction duration – d



J. Property tax rate – ψ



K. Risk-free rate – r

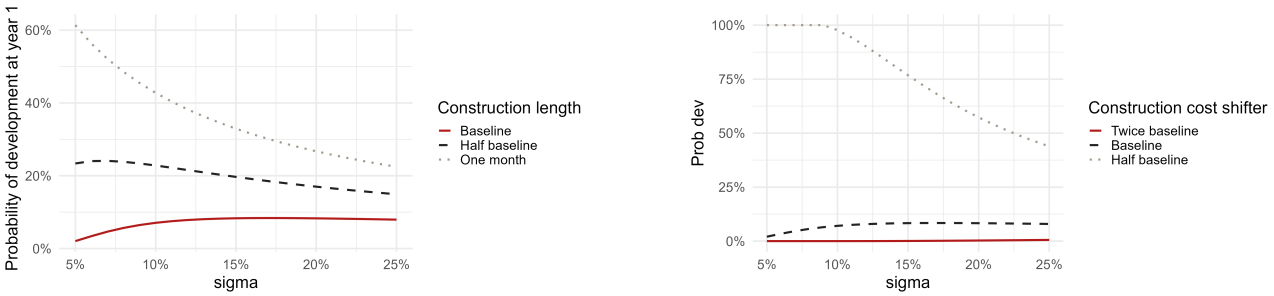


L. Volatility – σ

Note: These figures show the effects of changing the one input parameter on the change in the property value (left panels) and the change in the probability of development starting within 10 years (right panels). These figures are obtained for a parcel of land built at 66% of its capacity with $F_B = 2$ and $\bar{F} = 3$, of age 150, with a rental growth of 4%, a volatility of 15%, and a potential rent of 50. All other parameters and elasticities are shown in Table II.

our setting of *lumpy and lengthy* investment, uncertainty alters timing, but once investment occurs, intensity is unaffected. Models that assume instantaneous or incremental investment, therefore, tend to overstate development probabilities and inflate housing supply forecasts, that variation in construction costs cannot capture.

Figure B5: Uncertainty, Construction Length, Construction Cost, and Probability of Development



A. Development probability and duration

B. Development probability and construction cost

Note: This chart shows the effects of varying the rental volatility σ on the the probability of development within 10 years. Each line shows this effect for different assumptions regarding the length of construction d (Panel A) or the baseline cost of construction k_c (Panel B). These figures are obtained for a parcel of land built at 66% of its capacity with $F_B = 2$ and $\bar{F} = 3$, of age 150, with a rental growth of 4%, a volatility of 15%, and a potential rent of 50. All other parameters and elasticities are shown in Table II.

C Additional Details on Data and Calibration

C.1 Parcel-level Data

We begin with the 2023 PLUTO dataset, which contains 857,944 tax lots. We apply a sequence of restrictions to isolate parcels relevant for the counterfactual analysis that we highlight in Table C1. Particularly important:

- **Residential parcels.** We retain lots that are zoned or partially zoned for residential use. To retain parcels eligible for residential use, we keep those with an "R-x" zoning classification in the first through fourth zoning categories. We also retain parcels with observed residential square footage regardless of zoning classification.
- **Complete and consistent information.** We keep parcels that have recorded built year and FAR in addition to parcels without building. We exclude parcels with extreme lot sizes by retaining parcels larger than 1,250 square feet (half of a standard Manhattan lot) and smaller than 250,000 square feet (roughly one hundred times a standard Manhattan lot).
- **Rental and caprate data availability.** We keep parcels with (i) an ACS-based rental estimate and (ii) an observed CoStar caprate measure, leaving 765,966 parcels in the final dataset.

In total, we keep 89.3% of all parcels of New York City. The same procedure is used when constructing the 2013 parcel-level data we use to predict construction activity, which we compare with realized construction as a model fit exercise (89.3% are retained).

Table C1: Parcel-level Cleaning Steps

Category	Parcels	Share of Total	Loss
PLUTO 2023	857,944	100.00%	
with FAR information	825,703	96.24%	-3.76%
residential or partially residential	803,026	93.60%	-2.75%
with acceptable parcel size	778,060	90.69%	-3.11%
with spatial information	777,211	90.59%	-0.11%
with age information	776,872	90.55%	-0.04%
with rental (ACS) data	766,558	89.35%	-1.33%
with return (CoStar) data	765,885	89.27%	-0.09%
with all variables	765,830	89.26%	0.00%

C.2 Rental Obsolescence due to Aging

To estimate rental discount to obsolescence z_i, we follow Rosenthal (2014) and compute the age elasticity of real estate prices using individual transaction data. Although the estimation relies on transaction prices rather than rents, the estimated price discount ϵ_z can be applied directly to rents because the year and location fixed effects account for variations in capitalization rates. We use multifamily transactions from CoStar between 2000 and 2023 and estimate a hedonic pricing regression of the form

$$\log(\text{SalePrice})_{ijt} = \beta_j + \beta_t + \epsilon_z \log(\text{Age}_{it}) + X_i\beta + \epsilon_{ijt},$$

where $\log(\text{SalePrice})_{ijt}$ is the log building price in year t and location j, β_j and β_t denote spatial and time fixed effects, Age_{it} is the difference between the sales year and the building's construction year, and X_i includes covariates such as log building size, log number of floors, a retail-use indicator, and distance to the nearest MTA subway station. The log–log specification allows for faster depreciation at earlier ages, consistent with Lopez and Yoshida (2022).

Table C2 reports results across several fixed-effect specifications. Estimates of ϵ_z, which capture the decline in prices due to aging, range from -0.096 to -0.089, implying an annual rental depreciation pattern that is steeper in the early years (averaging -2% over the first 10 years), consistent with the findings. We set $\varepsilon_z = -0.093$ in the baseline calibration and compute $z_i = \text{Age}_i^{\epsilon_z}$ to obtain parcel-level rental depreciation. Spatial variation in z_i is shown in Panel B of Figure D1.

C.3 Rental Data Construction

For the model, we need to measure rental income that reflects the potential rent per unit of space, net of the effects of height, obsolescence, and affordable-unit requirements. We use the ACS median gross rent variable (B25064_001) that reports the median contract rent at the block group or census tract level. First, we assign to each parcel either the block group level rent, $Rent_{bg}$, or the tract level rent, $Rent_{tract}$, when the former is unavailable. This procedure preserves geographic heterogeneity while maintaining close to full data coverage.

To recover a rent measure consistent with the model, we adjust the ACS data in several steps. First, because ACS rent is reported per dwelling unit, we normalize it by the median apartment size in the corresponding geography. We compute the median size of residential

Table C2: Estimation of the Age Elasticity

	Dependent variable:			
	log(SalePrice)			
	(1)	(2)	(3)	(4)
log(Age+1)	-0.096^{***}	-0.095^{***}	-0.093^{***}	-0.089^{***}
	(0.006)	(0.005)	(0.005)	(0.006)
Controls	X	X	X	X
Community District FE	X	X		
Year FE	X			
Borough x year YE		X		
Community district x year FE			X	
Neighborhoods x year FE				X
Observations	27,342	27,342	27,342	27,342
R^2	0.739	0.745	0.768	0.795
Adjusted R^2	0.738	0.743	0.755	0.766

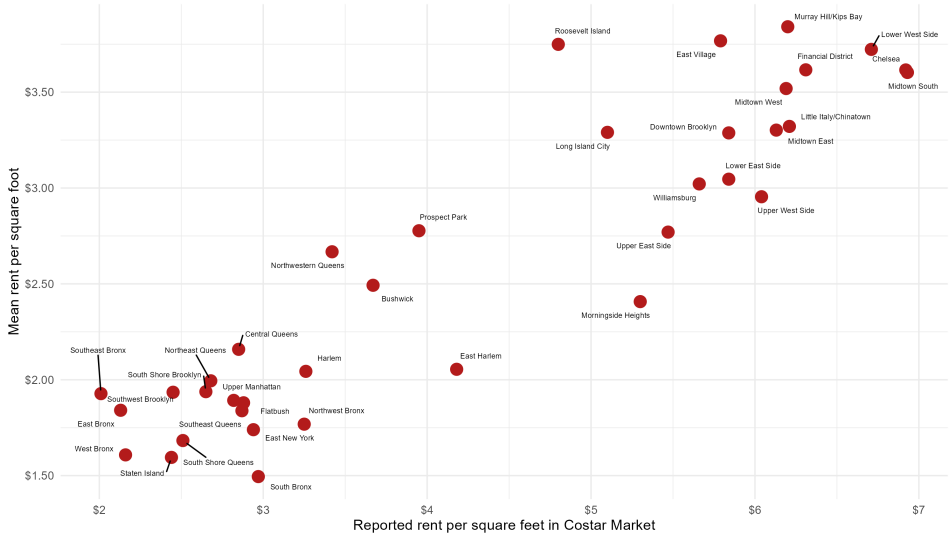
Notes: *This table reports the estimates of $log(SalePrice)_{ijt} = \beta_j + \beta_t + \varepsilon_Z log(Age_i) + X_i\beta + \epsilon_{ijt}$, where $log(PPU)$ is the log of the building price transacted in year t in location j, β_j and β_t are spatial and time fixed effects, respectively, Age_{it} is the age of the building at the time of transaction, X_i are covariates including the log size of the building, and the log number of floors, an indicator for whether the property has a retail component, and the distance to the closest MTA metro station. The sample consists of all building transactions from 2000 to 2023 in New York City, collected from Costar. Estimates followed by ***, **, and * are statistically significant at the 1%, 5%, and 10% levels, respectively.*

units using PLUTO records for buildings with reliable information on total residential square footage and number of units. We then divide each block-group (or tract) median rent by this median size of apartment to obtain the rent per square foot in each geography: $RentPSF_{bg} = MedianRent_{bg}/UnitSize_{bg}$.

We acknowledge that ACS rents are top-coded and therefore underestimate rent levels in the highest value neighborhoods. This bias affects primarily parts of Manhattan and Western Brooklyn. As a result, the calibrated model likely understates property values and redevelopment probabilities in these areasand parcels in these neighborhoods will respond less intensively to policy interventions, as illustrated in Figure I. This downward bias is evident in Figure C1, which compares our constructed ACS rents per square foot to market rents from CoStar, yet the two measures show a positive correlation ($R^2 = 0.82$). Despite this limitation, the ACS based construction remains essential because it delivers the finer spatial heterogeneity in rents. Market-based datasets such as CoStar cannot serve this purpose because their spatial units cover much larger geographic areas (47 sub-markets vs. 5,426 different rents with ACS geographies).

We finally convert this "realized" rent per square foot into the potential rent R_i required by the model. The ACS rent is collected through a survey of current residents and therefore reflects rental payments that depend on the existing buildings. Thus, it embeds the effects of current height, depreciation, and the share of affordable units. For instance, if we observe very low rent per square foot in a neighborhood, it might reflect low potential rent R_j or simply the fact that

Figure C1: Constructed ACS Rents per Square Foot versus CoStar Market Rents



Note: This scatter plot compares our constructed rent per square foot to CoStar market level rents. The vertical axis reports ACS based rents adjusted for median unit size and for average values of density, depreciation, and affordable share. The horizontal axis reports CoStar rents per square foot, aggregated at the market level. A perfect match would place all points on the 45 degree line. Most observations fall below this line, indicating that ACS based rents understate CoStar rents, with the gap strongest in high rent neighborhoods where ACS top coding is most binding. In contrast, lower rent neighborhoods lie close to the benchmark, suggesting that ACS rents provide reliable coverage in these areas. The pattern is consistent with the known censoring of ACS rental data above three thousand five hundred dollars.

many buildings are obsolete. In our model, R_i is the rental income per square foot of residential space in a building of height 1 ($F_B = 1$), not obsolete ($z_B = 1$), with no affordable units ($\alpha_B = 0$). To compute this potential rent, we scale the observed rent by the median values of F_B, z_B, and α_B in the corresponding geography. This adjustment removes the influence of existing building characteristics and yields an estimate of the underlying potential rent that would prevail on parcel i. Specifically, we define

$$R_{i(j)} = \frac{\text{Rent}_{i(j)}}{\Gamma\left(\tilde{F}_{B,i(j)},\ \tilde{z}_{B,i(j)},\ \tilde{\alpha}_{B,i(j)}\right)},$$

where $R_{i(j)}$ denotes the potential rent assigned to the geography j where parcel i is located, $\tilde{F}_{B,i(j)}$, $\tilde{z}_{B,i(j)}$, and $\tilde{\alpha}_{B,i(j)}$ are the weighted median built density, rental depreciation, and affordable unit share across parcels in geography j, respectively. Weighting by built square footage $F_{B,i} \times L_i$ ensures that the representative building characteristics reflect the stock of space actually inhabited by renters, consistent with the ACS rent measure. Panel A of Figure C3 shows the geographical variation in this constructed variable.

C.4 Returns, Cap Rates, and Rental Growth

We use market-level data from CoStar to construct the return series that underpins the stochastic process for rents. New York City is composed of 47 Costar submarkets that we manually mapped and assign to individuals lot in our database. The dataset covers the last twenty years (2004 to 2023). Returns are computed in three steps.

1. **Asset value per square foot.** For each market m and year t, we construct the implied asset value per square foot using market rents and cap rates:

$$\text{ValuePSF}_{m,t} = \frac{\text{RentPSF}_{m,t}}{\text{Caprate}_{m,t}}.$$

2. **Asset and rental returns.** We compute asset returns and rental returns as follows and report the summary statistics across market in Table C3:

$$\text{AssetReturn}_{m,t} = \frac{\text{ValuePSF}_{m,t}}{\text{ValuePSF}_{m,t-1}}, \qquad \text{RentalReturn}_{m,t} = \frac{\text{RentPSF}_{m,t}}{\text{ValuePSF}_{m,t-1}}.$$

3. **Total return.** The annual total return in market m is the sum of the two components:

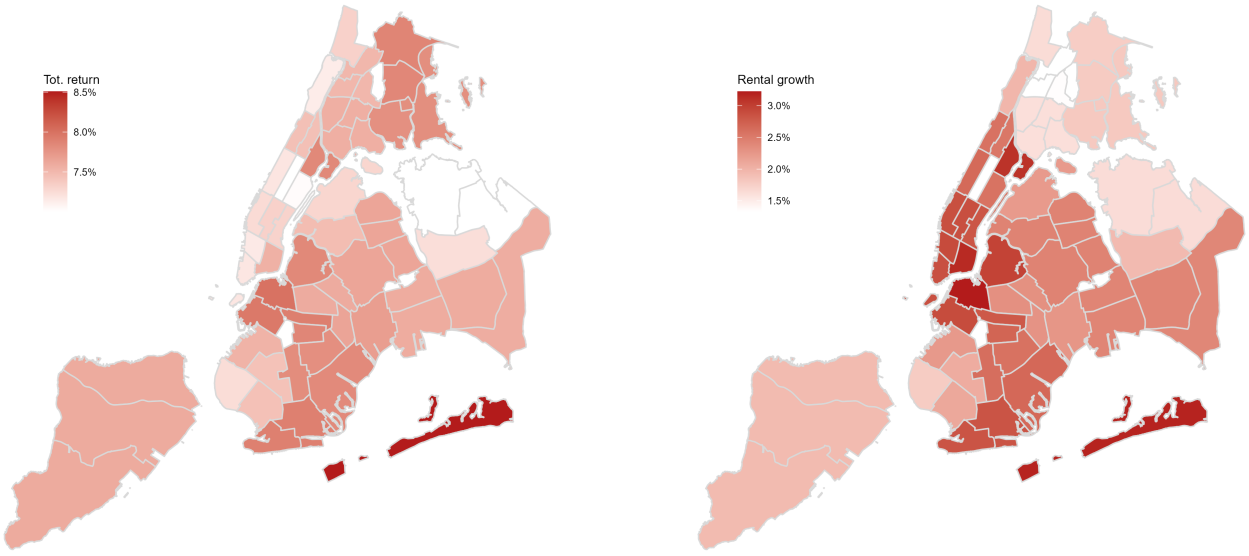
$$\text{TotalReturn}_{m,t} = \text{AssetReturn}_{m,t} + \text{RentalReturn}_{m,t}.$$

Table C3: Costar Market Level Returns

Statistic	N	Mean	St. Dev.	Min	Median	Max
Asset Return (%)	37	2.39	0.58	1.26	2.46	3.64
Rental Return (%)	37	4.85	0.59	4.05	4.85	5.98
Total Return (%)	37	7.23	0.40	6.60	7.26	8.14

We note that the average total returns across the 61 CoStar markets in New York City is 7.74%. This value falls within the estimates reported by Lyons et al. (2026) and Amaral et al. (2025) for New York City. The advantage of our approach is that it preserves meaningful spatial variation in returns, rental growth, and volatility. Figure C2 shows that expected total returns decline as one moves away from the city center, a pattern consistent with the argument in Amaral et al. (2025) that dense urban locations tend to deliver lower total returns.

Figure C2: Total Housing Return and Expected Rent Growth

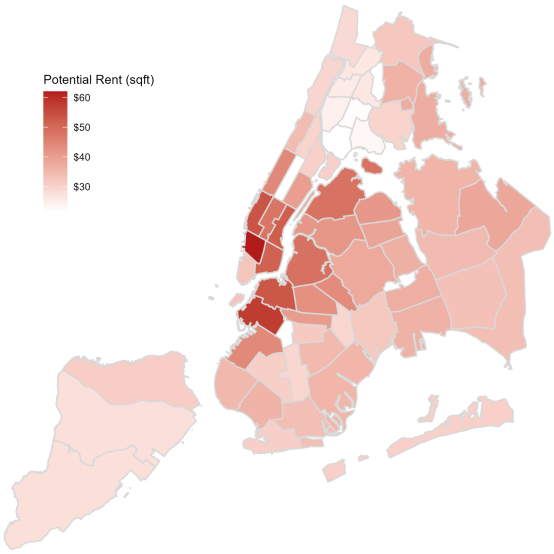


A. Total return (%)

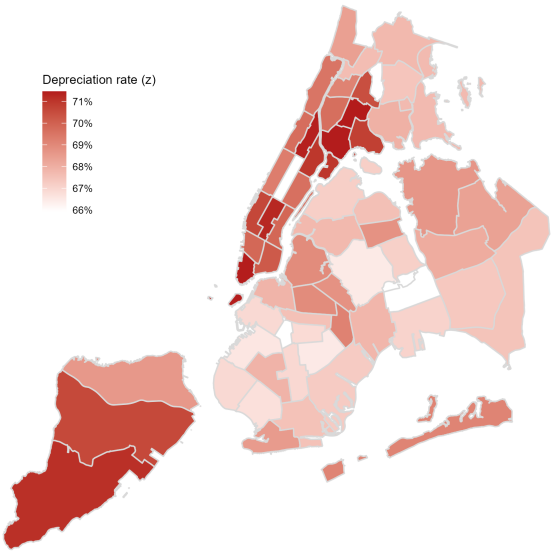
B. Volatility (σ_i)

Note: These maps show the average total return (asset and rental returns) in Panel A, and the 2023 estimated rental growth (total return minus 2023 cap rate) in Panel B computed across all parcels of the community districts. These statistics are drawn from Costar market data from 2004 to 2023.

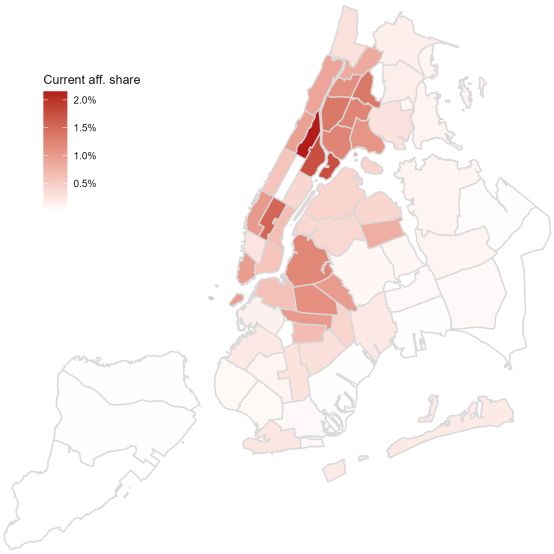
Figure C3: Spatial Variations of Key Variables



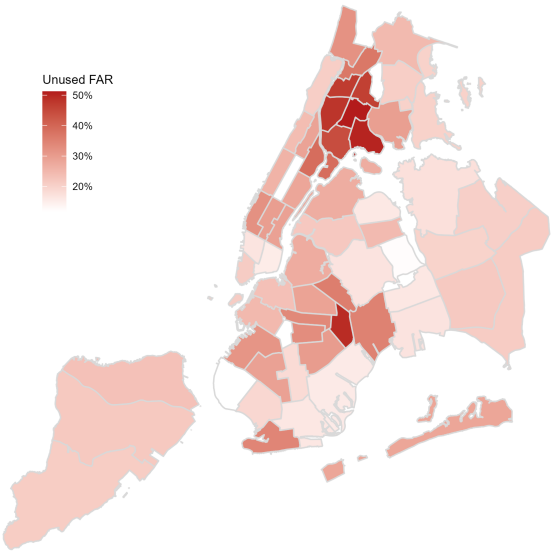
A. Potential rent per unit (R_i)



B. Rental depreciation Rate ($z_{B,i}$)



C. Pre-policy affordable share ($\alpha_{B,i}$)



D. Unused density ($1 - (F_{B,i}/\bar{F}_i)$)

Note: These maps show the average across all parcels of each community district of key parameters of the calibration. Panel A shows the potential rent per unit of density R_i that reflects market-rate rents for one non-obsolete unit, obtained by adjusting the annual rent for the average age and size of buildings within each neighborhood. Panel B shows the average discount due to the aging of properties $z_{B,i}$. Panel C shows the average share of buildings with affordable units. Panel D shows the unused density computed as the share of allowed FAR that is currently not built. All statistics are computed with 2023 data.

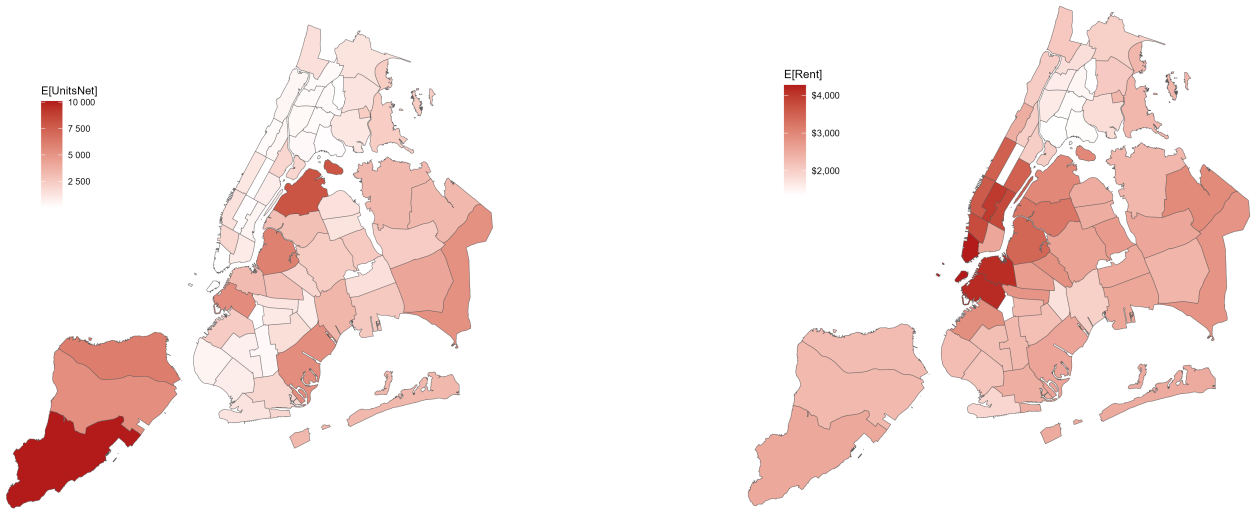
D Baseline Outcomes Additional Results and Details

We aggregate outcomes at the city and market level at the 10-year horizon. The two main outcomes are the expected number of net additional housing units, $\mathbf{E}[Apt_j^{net}]$, and the expected rent per housing unit, $\mathbf{E}[Rent_j]$. We also compute related measures including: the expected total supply $\mathbf{E}[S_j]$, expected density $\mathbf{E}[Density]$, the present value of all parcels Π, and the average share of option value $\mathbf{E}[Option]$. Aggregated outcomes are defined from the parcel-level outcomes as:

$$\begin{aligned}
\mathbf{E}[AptConst_j|\mathcal{P}] &= \sum_{i\in j} \mathbf{P}_i(\mathcal{P};\Theta)\frac{L_i F_i^*(\mathcal{P};\Theta)}{UnitSize_i} \\
\mathbf{E}[AptNet_j|\mathcal{P}] &= \sum_{i\in j} \mathbf{P}_i(\mathcal{P};\Theta)\frac{L_i (F_i^*(\mathcal{P};\Theta) - F_{B,i})}{UnitSize_i} \\
\mathbf{E}[Apt_j|\mathcal{P}] &= \sum_{i\in j} \left(\mathbf{P}_i(\mathcal{P};\Theta)\frac{L_i (F_i^*(\mathcal{P};\Theta))}{UnitSize_i} + (1-\mathbf{P}_i(\mathcal{P};\Theta))\frac{L_i F_{B,i}}{UnitSize_i} \right) \\
\mathbf{E}[Rent_j|\mathcal{P}] &= \frac{\sum_{i\in j} \mathbf{E}[RentInc_{it}(\mathcal{P};\Theta)]}{\mathbf{E}[Apt_j|\mathcal{P}]} \\
\mathbf{E}[Density_j|\mathcal{P}] &= \frac{\mathbf{E}[Apt_j|\mathcal{P}_0]}{\sum_{i\in j} L_i/43560} \\
\Pi_j(\mathcal{P}) &= \sum_{i\in j} \pi_i(\mathcal{P};\Theta) \\
Option_j(\mathcal{P}) &= \frac{\sum_{i\in j} \tilde{\pi}_i(\mathcal{P};\Theta)}{\sum_{i\in j} \pi_i(\mathcal{P};\Theta)} \\
PV_j^{Tax}(\mathcal{P}) &= \sum_{i\in j} \pi_i^{Tax}(\mathcal{P};\Theta).
\end{aligned} \tag{D.1}$$

where $\tilde{\pi}_i(\mathcal{P};\Theta)$ is the redevelopment option value computed by the difference between the property value π_i and its counterpart when no building can be rebuilt (i.e., $k_c = \infty$). The present value of the taxes for a parcel, $\pi_i^{Tax}(\mathcal{P};\Theta)$, is computed by the sum of the last integral of Equation (3) and the ψ component of the first integral. Together, these aggregates summarize supply, rents, and asset values, providing the key metrics through which we evaluate counterfactual policy scenarios.

Figure D1: Baseline - Market-level Aggregated Outcomes

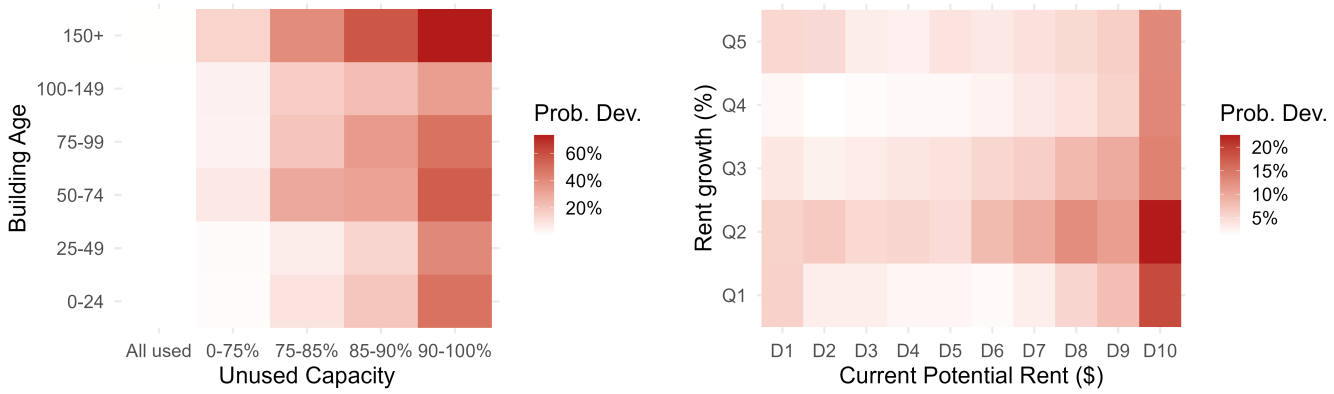


A. Expected net units

B. Expected rent

Note: These maps show the market-level aggregated outcomes of our baseline simulation as described in Table II. Panel A shows the expected net units addition and Panel B shows the expected rents per units.

Figure D2: Parcel Heterogeneity and Determinants of Probability of Development



A. Built environment

B. Rental potential

Note: These panels show the unconditional average probability of development computed for each grid cell. Panel A splits cells into deciles based on the current density ($F_{B,i}$) and the current age of the building ($z_{B,i}$). Panel C splits cells into deciles based on the potential rent (R_i) and rental growth (g_i) using the model baseline calibration with parameters described in Table II.

Table D1: Partial Correlations Between Inputs and Outcomes of Baseline Model

	Baseline Outcomes:				
	Prob	F opt	log(PV)	Option	PV/F
	All parcels				*Built parcels*
	(1)	(2)	(3)	(4)	(5)
Rent potential (R_i)	0.289	−0.015	0.457	0.150	0.792
Rent growth (g_i)	0.056	0.020	0.037	0.028	0.096
Quality index ($z_{B,i}$)	−0.058	−0.017	0.274	−0.016	0.328
Current density ($F_{B,i}$)	−0.140	0.825	0.652	−0.077	0.087
Non-built parcel ($\mathbf{1}_{F_{B,i}=0}$)	0.685	−0.0001	−0.377	0.972	

Notes: *This table reports the partial correlations between key inputs (rows) and outcomes (columns) of our baseline model results. The partial correlations are conditional on community districts as well as all other inputs listed in the rows. It uses the outcomes of the model with horizon 10-years for the 781,226 parcels under the baseline calibration described in Tables I and II. In Column (1), the outcome is the estimated probability of redevelopment decision $\mathbf{P}_i(\mathcal{P}_0;\Theta)$. In Column (2), the optimal density chosen endogenously to maximize property value ($F^*(\mathcal{P}_0;\Theta)$). In Column (3), the log of the present value of the parcel $\pi_i(\mathcal{P}_0;\Theta)$. In Column (4), the option value share of total value $\tilde{\pi}_i(\mathcal{P}_0;\Theta)/\pi_i(\mathcal{P}_0;\Theta)$. In Column (5), the present value per square foot of built units $\pi_i(\mathcal{P}_0;\Theta)/F_iL_i$.*

E Counterfactual Results – Additional Tables & Figures

E.1 Distribution of rent

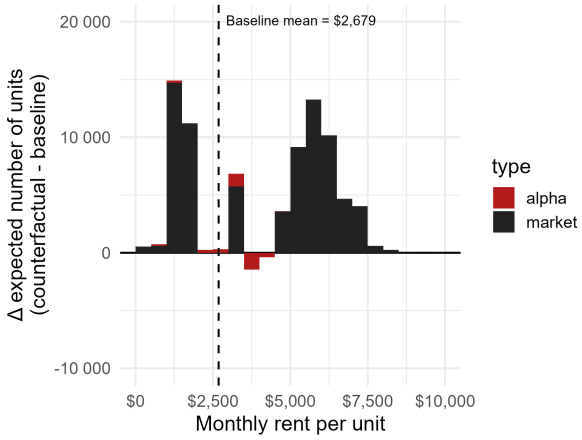
Figure E1: Counterfactuals – Change in Distribution of Rent



A. Upzoning ($\phi = .25$)



B. Density incentive zoning ($\alpha = 0.3$ & $\phi = .25$)



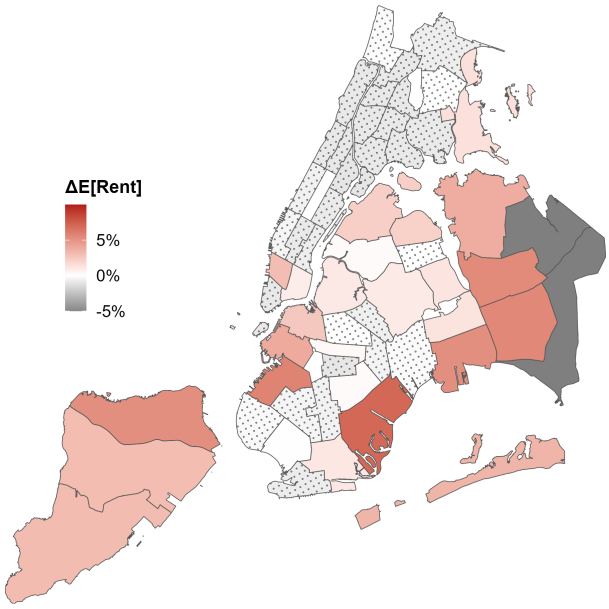
C. Tax exemption ($\tau = 20$)



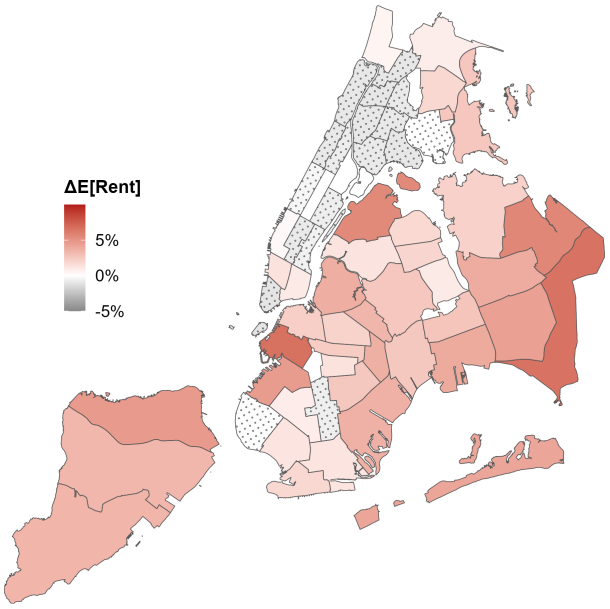
D. Fiscal incentive zoning ($\alpha = 0.30$ & $\tau = 20$)

Note: The histograms report the change in the expected number of apartments in each $500 rent bin under the counterfactual policy relative to the baseline, evaluated at a 10-year horizon. Bars above (below) zero indicate rent bins in which the expected number of units increases (decreases). Changes are decomposed into market-rate units (black bars) and units subject to affordability mandates (red bars).

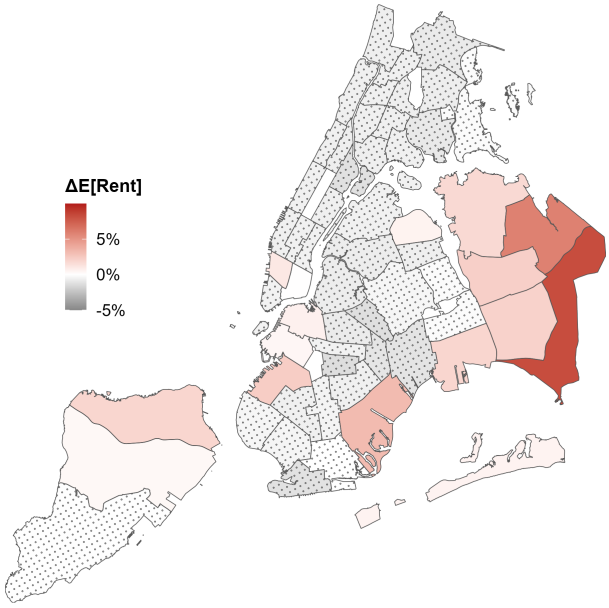
Figure E2: Counterfactuals – Change in Expected Average Rent



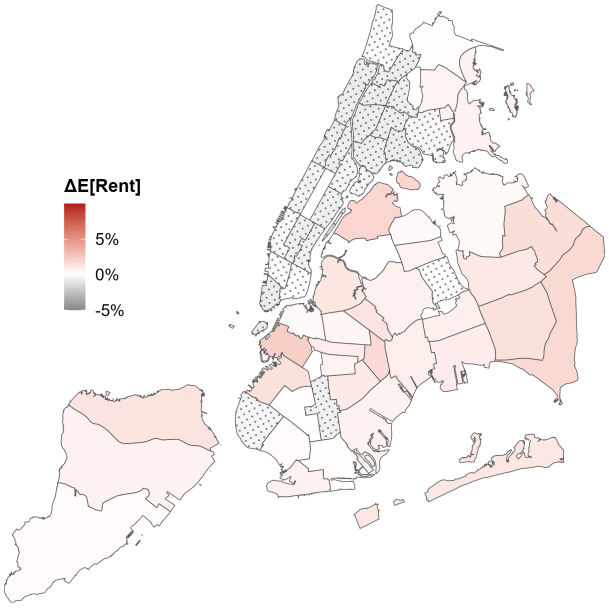
A. Upzoning ($\phi = .25$)



B. Tax exemptions ($\tau = 20$)



C. Density incentive zoning ($\alpha = 0.3$ & $\phi = .25$)

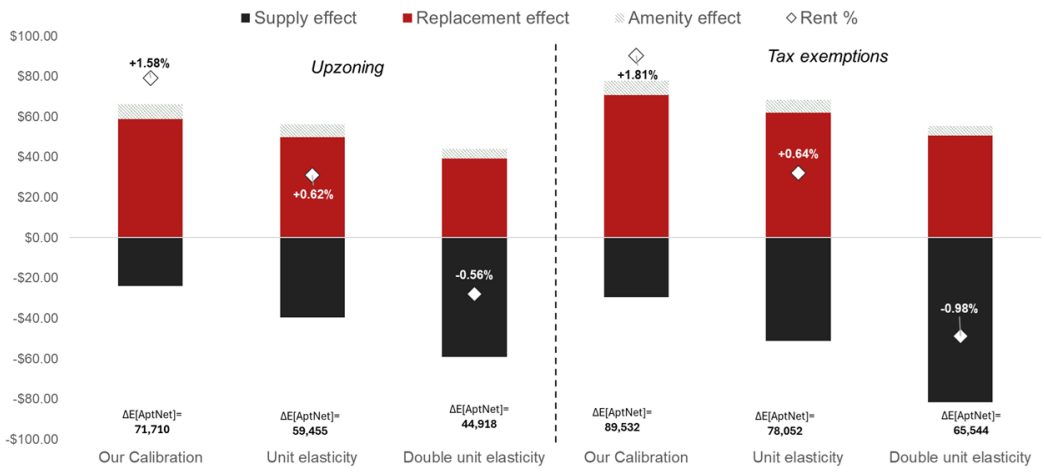


D. Fiscal incentive zoning ($\alpha = 0.3$ & $\tau = 20$)

Note: These maps show the percentage change in average expected rent per unit for different counterfactual policy analyses. It shows for each community district the change compared to the baseline outcomes with horizon 10-year.

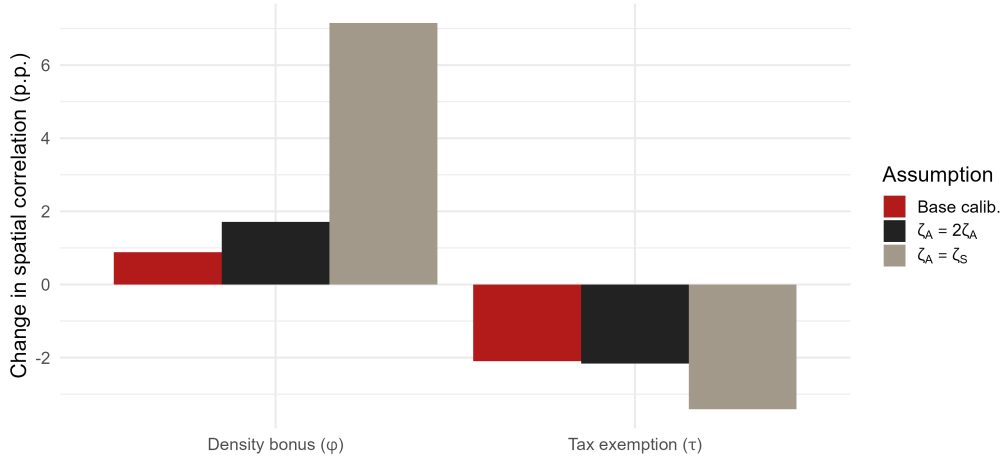
E.2 Robustness to different elasticities

Figure E3: Demand Elasticity, Rents, and Housing Production



Note: The points report the change in average expected rent under each policy relative to the baseline, evaluated at a 10-year horizon, together with its decomposition into the main channels described in the text. For each counterfactual, upzoning in the left panel and tax exemption in the right panel, outcomes are reported for alternative values of the citywide inverse demand elasticity $\zeta_S = \{-0.50; -1.00, -2.00\}$ *as indicated in the bottom row. Endogenous changes in housing production associated with a policy/elasticity bundle are reported at the bottom.*

Figure E4: Local Spillover Strength and the Spatial Correlation of Rents

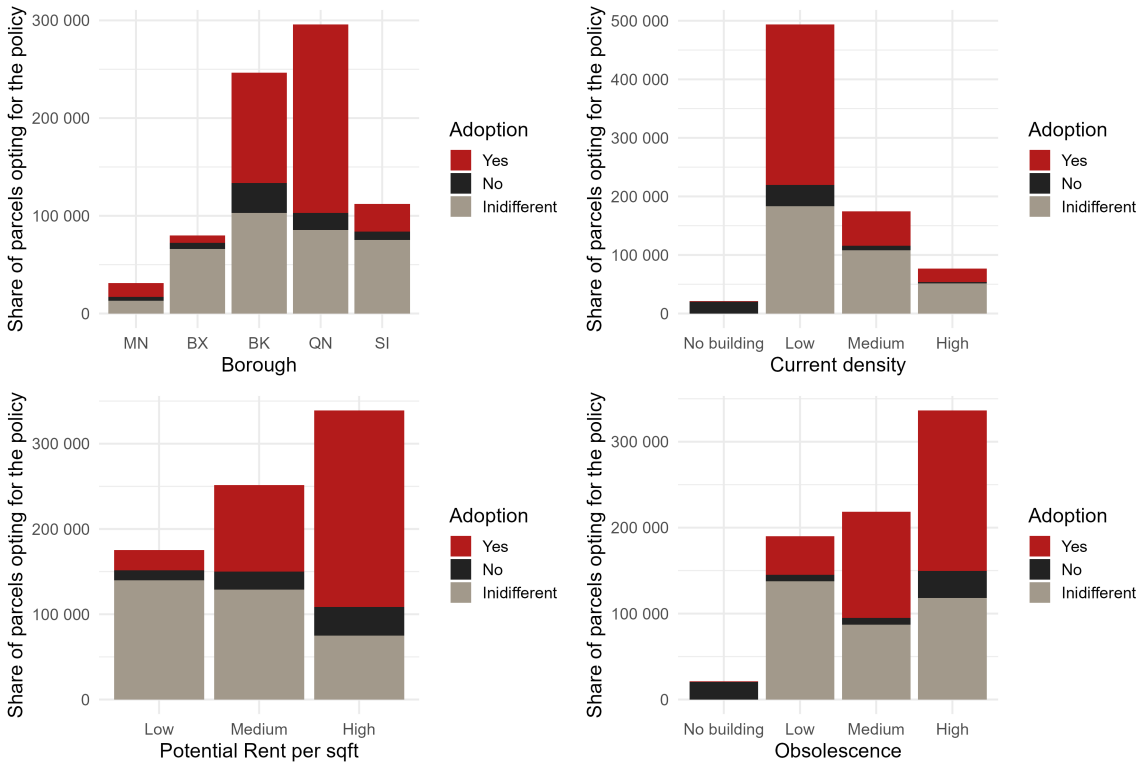


Note: The bars report changes in the spatial correlation of construction probabilities. Spatial correlations are measured using Moran's I, computed with inverse-distance weights over all parcels within 500 meters of each target parcel. Red bars correspond to the baseline calibration, with $\zeta_A = 0.05$ *and* $\zeta_S = -0.30$*. Black bars use* $\zeta_A = 0.10$ *and* $\zeta_S = -0.35$*, holding the sum of elasticities constant. Grey bars report results with* $\zeta_A = 0.30$ *and* $\zeta_S = -0.30$*. All values are expressed as deviations from the baseline spatial correlation at the 10-year horizon.*

E.3 Voluntary Adoption of Policies

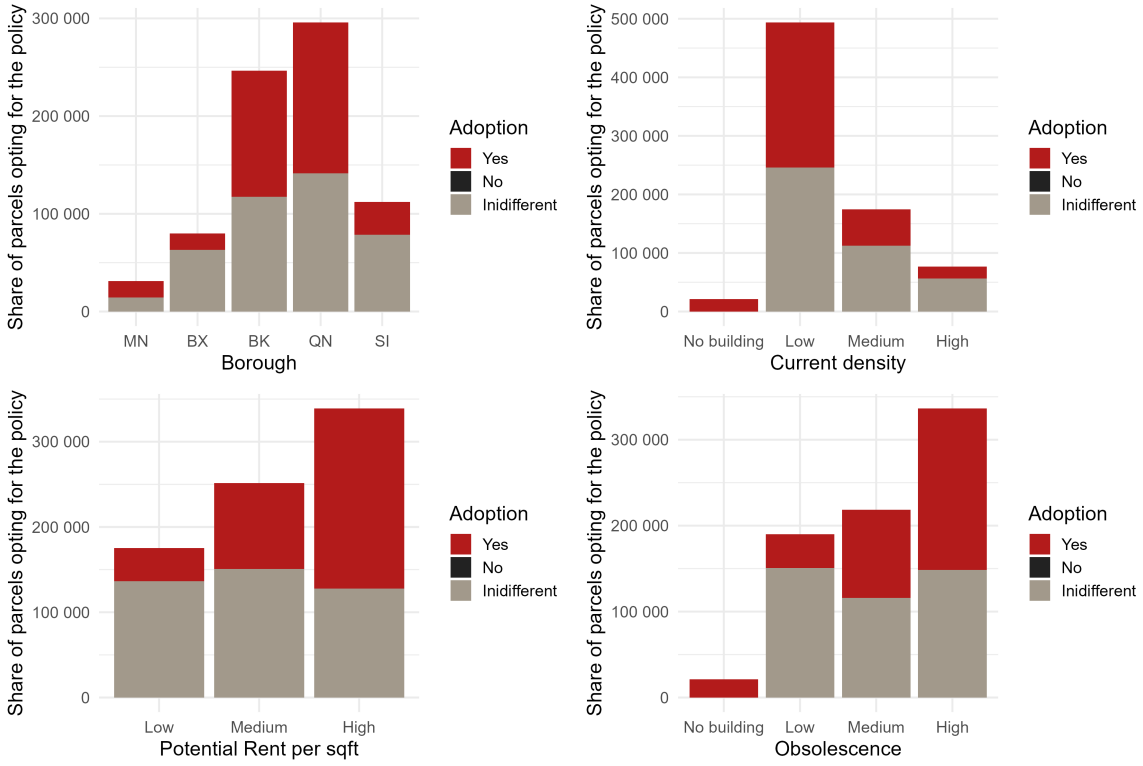
Table E1 reports the share of parcels that would opt into each policy. Approximately 45% of parcels adopt either the voluntary Density Incentive Zoning or the Fiscal Incentive Zoning. Notably, about 12% of adopters differ across these two bundles, underscoring the importance of parcel-level heterogeneity in the adoption decision. When density and fiscal incentives are combined, adoption rises sharply to 74.7%, with 28.6% of parcels switching from non-adoption to adoption once the fiscal incentive is added to the density incentive zoning. Figures E5 and E6 decompose adoption rates by location and building characteristics. Participation is systematically higher among parcels with low current density, high potential rent, and those located in Queens and Brooklyn.

Figure E5: Voluntary Adoption of Density Incentive Policy



Note: These bar graphs show the share of parcels that opt-in ($\pi_i(\mathcal{P}) > \pi_i(\mathcal{P}_0)$), opt-out of the policy $\mathcal{P}$, or are indifferent under the policy counterfactual that combine density bonuses ($\phi = 0.50$), and an affordable mandate ($\alpha = .30$), compared to the status-quo policies.

Figure E6: Voluntary Adoption of Fiscal Incentive Policy



Note: These bar graphs show the share of parcels that opt-in ($\pi_i(\mathcal{P}) > \pi_i(\mathcal{P}_0)$), opt-out of the policy $\mathcal{P}$, or are indifferent under the policy counterfactual that combine tax exemptions ($\tau = 20$), and an affordable mandate ($\alpha = .30$), compared to the status-quo policies.

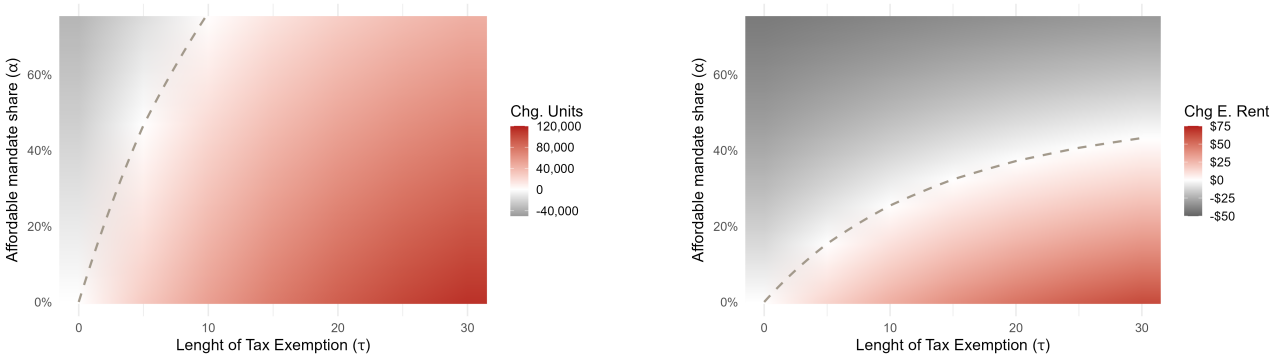
Table E1: Share of Parcels that Opt-in *Voluntary* Policy Interventions

	Number of Parcels	Share (%)
All Parcels	**765,830**	**100**
(7) Density Incentive Zoning ($\alpha = 0.30$ & $\phi = 0.50$)	355,930	46.5
but not in fiscal IZ	94,390	12.3
(8) Fiscal Incentive Zoning ($\alpha = 0.30$ & $\tau = 20$)	350,894	45.8
but not in density IZ	89,354	11.7
(9) All Policies	564,752	73.7
but not in density IZ (i.e., switchers with τ)	208,822	27.3
but not in fiscal IZ (i.e., switchers with ϕ)	215,553	28.1

Notes: *This table reports the number and the share of parcels that would opt-in the policy bundle $\mathcal{P}$ under voluntary adoptions. These parcels are defined as those that are better off under the new policy as in the baseline policy ($\pi_i(\mathcal{P}) \geq \pi_i(\mathcal{P}_0)$).*

E.4 Other Results

Figure E7: Continuous Policies Outcomes - Fiscal Incentive Zoning

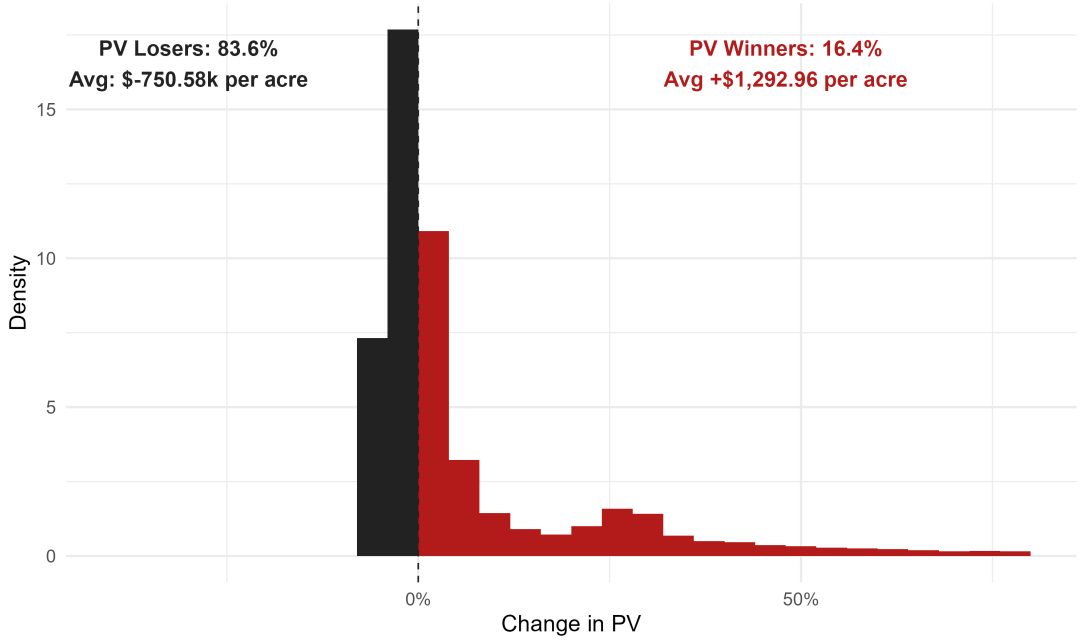


A. Change in housing unit

B. Change in expected average rent

Note: These heatmaps show the outcomes of a Fiscal Incentive Zoning program under continuous values of τ (x-axis) and α (y-axis). Changes are computed over the outcomes of the status-quo under policy $\mathcal{P}_0$. Panel A shows the net change in the number of housing units $E[AptNet|\mathcal{P}]$. Panel B shows the change in average expected rents per unit. The dotted lines show outcomes that equate the value under the status-quo policy $\mathcal{P}_0$.

Figure E8: Distribution of change of present values with combined incentive policy



Note: These bar graphs show the distribution of the percentage change in parcel present value $\Delta\pi_i(\mathcal{P})$ for the combined incentive zoning policy that combines density bonuses ($\phi = 0.50$), tax exemptions ($\tau = 20$), and an affordable mandate ($\alpha = 0.30$), relative to the baseline $\mathcal{P}_0$. Each bar represents the density of parcels experiencing a given percentage change in present value. Red bars denote parcels whose present value increases under the policy (winners, $\pi_i(\mathcal{P}) > \pi_i(\mathcal{P}_0)$), while black bars denote parcels whose present value decreases (losers, $\pi_i(\mathcal{P}) < \pi_i(\mathcal{P}_0)$). Average changes are expressed per acre of land.

Table E2: Counterfactual Results

		Built Environment				Public Potential Costs		
		$\Delta E[NetUnit]$ # of Apt.	$\Delta E[\text{Aff}Net]$ # of Apt	$\Delta E[MarketNet]$ # of Apt.	$\Delta E[Rent]$ (%)	$\Delta E[Density]$ (%)	$\Delta PVTax$ (%)	ΔPV (%)
		(1)	(2)	(3)	(4)	(5)	(6)	(7)
			Unilateral Policy					
(1)	*Upzoning* - $\phi = 50\%$	71,710	22	71,688	1.58	1.76	0.44	−1.20
(2)	*Tax abatement* - $\tau = 20$	89,532	269	89,263	1.81	2.18	−2.61	−0.93
(3)	*Affordable mandate* - $\alpha = 30\%$	−15,124	41,656	−56,780	−0.77	−0.37	−0.42	0.17
			Mandatory Carrot & Stick Zoning					
(4)	*Density Incentive Zoning* - $\alpha = 30\%$ & $\phi = 50\%$	43,552	67,502	−23,950	0.23	1.08	−0.25	−0.85
(5)	*Fiscal Incentive Zoning* - $\alpha = 30\%$ & $\tau = 20$	65,007	84,479	−19,472	0.31	1.58	−2.73	−0.75
(6)	*All* - $\alpha = 30\%$, $\phi = 50\%$, & $\tau = 20$	195,457	144,759	50,698	2.25	4.80	−3.89	−2.74
			Voluntary Carrot & Stick Zoning					
(7)	*Density Incentive Zoning* - $\alpha = 30\%$ & $\phi = 50\%$	42,338	34,538	7,800	0.65	1.04	0.29	−0.46
(8)	*Fiscal Incentive Zoning* - $\alpha = 30\%$ & $\tau = 20$	65,834	84,901	−19,067	0.47	1.59	−2.42	−0.45
(9)	*All* - $\alpha = 30\%$, $\phi = 50\%$, & $\tau = 20$	200,158	147,028	53,131	2.71	4.91	−3.10	−1.98
			Carrot & Stick Zoning with no supply effect					
(10)	*Density Incentive Zoning* - $\alpha = 30\%$ & $\phi = 50\%$	42,698	66,662	−23,964	0.53	1.04	0.33	−0.02
(11)	*Fiscal Incentive Zoning* - $\alpha = 30\%$ & $\tau = 20$	68,393	86,412	−18,019	0.97	1.65	−1.46	0.52
(12)	*All* - $\alpha = 30\%$, $\phi = 50\%$, & $\tau = 20$	219,790	156,370	63,420	4.41	5.35	−0.19	0.97

Notes: *This table reports the aggregate outcomes of our counterfactual policy analyses. Each row corresponds to a counterfactual regulatory environment $\mathcal{P}$, and all reported quantities reflect deviations from the baseline calibration $\mathcal{P}_0$ over a 10-year horizon. Column (1) reports the change in the expected number of housing units net of demolitions. Columns (2) and (3) decompose this change into net affordable and net market-rate units, respectively. Column (4) reports the percentage change in expected citywide rent per housing unit. Column (5) reports the percentage change in expected residential density, where density is defined as the expected number of built square footage per acre of land. Columns (6) and (7) report the percentage change in the present value of property tax revenues and total residential asset values, respectively. Rows (7-9) report outcomes under non-obligatory versions of the corresponding policy bundles. In these counterfactuals, developers of each parcel endogenously select whether to adopt policy $\mathcal{P}$ or remain under the baseline regime $\mathcal{P}_0$. The last three rows show counterfactual results computed by assuming there is not spatial feedback across parcels (i.e., $\zeta_S = 0$ and $\zeta_A = 0$).*